Faculty of Sciences

Group of Fundamental Theoretical Physics

Two aspects of Strong Interactions

Non Static Extension of the Color Singlet Model and Structure Functions of the Pion and of a Scalar Particle

Jean-Philippe Lansberg

Research report presented in partial fullfillement of the requirements for the Grade of Diplomé d'études approfondies en Sciences

Academic year 2001-2002

Preface

In Part I, I shall present some aspects of the production of heavy quarkonia in hadronic collisions. This is the direct continuation of my undergraduate dissertation [1].

More precisely, I shall consider the uncertainties specific to the theoretical model used, *i.e.* the Color Singlet Model [2]. I shall give an analysis of the influence of the uncertainties of the proton parton distribution functions on the differential cross-sections of hadronic heavy quarkonia production as well as the influence of the uncertainties on the wave function. The point of this study is to show – even if this was commonly believed – that theoretical errors are not sufficient to explain the discrepancies between Tevatron measurements [3, 4, 5] and the predictions of the CSM as exposed in the Chapter 2 of [1]. This study moreover allowed me to quantify the theoretical errors with a better precision.

Still in Part I, I shall then expose my work on the introduction of a non-vanishing relative three-momentum between quarks constituting the heavy mesons. Another step in the improvement of the classical CSM which I shall mention is the introduction of a non-vanishing relative energy and of a relativistic wave function for the mesons. In the following, I shall talk about *the non static extension of the CSM* when refering to this improvement.

Part II will be devoted to the study of pion and scalar structure functions. The study of these is part of a wider project related to off-diagonal hadron structure functions and is done in context of the ESOP European Network.

The subjects of Part I and Part II, although a priori not linked, do not differ substantially. As it will appear, the structure of the calculations of quarkonia production and of our model for pion structure functions are somehow very similar. In a general point of view, the main differences come from the nature of the particules which induce different vertex functions and differences in kinematics.

Acknowledgements and thanks

I would like to express my full gratitude to Jean-René Cudell for a careful reading of this report which is my first long written-work in English, but also for having proposed me to enter our ESOP working group and hence for having offered me the possibility to work on a brand new domain of particle physics to me, *i.e.* the light hadron physics.

I would like also to thank Pr. Joseph Cugnon. Without the position of IISN researcher he offered me in the group of Fundamental Theoretical Physics –nearly two years ago–, this work would not exist. I am also grateful to him for the numerous possibilities to attend scientific meetings he gave me.

Finally, and obviously, I want to thank all the other people of our group, especially the people of our ESOP working group and the young researchers for the motivation and/or the entertainment they provide me.

Contents

Part I

Non Static Extension of the Color Singlet Model

Context and Presentation of the Problem

As I pointed out in my undergraduate dissertation [1], a simple transposition of the factorization theorem [6](proved for some definite cases, *e.g.* Drell-Yan process) with the introduction of a nonrelativistic and universal wave function is not sufficient to describe hadronic production of heavy mesons such as the J/ψ, $\psi(2S)$ or the $\Upsilon(1S)$, $\Upsilon(2S)$ and $\Upsilon(3S)$ in the high-energy regime. This way of proceeding is the so-called Color Singlet Model [2].

In order to solve this problem, several models were proposed. The most discussed were and are the Color Evaporation Model [7] [1] (CEM), a model of reinteraction with a comoving color field presented by Hoyer & Peigné [8] [2] and Non Relativistic Quantum Chromodynamics (NRQCD) applied to heavy quarkonia production and decay.

The CEM is not anymore considered as *the* solution: its simplicity must indeed accomodate parameters which were supposed to be constant and which are now neither constant neither universal[3]. Nevertheless this model shows the necessity of introducing color-specific effects which are totally transparent in the CSM, this is somehow due to the interpretation of the wave function in this model, which is assumed to include all the non-perturbative effects. Actually the simplification is even stronger, as one simply considers its value at the origin (in position space), that is the first term in a Taylor expansion of

$$\int \psi(\vec{\ell})\mathcal{M}\mathrm{d}\vec{\ell}, \tag{.1}$$

where $\mathcal{M}$ is the amplitude to produce two free (on-shell) heavy quarks (with a flavor depending on the nature of the quarkonium) with a relative three-momentum $\vec{\ell}$.

[1]Exposed in Chapter 4 of [1].

[2]Exposed in Chapter 5 of [1].

[3]It worth pointing out however that the CEM can be improved with the help of event generators techniques simulating the non-perturbative effects included in the previously cited parameters, but I shall not speak about this in this work (see *e.g.* [9]).

In this context, except for the calculation of the second non-vanishing term of the expansion, the first improvement that comes to mind is to consider the full ℓ phase space contribution.

In order to do this, I shall first consider only the integration with $\ell^0 = 0$ (nonrelativistic bound state approximation) and a gaussian wave function compatible with the commonly admitted values of $\psi(0)$.

But doing that, we directly face a problem: the appearance of poles in some propagators in the amplitude. To solve this problem, there seems to be two solutions. The first one is to limit the phase space to avoid the singularities. The second solution is, supposing that the poles of the different propagators do not occur at the same momenta loop value, to evaluate (numerically) their principal parts.

Before exposing this, I shall present in the next Chapter the study of the model-specific theoretical uncertainties, *i.e.* from the parton distribution function and from the wave function value at the origin deduced from the leptonic decay width.

Chapter 1

Theoretical Uncertainties of the Color Singlet Model[1]

1.1 Recalling the Model

This model is based on several approximations or postulates:

- Decomposing the quarkonium production in two steps, first the creation of the 2 heavy quarks (Q & $\bar{Q}$) and then the binding of these two quarks forming the meson, one *postulates the factorization* of these two processes.

- As the scale of the first process is approximately $M^2 + p_T^2$ one considers it as a *perturbative* one. One can thus calculate its cross-section with classical Feynman-diagram methods.

- Considering only bound states of heavy quarks, their velocity in the meson must be small. One therefore supposes that the meson is created with its 2 constituent quarks *at rest* in the meson frame. This is *the static approximation.*

- One finally assumes that the color and the spin of the pair $Q\bar{Q}$ don't change during the binding. As physical states are colorless, one requires the pair to be produced in a *color singlet state.*

In high-energy hadronic collisions, the leading contribution comes from a gluon fusion process. Using a meson production vertex function with the required tensorial structure and prescriptions relative to the propagators, one has six diagrams for the $^3S_1$ states,

[1] This chapter is based on my contribution to the proceedings of the JJC2001 [11]. An electronic version is available on the `arXiv.org` preprint server under the reference **hep-ph/0201111**.

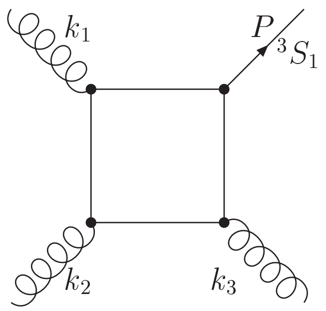

+ 5 crossed diagrams ...

which give

$$\frac{d\sigma}{d\hat{t}} = \frac{20\pi^2 M\alpha_s^3 |\psi(0)|^2}{9\hat{s}^2} \times \frac{[\hat{s}^2(\hat{s}-M^2)^2] + [\hat{t}^2(\hat{t}-M^2)^2] + [\hat{u}^2(\hat{u}-M^2)^2]}{(\hat{s}-M^2)^2(\hat{t}-M^2)^2(\hat{u}-M^2)^2}. \tag{1.1}$$

1.2 Theoretical Uncertainties

1.2.1 Wave Function

The first source we consider is related to the wave function at the origin, which enters directly the expression of the cross-section (1.1).

Its value is in fact extracted from the leptonic decay width, which can be written

$$\Gamma(^3S_1 \to \ell\bar{\ell}) = \frac{64\pi}{9}\frac{\alpha^2 e_Q^2 \psi^2(0)}{M^2}. \tag{1.2}$$

This is one of the consequences of the factorization postulate.

We thus find that the error on $\Gamma_{^3S_1\to\mu\mu}$ introduces an error of at least 10% on the cross-section.

Meson	$\lvert\psi(0)\rvert^2 \pm \sigma_{\lvert\psi(0)\rvert^2}$	Relative error
J/ψ	0.041 ± 0.0042 GeV^3	10%
$\psi(2S)$	0.024 ± 0.0025 GeV^3	10%
$\Upsilon(1S)$	0.397 ± 0.015 GeV^3	4%
$\Upsilon(2S)$	0.192 ± 0.030 GeV^3	16%
$\Upsilon(3S)$	0.173 ± 0.032 GeV^3	18%

1.2.2 Parton Distribution Functions

Let us now analyze the uncertainties due to the parton distribution functions (pdf). As there are two gluons coming from the initial hadronic state, these can induce non-negligible uncertainties upon the cross-section (1.1).

There exist two ways through which the pdf's can introduce errors in the cross-section. First the value of $\alpha_S(Q^2)$ attached with the pdf and then the pdf's themselves for the hadronic cross-section.

Here are different plots obtained for a set of 12 pdf's (see the legend of Fig. 1.1) coded in PDFLIB [12] which illustrate this:

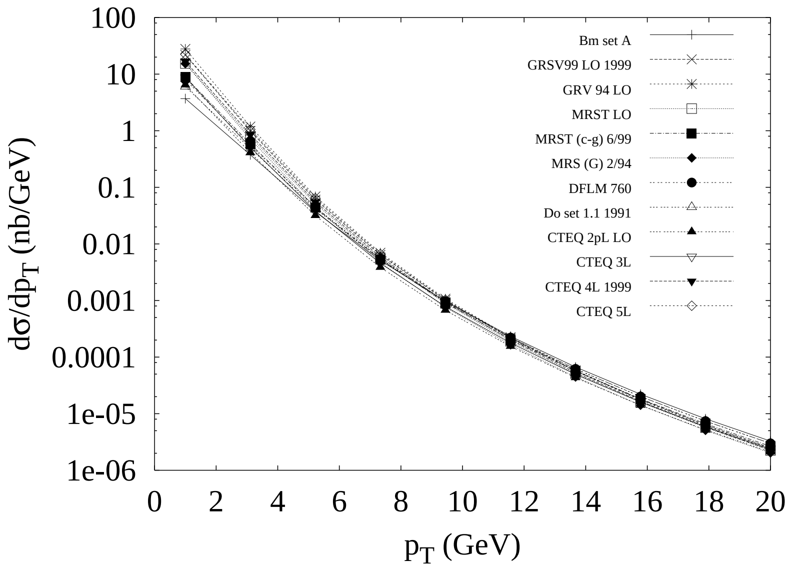

Figure 1.1: Variation of the cross-sections obtained with various pdf's [12] due to the pdf's only.

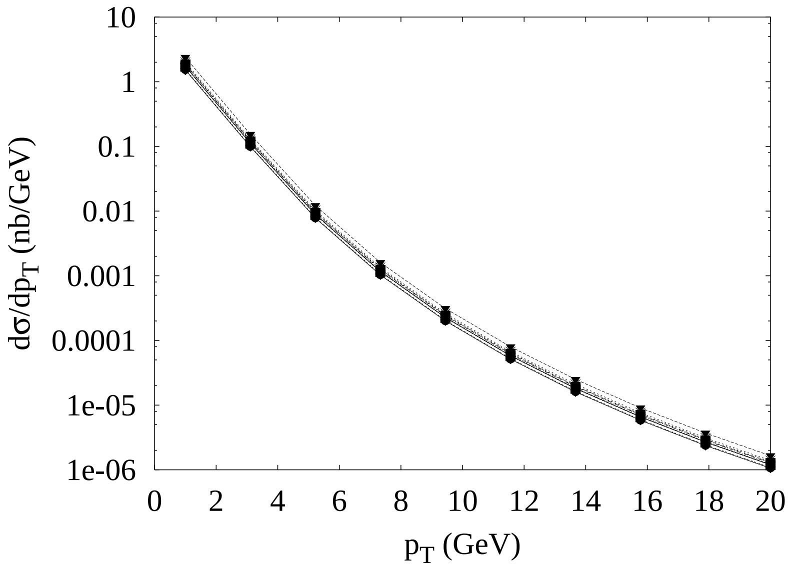

Figure 1.2: Variation of the cross-sections obtained with various pdf's [12] due to α_S only.

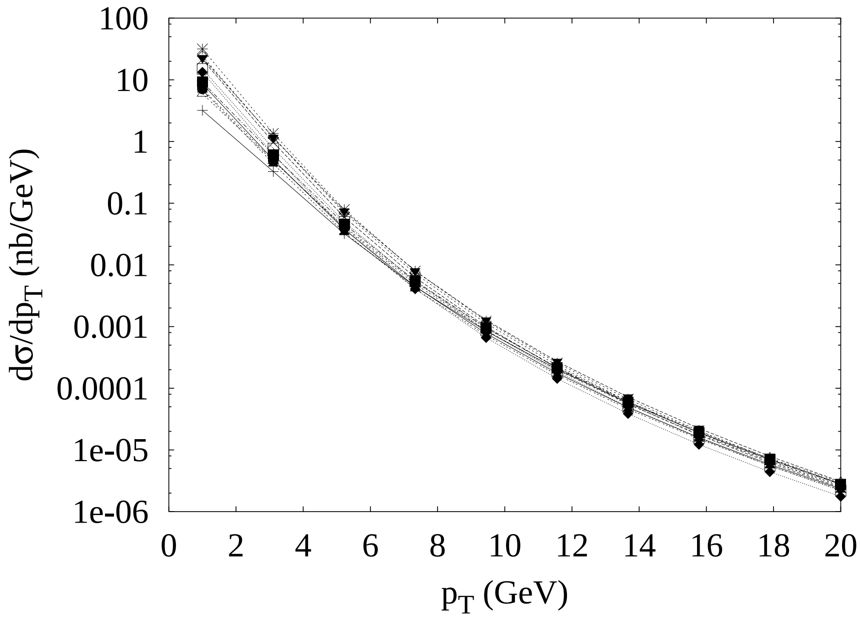

Figure 1.3: Variation of the cross-sections obtained with various pdf's [12] due to α_S and the pdf's.

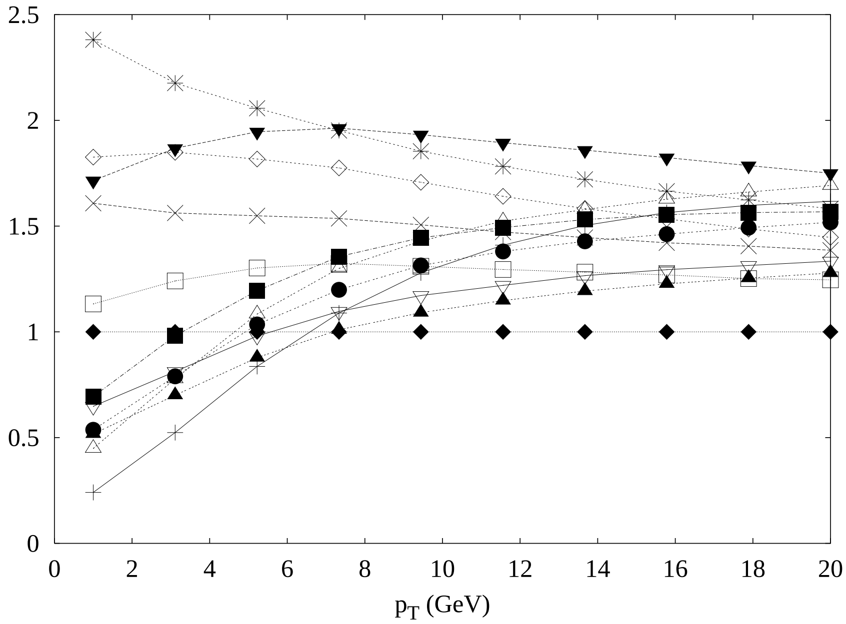

Figure 1.4: Ratio of the cross-sections obtained with various pdf's [12] to the cross-section obtained with MRS(G) 2-94.

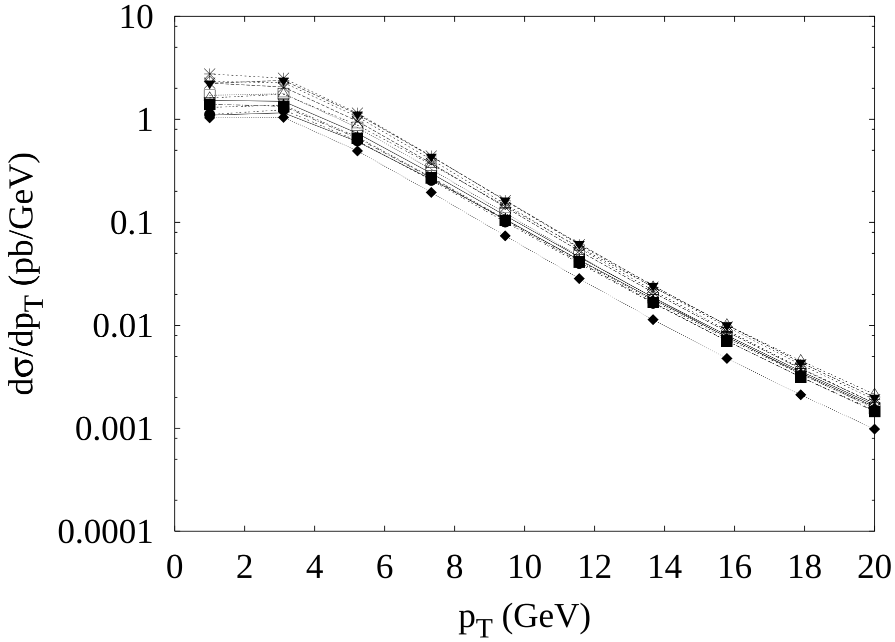

Figure 1.5: Variation of the cross-sections obtained with various pdf's [12] for $\Upsilon(3S)$.

We thus found that the overall factor resulting from these 3 sources of uncertainties is about 2-3 and roughly constant for different values of p_T.

Chapter 2

Interlude: Sudakov Variables

In this short chapter, we will introduce some useful variables, the so-called Sudakov variables of a given four-vectors. In a few words, these are the projections of this four-vectors upon two or three four-vectors, plus one or two transverse parts.

We shall derive the jacobian of the change of variable in two cases, one with two parameters and another with three parameters. Depending on the kinematics, one decomposition could be more fruitful than the other and further changes of variable (*e.g.* taking the square of the decomposed variable as a new one) could provide even further simplifications.

2.1 Decomposition upon Two Four-Vectors

I shall consider here the case of two initial particles with **non vanishing masses**. Let thus p and q be the four-momenta of these particles and define the scalars ξ and η and the transverse vector ℓ_T such as

$$\ell = -\xi p + \eta q + \ell_T, \tag{2.1}$$

with

$$\begin{aligned} \ell_T \cdot p =& 0, \\ \ell_T \cdot q =& 0. \end{aligned} \tag{2.2}$$

In the center of momentum (CM) frame, it is possible to choose the z-axis such that

$$q = \begin{pmatrix} q_0 \\ 0 \\ 0 \\ q_z \end{pmatrix} \text{ and } p = \begin{pmatrix} p_0 \\ 0 \\ 0 \\ -q_z \end{pmatrix}. \tag{2.3}$$

Hence we get the jacobian of the change variables

$$\{\ell_0, \underbrace{\ell_x, \ell_y}_{\vec{\ell}_T}, \ell_z\} \to \{\xi, \eta, \vec{\ell}_T\} \tag{2.4}$$

by calculating as usual the absolute value of the determinant of the following jacobian matrix

$$\begin{pmatrix} \frac{\partial \ell_0}{\partial \xi} & \frac{\partial \ell_0}{\partial \eta} \\ \frac{\partial \ell_z}{\partial \xi} & \frac{\partial \ell_z}{\partial \eta} \end{pmatrix} = \begin{pmatrix} p_0 & q_0 \\ -q_z & q_z \end{pmatrix}, \tag{2.5}$$

that is $|q_z|\sqrt{s}$.

For the process $\gamma^\star \pi^0 \to X$ and in accordance with the notations of Part II[1], let

$$\begin{aligned} q^2 &= -Q^2 = -2x\nu, \\ p^2 &= m_\pi^2, \end{aligned} \tag{2.6}$$

and

$$\begin{aligned} q_z &= |\vec{q}| = \sqrt{E^2 + Q^2}, \\ E &= \frac{s - m_\pi^2 - Q^2}{2\sqrt{s}}, \end{aligned} \tag{2.7}$$

with $q_0 = E$.

The jacobian is then given by

$$d^4\ell = \sqrt{\nu^2 + 2\nu m_\pi^2 x}\ d\xi\ d\eta\ \underbrace{\frac{d\ell_T^2}{2} d\phi}_{d\vec{\ell}_T}. \tag{2.8}$$

We can now calculate the scalar products involving the different momenta of the process

$$\begin{aligned} \ell.p =& \eta\nu - \xi m_\pi^2, \\ \ell.q =& -\nu(\xi + 2x\eta), \\ \ell.\ell =& \xi^2 m_\pi^2 - \eta^2 Q^2 + \ell_T^2 - \xi\eta\nu. \end{aligned} \tag{2.9}$$

2.2 Decomposition upon Three Four-Vectors

Let us take the example of the production of $^3S_1$ quarkonium state by the fusion of two gluons and the emission of a third one. This process is represented by the following Feynman diagram:

[1]The photon momentum is thus q with $q^2 = -Q^2$ and the pion momentum is p with $p^2 = m_\pi^2$.

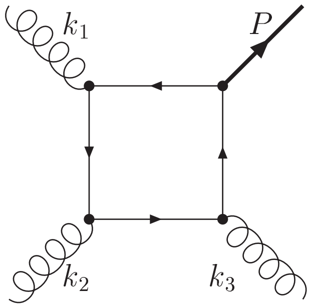

Figure 2.1: $g + g \to^3 S_1 + g$

Assuming that ℓ is a four-vector (in our example the four-momentum in the loop), we can decompose it as follows:

$$\ell = xk_1 + yk_2 + zk_3 + \kappa, \tag{2.10}$$

where x, y, z are scalars and κ is a one-dimensional vector[2]. Moreover κ is orthogonal to the k_i's – we could have added a subscript to κ to emphasize this transverse property–. In other words, we have

$$\begin{aligned} k_1.\kappa =&0, \\ k_2.\kappa =&0, \\ k_3.\kappa =&0. \end{aligned} \tag{2.11}$$

x, y, z and κ are called the Sudakov variables.

This change of variables gives

$$d^4\ell = \frac{1}{2}\sqrt{stu}\; dx\; dy\; dz\; d\kappa, \tag{2.12}$$

with s, t and u the Mandelstam variables. The jacobian $\frac{1}{2}\sqrt{stu}$ is evaluated in the same way as in section 2.1.

We can also express ℓ^2 as an independent variable by dropping another one. For instance let us choose x.

We have

$$\ell^2 = xys - xzu - yzt - \kappa^2, \tag{2.13}$$

where $s = (k_1 + k_2)^2 = 2k_1.k_2$, $t = (k_2 + k_3)^2 = -2k_2.k_3$, $u = (k_1 + k_3)^2 = -2k_1.k_3$ for massless particles.

[2]We mean that $\ell = xk_1 + yk_2 + zk_3 + \kappa$ is in fact equivalent to $\ell = xk_1 + yk_2 + zk_3 + \ell_T$ with the four-momentum ℓ_T defined by $(0, 0, 0, \kappa)$ if we had chosen the z-axis to be orthogonal to the plane of the collision.

We simply take

$$x = \frac{yzt + \ell^2 + \kappa^2}{ys - zu}. \tag{2.14}$$

The jacobian gives:

$$d^4\ell = \left| \frac{\sqrt{stu}}{2(ys - zu)} \right| \; d\ell^2 \; dy \; dz \; d\kappa. \tag{2.15}$$

We can now calculate the scalar products involving the different momenta of the process:

$$\begin{aligned} \ell.k_1 =& \frac{ys - zu}{2}, \\ \ell.k_2 =& \frac{xs - zt}{2}, \\ \ell.k_3 =& -\frac{xu + yt}{2}, \\ \ell.p =& \frac{x(s+u) + y(s+t) - z(t+u)}{2}. \end{aligned} \tag{2.16}$$

Chapter 3

Non Static Extension

3.1 Phase Space and Integration in the Meson Rest Frame with $\ell.p = 0$

The nonrelativistic description of the heavy meson assumes that the relative energy in the meson rest frame between the two constituent quarks is so small than it can be neglected.

Thus we have

$$\ell \simeq \begin{pmatrix} 0 \\ \ell_x \\ \ell_y \\ \ell_z \end{pmatrix}. \tag{3.1}$$

In this frame we have $\ell.p = 0$ and therefore in every other frame by invariance.

3.1.1 Sudakov Variables

We shall now impose the condition $\ell.p = 0$ using the fourth relation in Eq. (2.16). We immediately get the following equation

$$x(s+u) + y(s+t) - z(t+u) = 0. \tag{3.2}$$

This removes another degree of freedom by fixing the value of either y or z as x is already fixed ($x = x(\ell^2, y, z, \kappa)$). If we choose to eliminate y, we have to solve a second-order equation. Equating the value of x in Eq. (2.14) with the one given by Eq. (3.2), we get

$$y^2 s(s+t) - 2yzus + \left[(\kappa^2 + \ell^2)(s+u) + z^2 u(u+t)\right] = 0. \tag{3.3}$$

Note here the main advantage of the Sudakov variables, which make Eq. (3.3) covariant. To solve the latter, we have to respect the following condition[1], stating

[1] If $(u - M^2)(t - M^2) < 0$, then the sign of inequality in Eq. (3.4) must be inverted.

that the discrimant of this second-order equation is greater than zero,

$$\kappa^2 < -\ell^2 - \frac{z^2 M^2 ut}{(s+t)(s+u)}. \tag{3.4}$$

Solving Eq. (3.3) for y, we get the following two solutions,

$$\begin{aligned} y_1 &= \frac{zus + \sqrt{s}\sqrt{-\left[(s+t)(s+u)(\ell^2+\kappa^2) + M^2utz^2)\right]}}{s(s+t)}, \\ y_2 &= \frac{zus - \sqrt{s}\sqrt{-\left[(s+t)(s+u)(\ell^2+\kappa^2) + M^2utz^2)\right]}}{s(s+t)}. \end{aligned} \tag{3.5}$$

Thus to choose $y = y_1$ or $y = y_2$ is equivalent to the choice of ℓ such that $\ell.p = 0$.

We can go further in the analysis of the constraint on the phase space coming from approximation (3.1). Solving Eq. (3.2) for x and equating the result with the value of x given by Eq. (2.14), we obtain a new condition on ℓ^2, that is

$$\ell^2 = \frac{y(s+t) - z(t+u)}{(s+u)}(ys - zu) - uzt - \kappa^2. \tag{3.6}$$

This enables us to express the condition $\ell^2 < 0$ coming from the constraint $\ell_0 = 0$ and the signature of the Minkowsly space. By means of Eq. (3.6), we can indeed express the latter condition in term of κ^2 as

$$\kappa^2 > \frac{y(s+t) - z(t+u)}{(s+u)}(ys - zu) - uzt. \tag{3.7}$$

We thus have an upper and a lower bound – Eqs. (3.4) and (3.7)– on κ if the external kinematics is fixed as well as ℓ^2 and z.

We can interpret these conditions in the following way. The fact that we fix the value of ℓ^2 imposes that the square of the sum $xk_1 + yk_2 + zk_3 + \kappa$ lies on a four-sphere of radius ℓ^2. So it is straightforward to state that κ^2 (in absolute value) must be lower than ℓ^2 and even that the constraint is stronger depending on the value of the other vectors contributing to ℓ^2, these are k_1, k_2 and k_3. Their *contributions* to ℓ^2 depend however on the last free Sudakov variables, that is z. In terms of the Mandelstam variables, this contribution is

$$\frac{z^2 M^2 ut}{(s+t)(s+u)}. \tag{3.8}$$

If now κ is actually lower than its upper bound, we have enough phase space to have a contribution due to y. The equation (3.5) even tell us that y can have two values in order to make the square of the sum $xk_1 + yk_2 + zk_3 + \kappa$ lies on the fixed ℓ^2-radius sphere. This is illustrated in Fig. 3.1.

For $f(\ell)$ a function to be integrated over the hyperspace $\ell.p = 0$, we have:

$$\int d^4\ell \ \delta(\ell.p) f(\ell) = \int \left| \frac{\sqrt{stu}}{2} \times \frac{1}{(ys - zu)} \times \frac{2(ys - zu)^2}{(s+t)(ys-zu)^2 - (u+s)(s(\ell^2+\kappa^2) + utz^2)} \right| \times \\ \times \left(\delta\left(y - \frac{zus + \Delta}{s(s+t)} \right) f(\ell) + \delta\left(y - \frac{zus - \Delta}{s(s+t)} \right) f(\ell) \right) d\ell^2 \ dy \ dz \ d\kappa, \tag{3.9}$$

with $\Delta = \sqrt{s}\sqrt{-[(s+t)(s+u)(\ell^2+\kappa^2) + M^2utz^2)]}$. .

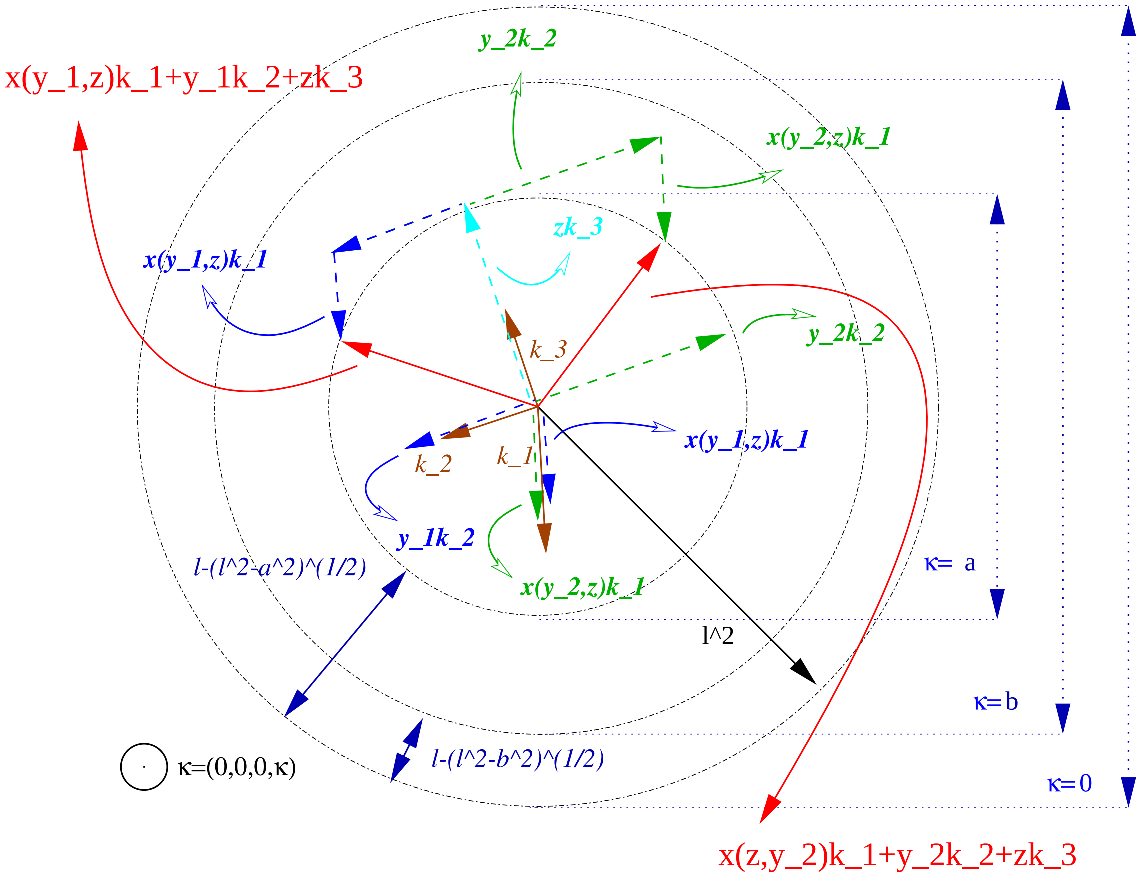

Figure 3.1: Illustration of the different quantities defined above: choosing $\kappa = a$, hence we have $xk_1+yk_2+zk_3$ (in red) on the first circle. For a given value of z– which is not constrained–, zk_3 (in cyan) is fixed and there exists two linear combinations, $x(y_1,z)k_1+y_1k_2$ (in blue) and $x(y_2,z)k_1+y_2k_2$ (in green) such as to reach this circle.

3.1.2 Cartesian Variables

Supposing that we want to integrate in cartesian coordinates a function of ℓ in the laboratory frame where the collision $p\bar{p}$ takes place producing two gluons such as drawn in Fig. 2.1, we have to calculate the value of ℓ_0 in this frame which is fixed by $\ell.p = 0$.

Writing explicitely the values of the four-components of p with y the rapidity of the meson in the new frame, that reads

$$p = (\sqrt{M^2 + p_x^2 + p_y^2}\cosh y, p_x, p_y, \sqrt{M^2 + p_x^2 + p_y^2}\sinh y), \tag{3.10}$$

we can easily express the condition $\ell.p = 0$.

Choosing the axes as to have $p_y = 0$, Eq. (3.10) becomes

$$p = (\sqrt{M^2 + p_T^2}\cosh y, p_T, 0, \sqrt{M^2 + p_T^2}\sinh y). \tag{3.11}$$

So we have

$$0 = \ell.p = \ell_0\sqrt{M^2 + p_T^2}\cosh y - \ell_x p_T - \ell_z\sqrt{M^2 + p_T^2}\sinh y. \tag{3.12}$$

Solving for ℓ_0, we obtain

$$\ell_0 = \tanh y \ell_z + \ell_x \frac{p_T}{\sqrt{M^2 + p_T^2}\cosh y}. \tag{3.13}$$

We finally have

$$\begin{aligned} &\int d^4\ell\ \delta_{\mathrm{MRF}}(\ell_0) f(\ell) = M \int d^4\ell\ \delta(\ell.p) f(\ell) \\ &= M \int \frac{d^4\ell}{\sqrt{M^2 + p_T^2}\cosh y_{\mathrm{Lab}}} \delta_{\mathrm{Lab}}(\ell_0 - \tanh y_{\mathrm{Lab}}\ \ell_z - \ell_x \frac{p_T}{\sqrt{M^2 + p_T^2}\cosh y_{\mathrm{Lab}}}) f(\ell). \end{aligned} \tag{3.14}$$

Note however that the last formula applies also in the MRF frame. In this frame, y as well as p_T are indeed zero and hence the last formula reduce to the first one.

3.1.3 Test of Equivalence of the Two Methods

In order to insure that the two ways of implementig the condition $\ell.p = 0$ were correctly coded, we used test-functions we integrated for different values of the transverse momentum p_T. As the calculation of the cross-section implies twice the loop integration[2], we have choosen the following test functions:

$$1, \quad \ell \cdot \ell', \quad (\ell \cdot \ell)(\ell' \cdot \ell'), \quad (\ell \cdot \ell)^2 (\ell' \cdot \ell')^2.$$

[2] The momentum in the loop of the conjugate process is not supposed to be same as the one in the first loop. Therefore, we have to perform two integrations for two different *loop-momenta* ℓ and ℓ'.

We have thus performed the following integrations for different values of p_T (from 2.0 GeV to 15 GeV):

$$\begin{aligned}
&\int d\ell d\ell' \delta(\ell \cdot p)\delta(\ell \cdot p') \\
&\int d\ell d\ell' (\ell \cdot \ell')\delta(\ell \cdot p)\delta(\ell \cdot p') \\
&\int d\ell d\ell' (\ell \cdot \ell)(\ell' \cdot \ell')\delta(\ell \cdot p)\delta(\ell \cdot p') \\
&\int d\ell d\ell' (\ell \cdot \ell)^2(\ell' \cdot \ell')^2\delta(\ell \cdot p)\delta(\ell \cdot p')
\end{aligned} \tag{3.15}$$

Taking account of the numerical errors of 5-10%[3], we can conclude that the two methods agree relatively well.

Another way to illustrate this agreement between the two methods is to analyse the phase space resulting from the two conditions. We put below a plot of $k_1 \cdot \ell$ and $k_2 \cdot \ell$ as a function of ℓ^2 for a given value of the transverse momentum (see Fig 3.2). For the Sudakov variables, ℓ^2 is constrained to be less than 20 and for the cartesian one, less than 50. In both cases, we can see the good agreement between the two methods.

If we remember that the Sudakov variable y (fixed by $\ell.p{=}0$ (Eq. 3.5)) is a function of $\sqrt{\ell^2}$, we easily understand the shape of the distribution of $\ell.k_1 = \frac{ys-zu}{2}$.

3.2 Propagators Poles for $gg \to g^3S_1$ in Cartesian Coordinates.

In order to tackle the difficulties of pole integrations, it is useful to determine the region where they occur. If these regions contribute only for a small part of the total integral, we shall have the possibilities to leave (or treat) them separately.

As already mentioned, the dominant sub-process for $gg \to g^3S_1$ is represented by the diagram 2.1 to which we must add the crossed diagrams. This gives us six diagrams. As the integration over the loop is performed with the four-elements $d^4\ell$, the integral of a given function $f(\ell)$ equals to that of $f(-\ell)$.

We shall first consider the case where ℓ_x, ℓ_y and $\ell_z > 0$ and limit ourself to $y = 0$ value for the $^3S_1$ bound state.

---

[3] This seemingly large numerical error comes from the fact that we had to perfom a 9-dimensional integral (4×2 for the loop integrals and 1 for the integration over the momentum fraction of the gluons). Indeed, we evaluated these integrals as a test of the overall code (not only as test of the loop integrals.)

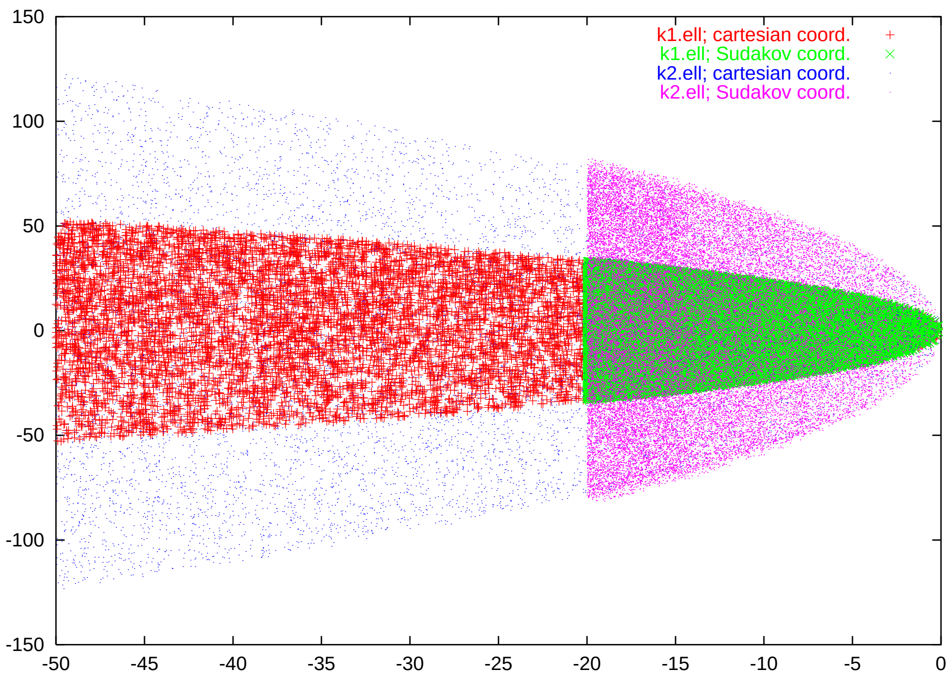

Figure 3.2: Comparison of the phase space: $k_1 \cdot \ell$ and $k_2 \cdot \ell$ as a function of ℓ^2.

3.2.1 Poles of $\frac{1}{(\frac{P}{2}-k_{1,2}-\ell)^2-m^2}$.

We simply search for the roots of

$$\begin{aligned} 0 = (\frac{P}{2} - k_1 - \ell)^2 - m^2 =& \frac{M^2}{4} - p.k_1 + 2k_1.\ell - m^2 + \ell^2 \\ =& \frac{1}{4}\left(M^2 - 4m^2 + 2t - 2M^2 + 8k_1.\ell + 4\ell^2\right). \end{aligned} \tag{3.16}$$

From the definition of $t \equiv (k_2 - k_3)^2 = (k_1 - p)^2 (\Rightarrow t = -2k_1.p + M^2)$ and u, we get

$$\begin{aligned} p.k_1 &= \frac{M^2 - t}{2}, \\ p.k_2 &= \frac{M^2 - u}{2}. \end{aligned} \tag{3.17}$$

Now we simply have to work out $k_1.\ell$, $k_1.\ell$ and ℓ^2. In the CM frame of the collision of the protons, with the two gluons as partons, we have

$$k_{1,2} = \begin{pmatrix} x_{1,2}\frac{\sqrt{s}}{2} \\ 0 \\ 0 \\ \pm x_{1,2}\frac{\sqrt{s}}{2} \end{pmatrix}, \tag{3.18}$$

where $x_{1,2}$ are as usual the part of the proton momentum taken off by the gluons.

And with the result (3.13) for $y = 0$, we are able to calculate the scalar products $k_i.\ell$ and get

$$\begin{aligned}\ell.k_1 &= \frac{x_1\sqrt{s}}{2}\frac{\ell_x}{\sqrt{1+\frac{M^2}{p_T^2}}} - \frac{x_1\sqrt{s}}{2}\ell_z,\\ \ell.k_2 &= \frac{x_2\sqrt{s}}{2}\frac{\ell_x}{\sqrt{1+\frac{M^2}{p_T^2}}} - \frac{x_2\sqrt{s}}{2}\ell_z.\end{aligned} \tag{3.19}$$

Moreover, we have

$$\ell^2 = \ell_0^2 - \vec{\ell}^2 = \ell_x^2\left(\frac{1}{1+\frac{M^2}{p_T^2}} - 1\right) - \ell_y^2 - \ell_z^2 = \ell_x^2\left(\frac{-1}{1+\frac{p_T^2}{M^2}}\right) - \ell_y^2 - \ell_z^2. \tag{3.20}$$

Taking account of the condition $\delta(\hat{s}+\hat{t}+\hat{u}-M^2)$, it can be easily shown that x_2 is related to x_1 as follows

$$x_2 = \frac{x_1\sqrt{M^2+p_T^2}\sqrt{s}e^y - M^2}{sx_1 - \sqrt{M^2+p_T^2}e^{-y}}, \tag{3.21}$$

with the Mandelstam variables for the partonic interaction[4] ,

$$\begin{aligned}\hat{s} =& sx_1x_2,\\ \hat{t} =& -x_1\sqrt{s}\sqrt{M^2+p_T^2}e^y + M^2,\\ \hat{u} =& -x_2\sqrt{s}\sqrt{M^2+p_T^2}e^{-y} + M^2.\end{aligned} \tag{3.22}$$

The condition of energy conservation give us the minimal value of x_1 and x_2 which are strictly equal at this limit, *i.e.*

$$x_{1,2,\mathrm{min}} = \frac{\sqrt{M^2+p_T^2}p_T + M^2 + p_T^2}{\sqrt{s}\sqrt{M^2+p_T^2}}. \tag{3.23}$$

Hence (still keeping $y = 0$), the annulation of the propagator occurs when the following equation is satisfied:

$$0 = M^2 - 4m^2 - 4\frac{x_1\sqrt{s}}{2}\sqrt{M^2+p_T^2} + \frac{8\frac{x_1\sqrt{s}}{2}\ell_x}{\sqrt{1+\frac{M^2}{p_T^2}}} - 8\frac{x_1\sqrt{s}}{2}\ell_z + 4\ell^2, \tag{3.24}$$

with x_1, ℓ_x, ℓ_y and ℓ_z the only quantities that may still vary.

[4]For instance, we have $t = M^2 - 2k_1.p = M^2 - 2(x_1\frac{\sqrt{s}}{2})(\sqrt{M^2+p_T^2}\cosh y) + 2(x_1\frac{\sqrt{s}}{2})(\sqrt{M^2+p_T^2}\sinh y) = M^2 - x_1\sqrt{s}\sqrt{M^2+p_T^2}e^y$. Therefore the sign of y in the expression depends on the choice of the direction of the parton 1.

3.3 Preliminary Results for the Calculation of the Principal Parts.

We present briefly in this section the results obtained for the calculation – within the code used for the obtention of the cross-section in the classical CSM– of the principal parts of test functions, *e.g.* $\frac{1}{k_1.\ell}$, $\frac{1}{(k_1.\ell)(k_2.\ell)}$, etc ...

The position of the poles is determined numerically and is used by the folding procedure in the following way: Let x_0 be the pole of the function $g(x)$ to be integrated from a to b. Instead of calculating

$$\int_a^b g(x)dx, \tag{3.25}$$

we simply divide the integration in three parts as follows

$$\int_a^b g(x)dx = \int_a^{x_0-\varepsilon} g(x)dx + \int_{x_0-\varepsilon}^{x_0+\varepsilon} g(x)dx + \int_{x_0+\varepsilon}^b g(x)dx. \tag{3.26}$$

Hence, we calculate $\int_a^{x_0-\varepsilon} g(x)dx$ and $\int_{x_0+\varepsilon}^b g(x)dx$ as usual, but $\int_{x_0-\varepsilon}^{x_0+\varepsilon} g(x)dx$ is replaced by

$$2\int_{x_0-\varepsilon}^{x_0} (g(x) + g(x + 2(x_0 - x)))dx. \tag{3.27}$$

We have indeed folded the integrand in order to get a suppression of the pole.

An important point to keep in mind, is that ε must be small enough such that $x_0 \pm \varepsilon$ stay within the interval $[a, b]$. In fact, this can become quite tricky as the boundary values of our integrals are not constant. They may be functions of other integration variables. We thus added a test to check this and chose a value of ε compatible with the boundary values for all the external values used.

Moreover, if there are several poles, we proceed to a similar decomposition for each pole (we only consider here the case when the different poles do not cross each other. In this case, the principal part would be infinite anyway !). Another problem which possibly occurs is when the poles are near each other. We must then be cautious that ε be small enough to avoid an overlapping of the folding regions.

Here are two precise examples of what we obtained, still within our main program used to obtain the cross-sections of the classical implementation of the CSM:

Integrand: $\frac{1}{(\ell_z+1)(\ell_z-2)}$

In order to get rid of the constant coming from the flux factor, the multiplicative constants and the integrals over the other variables than ℓ_z, we performed the integration with 1 as integrand. For definiteness, we got 14400. We chose to integrate the ℓ_i's between -10 and 10. Therefore the integral over ℓ_z with 1 as integrand gave 20. Hence, $\frac{14400}{20} = 720$ was the contribution to be rejected.

Now, putting $\frac{1}{(\ell_z+1)(\ell_z-2)}$ as integrand, we obtained -145 which, divided by 720, gives

$$\int_{-10}^{10} d\ell_z \frac{1}{(\ell_z+1)(\ell_z-2)} = -0.202. \tag{3.28}$$

This agrees with the results obtained with symbolic manipulation programs such as MATHEMATICA or DERIVE (with a TI-92).

Integrand: $\frac{1}{(\ell_z+1)(\frac{-1}{|\ell_x|+1}+\ell_z-2)}$

To get an idea of the efficiency of this method with a pole which is a function of another variable, we added $\frac{-1}{|\ell_x|+1}$ in the denominator. As above, we used the value of the full phase space contribution: 14400 and the contribution from ℓ_x (from -5 to 5) and ℓ_z (from -10 to 10): 200. The "ℓ_x-ℓ_z" contribution was then 72.

With this integrand, we got -146, which divided by 72, gives -2.03 as obtained with MATHEMATICA.

We can thus conclude that this method is fully efficient as long as the positions of the different poles are not too close.

Chapter 4

Towards a Relativistic Wave Function.

As previously announced, I will now explain briefly how can one extend the Color Singlet Model further than by introducing a finite relative three-momentum through the contribution of a nonrelativistic wave function.

It is in fact commonly believed that in decay process the contributions coming from the relativistic part of wave the function are not significant. Therefore the first corrections to the CSM that one considers are higher order Fock state contributions (as in the Color Octet Model which includes $|q\bar{q}g\rangle$ states in the description of the mesons).

On the other hand, in production processes, especially in the cases where no scale dominates, the physics is not as clear. It could indeed happen that corrections in $\vec{\ell}$ are not significant on the contrary of the relative energy corrections[1].

To answer this question is the aim of this further extension to the CSM. And this chapter opens the path to this by shedding light on the possible theoretical tools that would be used in this context.

4.1 Relativistic Wave Function and Normalisation

Let assume that the $Q\bar{Q}$ system (*i.e.* the quarkonium) can be described by a Green's function $G(W, p, q)$ which has poles at bound state energies:

$$M_n(Q\bar{Q}) = 2W_n, \tag{4.1}$$

so we can write

$$G(W, p, q) \simeq \frac{\psi(W_n, p)\bar{\psi}(W_n, q)}{W - W_n + i\varepsilon}\ , \ W \simeq W_n. \tag{4.2}$$

[1]Unlike the "$\vec{\ell}$-correction" which cannot –strictly speaking– be called relativistic corrections, these relative energy corrections are really relativistic, as well as contributions from other Fock states than the dominant $|q\bar{q}\rangle$ in mesons production.

$\psi(W_n, p)$ is the Bethe-Salpeter wave function.

For simplicity, we consider the quarkonium in its center of momentum frame which gives:

$$P_n^\mu = (2W_n, \vec{0}), \tag{4.3}$$

with p and q the relative four-momenta of the initial and of the final states.

The Green's function satisfies the Bethe-Salpeter equation [13]:

$$G(W,p,q) = (2\pi)^4\delta^4(p-q)G_F(W,p) + G_F(W,p)\int \frac{d^4q'}{(2\pi)^4}K(W,p,q')G(W,q',q), \tag{4.4}$$

with the free two-particle propagator $G_F(W,p) \equiv iS^{(1)}(\frac{1}{2}P+p)iS^{(2)}(-\frac{1}{2}P+p)$.

Equation (4.4) is a means to resum contributions from Feynman diagrams which arise in perturbation theory. It does not imply, of course, that $G(W,p,q)$ has poles corresponding to free quark-antiquark states, as in the case of $G_F(W,p)$. The mass parameters in $G_F(W,p)$ represent effective constituent quark masses.

On the other hand, the Bethe-Salpeter equation for the wave function is

$$\psi(W_n,p) = G_F(W_n,p)\int \frac{d^4q}{(2\pi)^4}K(W_n,p,q)\psi(W_n,q). \tag{4.5}$$

From Eqs. (4.2) and (4.4), we can derive the normalisation condition which can be written

$$\int \frac{d^4p}{(2\pi)^4}\frac{d^4q}{(2\pi)^4}\bar{\psi}(W_n,p)\frac{\partial}{\partial W_n}\left[G_F^{-1}(W_n,p)(2\pi)^4\delta^4(p-q) - K(W_n,p,q)\right]\psi(W_n,q) = 1. \tag{4.6}$$

Even if $\psi(W_n,p)$ is a non-perturbative quantity, in general, it will be necessary to turn to perturbation theory (through the contribution of K) to calculate $\psi(W_n,p)$. Writing the kernel as

$$K \equiv K_0 + \delta K, \tag{4.7}$$

one gets the following expression for the wave function:

$$\begin{aligned}\psi(W_n,p) =& \psi_0(W_n,p)\left(1 + \int \frac{d^4q}{(2\pi)^4}\frac{d^4q'}{(2\pi)^4}\bar{\psi}_0(W_n,q)(\frac{\partial}{\partial W_n}\delta K(W_n,q,q'))\psi_0(W_n,q')\right)\\ &+ \int \frac{d^4q}{(2\pi)^4}\frac{d^4q'}{(2\pi)^4}\hat{G}_0(W_n,p,q)\delta K(W_n,q,q')\psi_0(W_n,q') + \mathcal{O}(\delta K^2),\end{aligned} \tag{4.8}$$

where one has defined the $\hat{G}(W_n,p,q)$ as follows,

$$\hat{G}(W_n,p,q) = G_0(W_n,p,q) - \frac{\psi(W_n,p)\bar{\psi}(W_n,q)}{W - W_n + i\varepsilon}. \tag{4.9}$$

ψ_0 and G_0 are respectively the wave function and the Green's function corresponding to K_0. We also point out the replacement $W_n^0 \to W_n$ in Eqs. (4.8) and (4.9).

The success of potential models for quarkonia suggests that a natural choice for K_0 is an instantaneous kernel of the general form

$$K_0(W,p,q) = \sum_i V^i(W,(\vec{p}-\vec{q})^2,\vec{p}^{\,2},\vec{q}^{\,2})\Gamma_i^{(1)}\Gamma_i^{(2)}, \tag{4.10}$$

where $\Gamma_i^{(1)}(\Gamma_i^{(2)})$ are Dirac matrices acting on the particle (antiparticle) spinor indices.

Concerning the quark propagator, it reads

$$S(p) = \frac{\Lambda_+(\vec{p})\gamma_0}{p_0 - E_p + i\varepsilon} + \frac{\Lambda_-(\vec{p})\gamma_0}{p_0 + E_p - i\varepsilon}, \tag{4.11}$$

where

$$\begin{aligned} \Lambda_\pm(\vec{p}) &= \frac{1}{2E_p}\left[E_p \pm H(\vec{p})\right], \\ H(\vec{p}) = \gamma_0(\vec{\gamma}\cdot\vec{p}+m) &\text{ and } E_p = \sqrt{m^2+\vec{p}^{\,2}}. \end{aligned} \tag{4.12}$$

In the nonrelativistic limit, one obtains:

$$S^{NR}(p) = \frac{\left(\frac{1+\gamma_0}{2}\right)}{p_0 - m - \left(\frac{\vec{p}^{\,2}}{2m}\right) + i\varepsilon} - \frac{\left(\frac{1-\gamma_0}{2}\right)}{p_0 + m + \left(\frac{\vec{p}^{\,2}}{2m}\right) - i\varepsilon}. \tag{4.13}$$

Correspondingly, the Bethe-Salpeter equation for the wave function becomes

$$\begin{aligned} \psi_0^{NR}(W_n,p) = &\frac{1}{\left[p_0 + W_n - m - \left(\frac{\vec{p}^{\,2}}{2m}\right) + i\varepsilon\right]\left[p_0 - W_n + m + \left(\frac{\vec{p}^{\,2}}{2m}\right) - i\varepsilon\right]} \times \\ \times \int \frac{d^4q}{(2\pi)^4} &\sum_i V^i_{NR}(W,(\vec{p}-\vec{q})^2,\vec{p}^{\,2},\vec{q}^{\,2}) \left(\frac{1+\gamma_0}{2}\right)^{(1)} \Gamma_i^{(1)}\psi_0^{NR}(W_n,q)\Gamma_i^{(2)}\left(\frac{1-\gamma_0}{2}\right)^{(2)} \end{aligned} \tag{4.14}$$

as in the nonrelativistic limit only the small (large) components of the particle (antiparticle) survive.

The latter equation implies that the **scalar** wave function $\varphi_n(\vec{p})$ defined by

$$\int \frac{dp_0}{2\pi}\psi_0^{NR}(W_n,p) \equiv \varphi_n(\vec{p})\chi_n, \tag{4.15}$$

with χ_n containing Dirac matrices, obeys the Schrödinger equation

$$\left(2m + \left(\frac{\vec{p}^{\,2}}{2m}\right) - 2W_n\right)\varphi_n(\vec{p}) + \int \frac{d^3p}{2\pi}V(|\vec{p}-\vec{q}|)\varphi_n(\vec{p}) = 0, \tag{4.16}$$

if the nonrelativistic limit of the kernel satisfies the condition:

$$\sum_i V^i_{NR}(W,(\vec{p}-\vec{q})^2,\vec{p}^2,\vec{q}^2)\left(\frac{1+\gamma_0}{2}\Gamma_i\frac{1+\gamma_0}{2}\right)^{(1)}\left(\frac{1-\gamma_0}{2}\Gamma_i\frac{1-\gamma_0}{2}\right)^{(2)} \\ = V(|\vec{p}-\vec{q}|)\left(\frac{1+\gamma_0}{2}\right)^{(1)}\left(\frac{1-\gamma_0}{2}\right)^{(2)}. \tag{4.17}$$

We thus see that integrating out the relative-energy dependence of the Bethe-Salpeter equation leads to a nonrelativistic wave function satisfying a Schrödinger equation. The condition on the nonrelativistic limit of the kernel is obviously full-filled by the frequently employed linear combination of vector and scalar exchange (see [14] and references therein).

For a general combination of singlet and triplet states, the spinor part χ in Eq. (4.15) is conveniently written as

$$\chi = \frac{1}{\sqrt{2}}\frac{1+\gamma_0}{2}(a\gamma_5 + b\not{\varepsilon}),\ \ a^2+b^2=1, \tag{4.18}$$

where $\varepsilon^\mu = (0,\vec{\varepsilon})$ represents the spin polarisation in the CM system.

The nonrelativistic Bethe-Salpeter wave function $\psi_0^{NR}(W_n,p)$ is then

$$\psi_0^{NR}(W_n,p) = \frac{2W_n - 2m - \frac{\vec{p}^2}{2m}}{\left[p_0 + W_n - m - \left(\frac{\vec{p}^2}{2m}\right) + i\varepsilon\right]\left[p_0 - W_n + m + \left(\frac{\vec{p}^2}{2m}\right) - i\varepsilon\right]}\varphi_n(\vec{p})\chi_n, \tag{4.19}$$

and the normalisation condition of Eq. (4.6) reduces to

$$\int \frac{d^3p}{(2\pi)^3}\varphi_n^\star(\vec{p})\varphi_n(\vec{p}) = 1. \tag{4.20}$$

4.2 Application to the Leptonic Width

Before tackling the production processes, we expose here the simple case of the leptonic width. It is indeed sufficient to simply consider the decay in a virtual photon omitting the part of the process where the leptons appear.

In order to obtain this leptonic width one has thus to calculate the amplitude

$$\Gamma_{n\mu} = -ie_Q\int\frac{d^4p}{(2\pi)^4}\mathrm{Tr}[\gamma_\mu\psi(W_n,p)]. \tag{4.21}$$

This corresponds to the Feynman diagram of Fig. 4.1.

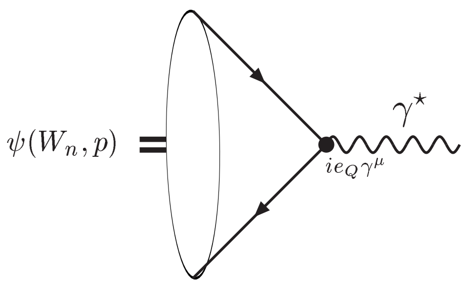

Figure 4.1: Feynman diagram contributing to the leptonic width of quarkonium.

This amplitude is given, in terms of δK (cf. Eqs. (4.7) and (4.8)), by

$$\begin{aligned}\Gamma_{n\mu} &= -ie_Q \int \frac{d^4p}{(2\pi)^4} \mathrm{Tr}[\gamma_\mu \psi_0(W_n,p)] \times \\ &\quad \times \left(1 + \int \frac{d^4q}{(2\pi)^4} \frac{d^4q'}{(2\pi)^4} \bar{\psi}_0(W_n,q)(\frac{\partial}{\partial W_n}\delta K(W_n,q,q'))\psi_0(W_n,q')\right) \\ &\quad -ie_Q \int \frac{d^4p}{(2\pi)^4} \frac{d^4q}{(2\pi)^4} \frac{d^4q'}{(2\pi)^4} \mathrm{Tr}[\gamma_\mu \hat{G}_0(W_n,p,q)\delta K(W_n,q,q')\psi_0(W_n,q')] \\ &\quad -ie_Q \mathcal{O}(\delta K^2) \\ &\equiv -ie_Q \left(\Gamma^{(0)}_{n\mu} + \Gamma^{(1)}_{n\mu} + \dots\right).\end{aligned} \tag{4.22}$$

In the nonrelativistic limit, we immediately obtain $\Gamma^{(0)}_{n\mu}$,

$$\Gamma^{(0)\,NR}_{n\mu} = \int \frac{d^4p}{(2\pi)^4} \mathrm{Tr}[\gamma_\mu \psi_0(W_n,p)] = \sqrt{2}\varepsilon_\mu \phi_n(0). \tag{4.23}$$

Notice here the presence of $\phi_n(0)$, the wave function at the origin, as in Eqs. (1.2) and (1.1) for the decay and the production of ${}^3S_1$ states.

As mentionned, the first-order correction in δK is

$$\Gamma^{(1)}_{n\mu} = \int \frac{d^4p}{(2\pi)^4} \frac{d^4q}{(2\pi)^4} \frac{d^4q'}{(2\pi)^4} \mathrm{Tr}[\gamma_\mu \hat{G}_0(W_n,p,q)\delta K(W_n,q,q')\psi_0(W_n,q')], \tag{4.24}$$

neglecting the derivative term (See discussion in [14]).

Integrations in Eqs. (4.22) and (4.24) involve all momentum transfers $(q-q')^2$ which occur in the kernel $\delta K(W_n,q,q')$.

For small momentum transfers the wave function occuring in $\hat{G}_0(W_n,p,q)$ can be treated nonrelativistically. This gives overlap integrals, such as

$$\int \frac{d^4q}{(2\pi)^4} \frac{d^4q'}{(2\pi)^4} \bar{\psi}_0(W_n,q)\delta K(W_n,q,q'))\psi_0(W_n,q') \tag{4.25}$$

which vanish in this kinematical regime as, by definition, $\delta K \to 0$ in the nonrelativistic limit. Therefore small mometum transfers do not contribute to integrals in Eqs. (4.22) and (4.24).

For large momentum transfers $\hat{G}_0(W_n, p, q)$ cannot be treated nonrelativistically. But now one can neglect the binding corrections and calculate the contribution to the corresponding integrals in perturbation theory. Replacing $\hat{G}_0$ by G_F and using the Bethe-Salpeter for the substraction term involving δK_0, one obtains

$$\begin{aligned}\Gamma^{(1)}_{n\mu} =& \int \frac{d^4p}{(2\pi)^4}\frac{d^4q}{(2\pi)^4}\mathrm{Tr}[\gamma_\mu G_F(W_n,p)K(W_n,p,q)\psi_0(W_n,q)] \\ &+ \int \frac{d^3p}{(2\pi)^3}\frac{d^3q}{(2\pi)^3}\frac{1}{2m + \left(\frac{\vec{p}^{\,2}}{2m}\right) - 2W_n}V(|\vec{p}-\vec{q}|)\varphi_n(\vec{q})\mathrm{Tr}[\gamma_\mu \chi_n]\end{aligned} \tag{4.26}$$

To leading order in α_S, $K(W_n, p, q)$ and $V(|\vec{p}-\vec{q}|)$ are given by

$$\begin{aligned}K(W_n,p,q) \sim& 4\pi\alpha_S C_2(R)\gamma^{(1)}_\mu\gamma^{(2)}_\nu D^{\mu\nu}(p-q,\lambda^2,\xi), \\ D^{\mu\nu}(k) =& \left(g_{\mu\nu} + \xi\frac{k_\mu k_\nu}{k^2+i\varepsilon}\right)\frac{(-i)}{k^2-\lambda^2+i\varepsilon}, \\ V(|\vec{p}-\vec{q}|) \sim& \frac{-4\pi\alpha_S C_2(R)}{|\vec{p}-\vec{q}|^2+\lambda^2}.\end{aligned} \tag{4.27}$$

Using the latter relations, the nonrelativistic, zero-binding limit of Eq. (4.26) becomes

$$\begin{aligned}\Gamma^{(1)}_{n\mu} = 4\pi\alpha_S C_2(R)\phi_n(0)\Bigg\{&-\int\frac{d^4p}{(2\pi)^4}\mathrm{Tr}\left[\gamma_\nu S(-\frac{1}{2}P_n+p)\gamma_\mu S(\frac{1}{2}P_n+p)\gamma_\lambda\chi_n\right]D^{\mu\nu}(p^2,\lambda^2,\xi) \\ &-\int\frac{d^3p}{(2\pi)^3}\frac{1}{\left(\frac{\vec{p}^{\,2}}{m}\right)(\vec{p}^{\,2}+\lambda^2)}\mathrm{Tr}[\gamma_\mu\chi_n]\Bigg\}.\end{aligned} \tag{4.28}$$

In terms of Feynman diagrams, this corresponds to diagrams of Fig. 4.2.

The integrals are readily evaluated, yielding

$$\Gamma^{(1)}_{n\mu} = \sqrt{2}\varepsilon_\mu\frac{\alpha_S}{2\pi}C_2(R)\phi_n(0)\left[\ln\frac{\Lambda}{m} - \frac{7}{4} + 2\pi\frac{m}{\lambda} + 2\ln\frac{\lambda}{m} + \xi(\ln\frac{\Lambda}{m} - \ln\frac{\lambda}{m}) - 2\pi\frac{m}{\lambda} - L^{(1)}\right], \tag{4.29}$$

where $L^{(1)}$ is the counterterm arising from self-mass insertions on the quark lines and the derivative term in Eq. (4.22),

$$L^{(1)} = \ln\frac{\Lambda}{m} + \frac{9}{4} + 2\ln\frac{\lambda}{m} + \xi(\ln\frac{\Lambda}{m} - \ln\frac{\lambda}{m}) \tag{4.30}$$

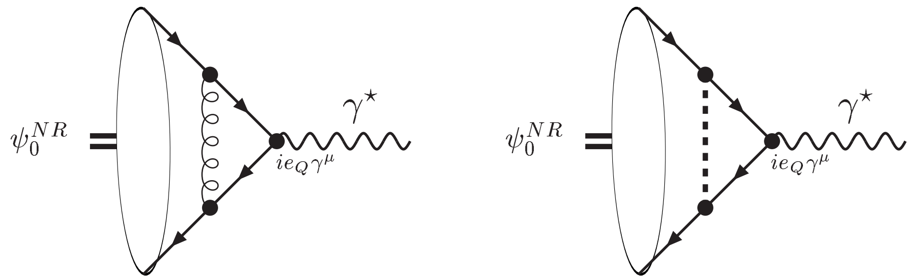

(a) Gluonic exchange correction

(b) Coulombic exchange correction

Figure 4.2: Feynman diagrams corresponding to the first order corrections to the leptonic width of quarkonium.

Equations (4.29) and (4.30) give the final result[2]

$$\Gamma_{n\mu} = \sqrt{2}\varepsilon_\mu \phi_n(0) \left(1 - \frac{8\alpha_S}{3\pi} + \dots\right) \tag{4.31}$$

implying the familiar corrections factor for the leptonic widths, first obtained by Barbieri *et al.* [15].

4.3 What about Production...

As we have already mentioned, the conclusions valid for decay are not necessarily relevant for production. However the two previous sections have given us a flavour of the formalism to be used to extend effectively the CSM in a relativistic regime. We have also seen how the wave function at the origin appears from the fully general Bethe-Salpeter formalism.

Beside that we can draw more technical conclusions: first Eq. (4.19) provides us with a nonrelativistic wave function from a given potential. This wave function has also the wanted form to be included in a Feynman diagram formalism just as it is, but without introducing propagators for the two quarks entering the bound state.

Therefore, as it appears clearly from the amplitude Eq. (4.21) describing the leptonic decay, there exists no risk to get infinite quantities in the amplitude as long as the wave function remains finite. In this sense, the taylor expansion of the product

$$\int \psi(\ell)\mathcal{M}d\ell, \tag{4.32}$$

[2] $C_2(R) = \frac{4}{3}$.

leading – at first order – to $\phi(0)\mathcal{M}|_0$ is licit.

On the other hand in the process $gg \to g^3S_1$, there are two off-shell propagators left. As the momentum in the loop is not *a priori* constrained (except $\ell^2 < 0$ if we keep the nonrelativistic condition $\ell.p = 0$), we have no reason to exclude cases where we get poles as we exposed in the previous Chapter.

Chapter 5

Conclusion and Outlook

In this part devoted to the study of heavy quarkonia, we have presented a detailed analysis of the theoretical uncertainties of the Color Singlet Model. We have concluded that these uncertainties, coming mainly from the parton distribution functions and the wave function of the bound state at the origin, are not sufficient to explain the large discrepancies observed with the experimental data coming from Tevatron detectors, *i.e.* CDF and D∅.

Beside this study, we presented the part of the work already done for the extension of the Color Singlet Model beyond the common static and thus nonrelativistic approximation. We explained how we implemented the integration over the momentum in the loop and particularly the condition $\ell.p = 0$ imposing that the relative energy of the constituents is zero. As we did this for either cartesian coordinates or Sudakov variables, we considered as worthy to mention and to show that both methods gave the same results even in the present case of a nine-dimension integral. As we made use of Sudakov variables, we devoted one short Chapter to these in order to explain their utility and the way one can use them.

As a complement to the presentation of the work already achieved, we also presented a way of introducing a relativistic wave function describing bound states of two particles. We have thus seen how to normalise this wave function, but also how to build a four-dimensional wave function, which directly matches the Feynman diagram formalism. This will perhaps enable us to quantify the relativistic corrections to production cross-sections in a coherent way in systems such as J/ψ where the square of the quark velocity is nearly one third of the velocity of light.

One of our conclusions was that, oppositely to processes such as leptonic decays, one cannot systematically brush aside the possibility of poles in the amplitude. These could arise for some values of the loop momentum when one of the intermediate quarks is put on its mass-shell.

Considering that models such as the Color Evaporation Model and Non Relativistic QCD are not fully satisfactory for the description of heavy quarkonia production, we might conclude that a correct tackling of this could be a decisive step in the way to the resolution of this well-known problem of QCD.

Part II

Structure Functions of the Pion and of a Scalar Particle

Chapter 6

Neutral Pion Structure Functions

In this chapter, we plan to calculate the structure functions of neutral pions. We shall use a simple model describing the pion, in which the pion vertex function is a constant g and in which we apply a cut-off simulating the finite size of the pion.

As a first approach, we shall concentrate on the diagonal case. Thus it will be sufficient to consider the cut diagrams for $\gamma^\star\pi_0 \to \gamma^\star\pi_0$ and therefore to limit ourselves to the calculation of total cross-section for $\gamma^\star\pi_0 \to q\bar{q}$.

From this cross-section, we shall be able to extract the two functions W_1 and W_2 defining the hadronic current in a complete analogous way to deep-inelastic scattering in the proton case. Taking the Bjorken limit, we shall then find the structure functions F_1 and F_2.

6.1 Model for the Pion

As we have just said, we use a simple model for the pion. In fact, it can be easily introduced in the context of the NJL model of strong interaction. Taking the limit $N_c \to \infty$ of NJL, we actually get a σ–model as the one we use for this calculation.

It has to be noticed that the introduction of a cut-off, simulating the size of the pion, does not break gauge invariance in this case. This will be discussed later. Moreover this cut-off disentagles the contribution of crossed diagrams from the contribution of direct ones, and turns out to be necessary for the very definition of structure functions. And finally the cut-off makes the momentum fraction of the quark –deduced from the first moment of $F_2(x)$ – independent of Q^2 as we could suppose with this constraint on the relative momentum.

6.1.1 Normalisation and Coupling Constant

In order to input a proper value of g in the calculation of the structure functions, we could have used the normalisation condition coming either from the form factor at $Q^2 = 0$ (the charge) or from a more rigourous derivation (see *e.g.* Chapter 12 of [16]) which gives the equivalent condition for the vertex function Γ:

$$1 = -\int \bar{\Gamma}\, \frac{\partial G}{\partial P^2}\bigg|_{P^2=m_\pi^2} \Gamma\,, \tag{6.1}$$

with P the total momentum of the two quarks constituting the pion. It can be explicitely shown that the two conditions are equivalent.

From this condition, we could have obtained [17, 18] a relation between the value of g and this of the cut-off, Λ. The following plot shows $g(\Lambda)$ and the quark mass $m_q(\Lambda)$.

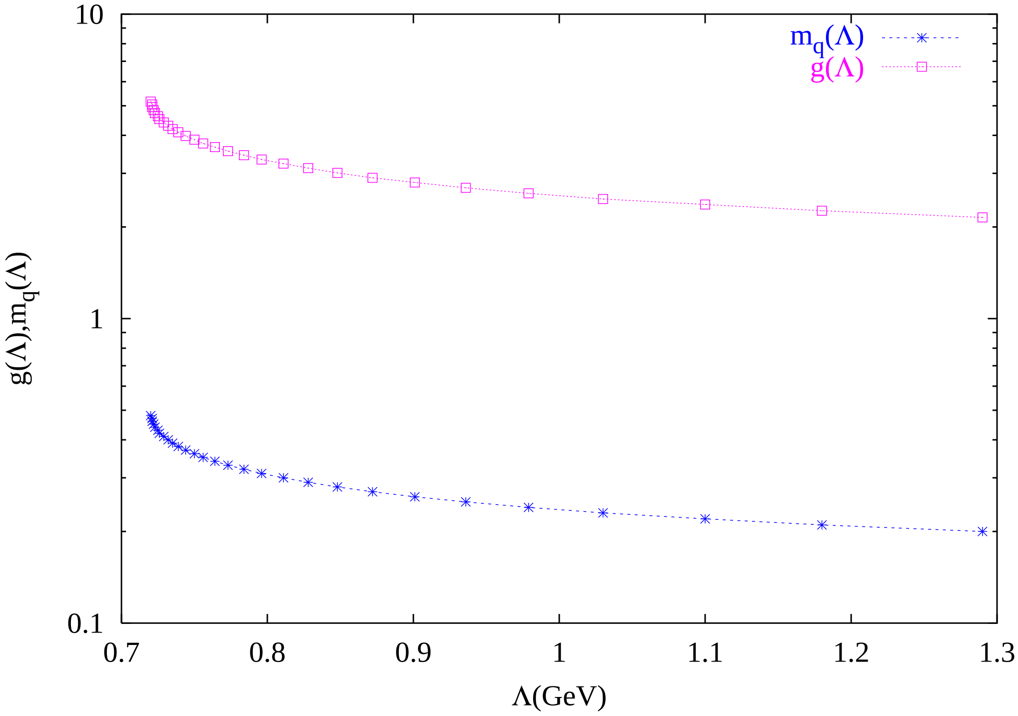

Figure 6.1: Evolution of $g(\Lambda)$ and of $m_q(\Lambda)$ (GeV) from the normalisation condition.

We did not proceed like this. The reason was to keep gauge invariance. The triangle diagram describing the form factor is normally divergent and must be regularized. We could have used a regularization method, as Pauli-Villars regularization, which does not break gauge invariance nor Lorentz invariance (oppositely to d^3k cut-off). In this case however Pauli-Villars regularization gave absurd results for the structure functions[1], this is why we stick to the use a cut-off, but with a different approach.

Therefore, to keep gauge invariance and a sort of coherence between the determination of the coupling constant and the calculation of the structure functions, we

[1]The latter are finite and independently of other considerations, they do not require any regularization. This could be one of the explanation of these absurd results.

used an alternate method based on the quark sum rule and which gave fully compatible coupling constants with the ones plotted in Fig. 6.1. The details are given in section 6.3.3.

6.2 Cross-Section Calculation for $\gamma^\star\pi_0 \to q\bar{q}$ by Integration over t

In this section, we calculate the **cross-section** for $\gamma^\star\pi_0 \to q\bar{q}$ which can be related to the functions W_1 and W_2 as we will see later. Another way to achieve this work would be to compute the imaginary part of the forward **amplitude** for $\gamma^\star\pi_0 \to \gamma^\star\pi_0$. The latter can also be related by tensorial manipulations to W_1 and W_2.

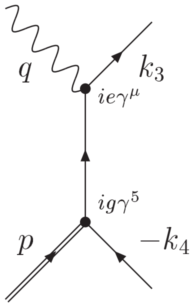

Figure 6.2: Feynman diagram for the process $\gamma^\star\pi_0 \to q\bar{q}$.

At the leading order in the perturbation expansion, we have two diagrams (one is shown in Fig. 6.2) which squared give two types of diagrams.The first –corresponding to box-diagrams for the amplitude of $\gamma^\star\pi_0 \to \gamma^\star\pi_0$– enables us to calculate the structure functions straightforwardly. The second involves crossed quark lines and is related to processes where the two photons –which normally appears in the context of structure functions– hit once a quark and once a anti-quark ! This is incompatible with the interpretation in terms of structure functions. As we will conclude from the calculations, the contributions of this type are fortunalety higher-twists, *i.e.* they scale as $\frac{1}{Q^2}$ when we introduce the cut-off.

One could raise as an objection that one could have simply modelized the interaction between the photons and the pions by the direct diagrams only. The reason why we considered the total contribution to $\gamma^\star\pi_0 \to q\bar{q}$ is that it is a physical process, observable and thus gauge invariant. Even avoiding gauge breaking regularization methods, the result would have been gauge dependent if one had not considered all the diagrams.

6.2.1 Kinematics of the Process

Before starting the calculation, we derive the value of the different momenta and scalar products involved (see Fig. 6.2). In order to do this we have to choose a frame and a set of coordinates. For the sake of simplicity, we choose the cartesian coordinates in the CM frame.

Hence we have the following four-momenta for the four particles:

$$\begin{aligned} q &= (E(=q_0), \vec{q}), \\ p &= (E_\pi, -\vec{q}), \\ k_3 &= (k_{3,0}, \vec{k}_3), \\ k_4 &= (k_{4,0}, -\vec{k}_3). \end{aligned} \tag{6.2}$$

Let us now introduce the Mandelstam variables in the classical way:

$$\begin{aligned} s =& (p+q)^2 = (k_3+k_4)^2 = E_{CM}^2 = (E+E_\pi)^2, \\ t =& (k_3-q)^2 = (k_4-p)^2, \\ u =& (k_3-p)^2 = (k_4-q)^2. \end{aligned} \tag{6.3}$$

Then we define the square momenta by means of the masses and the virtuality of the photon, as well as some scalar products using the Mandelstam variables:

$$\begin{aligned} q^2 =& -Q^2, \\ p^2 =& m_\pi^2, \\ k_3^2 =& m^2, \\ k_4^2 =& m^2 \Rightarrow \\ k_3 \cdot p =& \frac{-Q^2+m_\pi^2}{2} + q \cdot p - k_3 \cdot q, \\ q \cdot p =& \frac{s+Q^2-m_\pi^2}{2}, \\ k_3 \cdot q =& \frac{m^2-Q^2-t}{2}. \end{aligned} \tag{6.4}$$

In the CM frame, we obtain very simple expressions for k_3 and k_4's four-components:

$$\begin{aligned} k_{3,0} =& k_{4,0} = \frac{\sqrt{s}}{2}, \\ |\vec{k}_3| =& |\vec{k}_4| = \sqrt{\frac{s}{4} - m^2}. \end{aligned} \tag{6.5}$$

Now, in order to get four-invariant expressions during the calculation, it is always better to get rid of non-covariant quantities, as energies, angles, etc ... A first step is the elimination of E_π, which is carried out like this,

$$\begin{aligned} |\vec{q}|^2 &= E^2 + Q^2, \\ p^2 &= m_\pi^2 = E_\pi^2 - |\vec{q}|^2 \\ \Rightarrow E_\pi^2 &= m_\pi^2 + E^2 + Q^2. \end{aligned} \tag{6.6}$$

As $\sqrt{s} = E + E_\pi$, we have:

$$\sqrt{s} = E + \sqrt{m_\pi^2 + E^2 + Q^2}. \tag{6.7}$$

We can therefore directly obtain E from the last equation:

$$E = \frac{s - m_\pi^2 - Q^2}{2\sqrt{s}}. \tag{6.8}$$

As regards the squared three-momenta, we simply have:

$$\begin{aligned} |\vec{q}|^2 &= E^2 + Q^2 \\ \Rightarrow |\vec{q}|^2 = |\vec{p}|^2 &= \frac{(s - m_\pi^2 - Q^2)^2 + 4sQ^2}{4s}. \end{aligned} \tag{6.9}$$

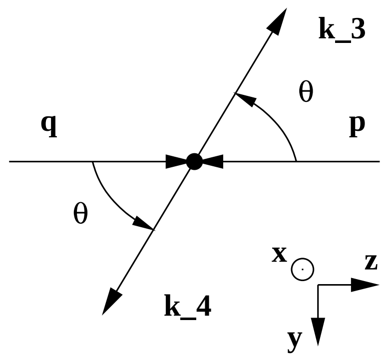

Figure 6.3: Kinematics and definition of the angle θ in the CM frame.

The last non-covariant variable left is the angle θ defined in Fig. 6.3. We want as well to emphasize that Fig. 6.3 implies that the x and y-axis are chosen in such a way as to have:

$$q_x = -p_x = 0 = q_y = -p_y, \tag{6.10}$$

the z-axis being fixed by the photon and pion directions in the CM frame.

To eliminate this angle, we simply use the variable t the expression of which explicitely involves θ,

$$\begin{aligned} t = (k_4 - p)^2 &= m^2 + m_\pi^2 - 2k_{4,0}\underbrace{E_\pi}_{E-\sqrt{s}} + \underbrace{(-1)^2\vec{k}_4 \cdot \vec{p}}_{2|\vec{k_4}||\vec{p}|\cos(\theta)} \\ &= m^2 + m_\pi^2 - s + \sqrt{s}\frac{s - m_\pi^2 - Q^2}{2\sqrt{s}} + 2\sqrt{\frac{s}{4} - m^2}\frac{\sqrt{(s - m_\pi^2 - Q^2)^2 + 4sQ^2}}{2\sqrt{s}}\cos(\theta) \end{aligned} \tag{6.11}$$

Eventually we obtain:

$$\cos(\theta) = \frac{t - m^2 - \frac{m_\pi^2}{2} + \frac{s}{2} + \frac{Q^2}{2}}{2\sqrt{\frac{s}{4} - m^2}\frac{\sqrt{(s-m_\pi^2-Q^2)^2+4sQ^2}}{2\sqrt{s}}} = \frac{t - m^2 - \frac{m_\pi^2}{2} + \frac{s}{2} + \frac{Q^2}{2}}{2\sqrt{\frac{s}{4} - m^2}\sqrt{E^2+Q^2}}. \tag{6.12}$$

Because we shall proceed to the integration of the cross-section over t, we also want to determine its boundary values. These are simply reached for the extremum values of $\cos(\theta)$, and are

$$t_{\substack{\max\\ \min}} = m^2 + \frac{m_\pi^2}{2} - \frac{s}{2} - \frac{Q^2}{2} \pm 2\sqrt{\frac{s}{4} - m^2}\frac{\sqrt{(s - m_\pi^2 - Q^2)^2 + 4sQ^2}}{2\sqrt{s}} \tag{6.13}$$

Finally, we get all the four-components of all the four-momenta involved in the reaction:

$$\begin{aligned}
q &= (\frac{s - m_\pi^2 - Q^2}{2\sqrt{s}}, 0, 0, \sqrt{\frac{(s - m_\pi^2 - Q^2)^2 + 4sQ^2}{4s}}) = (E, 0, 0, \sqrt{E^2 + Q^2}),\\
p &= (\sqrt{m_\pi^2 + \frac{(s - m_\pi^2 - Q^2)^2 + 4sQ^2}{4s}}, 0, 0, -\sqrt{\frac{(s - m_\pi^2 - Q^2)^2 + 4sQ^2}{4s}})\\
&= (\sqrt{m_\pi^2 + E^2 + Q^2}, 0, 0, -\sqrt{E^2 + Q^2}),\\
k_3 &= (\frac{\sqrt{s}}{2}, 0, -\sqrt{\frac{s}{4} - m^2}\sin(\theta), \sqrt{\frac{s}{4} - m^2}\cos(\theta)),\\
k_4 &= (\frac{\sqrt{s}}{2}, 0, \sqrt{\frac{s}{4} - m^2}\sin(\theta), -\sqrt{\frac{s}{4} - m^2}\cos(\theta)).
\end{aligned} \tag{6.14}$$

These quantities will be explicitely used in the determination of scalar products involving the polarisation vectors.

6.2.2 Amplitude Calculation

Analytical Expression

Applying Feynman rules for the process shown in Fig. 6.2, we obtain the analytical expression of the squared amplitude in a straightforward way. For a given polarisation of the virtual photon, $i = L, T_1, T_2$, and with well-known conventions[2] we have,

$$\begin{aligned}
|\mathcal{M}_i|^2 = 3g^2(e_u^2 + e_d^2)\mathrm{Tr}\Bigg(&(-\not{k}_4 + m)\gamma^5 \frac{\not{k}_3 - \not{q} + m}{(k_3 - q)^2 - m^2}\gamma^{\mu'}\\
&(\not{k}_3 + m)\gamma^\mu \frac{\not{k}_3 - \not{q} + m}{(k_3 - q)^2 - m^2}\gamma^5\Bigg)\,\varepsilon_{i\mu}\varepsilon^\star_{i\mu'}.
\end{aligned} \tag{6.15}$$

[2]For definiteness the different factors corresponding to the different elements of such diagrams involving hadrons are described and illustrated by examples in the Appendix A.

In order to calculate the latter, we need the expressions of the scalar products of the polarisation vectors with q, p, k_3 and k_4 for the three possible polarisation states.

We now proceed to the calculation of these :

Longitudinal Polarisation

We shall use the following definition of the longitudinal polarisation vector,

$$\varepsilon_{L,\mu} = \frac{1}{\sqrt{Q^2}}(q_z, 0, 0, E). \tag{6.16}$$

This and Eq. (6.14) enable us to work out the following scalar products:

$$\begin{aligned}
\varepsilon_L \cdot q &= 0, \\
\varepsilon_L \cdot p &= \frac{1}{\sqrt{Q^2}}\sqrt{s}\sqrt{E^2+Q^2} \text{ (recall that } \sqrt{s} = E + E_\pi), \\
\varepsilon_L \cdot k_3 &= \frac{1}{\sqrt{Q^2}}\left(\frac{\sqrt{s}\sqrt{E^2+Q^2}}{2} - \frac{E(t - m^2 - \frac{m_\pi^2}{2} + \frac{s}{2} + \frac{Q^2}{2})}{2\sqrt{E^2+Q^2}}\right), \\
\varepsilon_L \cdot k_4 &= \varepsilon_L \cdot (p + q - k_3).
\end{aligned} \tag{6.17}$$

Transverse Polarisations

We shall use the following definition of the linear transverse polarisation vectors:

$$\begin{aligned}
\varepsilon_{T_1,\mu} &= (0, 1, 0, 0), \\
\varepsilon_{T_2,\mu} &= (0, 0, 1, 0).
\end{aligned} \tag{6.18}$$

This and Eq. (6.14) lead to:

$$\begin{aligned}
\varepsilon_{T_i} \cdot q &= 0, \quad i = 1, 2, \\
\varepsilon_{T_i} \cdot p &= 0, \quad i = 1, 2, \\
\varepsilon_{T_1} \cdot k_3 &= 0, \\
\varepsilon_{T_2} \cdot k_3 &= \sqrt{\frac{s}{4} - m^2}\sqrt{1 - \left(\frac{t - m^2 - \frac{m_\pi^2}{2} + \frac{s}{2} + \frac{Q^2}{2}}{2\sqrt{\frac{s}{4} - m^2}\sqrt{E^2+Q^2}}\right)^2}, \\
\varepsilon_{T_i} \cdot k_4 &= \varepsilon_{T_i} \cdot (p + q - k_3).
\end{aligned} \tag{6.19}$$

6.2.3 Polarised Cross-Sections

The easiest way to obtain the total cross-section is to use the following relation [19], with $i = L, T_1, T_2$:

$$\frac{\mathrm{d}\sigma_i}{\mathrm{d}t} = \frac{1}{16\pi\lambda}\left|\mathcal{M}_i\right|^2 \tag{6.20}$$

with $\lambda = \lambda(s, -Q^2, m_\pi^2)$[3]. The latter directly links the amplitude –which is obtained, in our case, with REDUCE[4] – expressed in terms of well-chosen variables $(s, Q^2, t, \dots)$ and the differential cross-section upon t. Therefore its integration from $t_{\min}$ to $t_{\max}$ (see Eq. (6.13)) gives σ_{tot} for a given polarisation.

Hence we obtain, for the direct process, the following polarised cross-sections,

$$\begin{aligned}
\sigma_{T_1} &= \frac{1}{16\pi\lambda} 3g^2(e_u^2 + e_d^2) \int \mathrm{d}t \; T^{\mu\mu'} \varepsilon_{T_1,\mu} \varepsilon^\star_{T_1\mu'} \\
\sigma_{T_2} &= \frac{1}{16\pi\lambda} 3g^2(e_u^2 + e_d^2) \int \mathrm{d}t \; T^{\mu\mu'} \varepsilon_{T_2,\mu} \varepsilon^\star_{T_2\mu'} \\
\sigma_{L} &= \frac{1}{16\pi\lambda} 3g^2(e_u^2 + e_d^2) \int \mathrm{d}t \; T^{\mu\mu'} \varepsilon_{L,\mu} \varepsilon^\star_{L\mu'} \\
\sigma_{contr.} &= \frac{1}{16\pi\lambda} 3g^2(e_u^2 + e_d^2) \int \mathrm{d}t \; T^{\mu\mu'} (g_{\mu\mu'} + \frac{q_\mu q_{\mu'}}{Q^2}),
\end{aligned} \tag{6.21}$$

with $T^{\mu\mu'} \equiv \mathrm{Tr}\left((-\not{k}_4 + m)\gamma^5 \frac{\not{k}_3 - \not{q} + m}{(k_3-q)^2 - m^2} \gamma^{\mu'} (\not{k}_3 + m) \gamma^\mu \frac{\not{k}_3 - \not{q} + m}{(k_3-q)^2 - m^2} \gamma^5\right)$.

$\sigma_{contr.}$ does not correspond to any polarised cross-section, nevertheless as it involves no polarisation vectors but a simple tensor, its calcution is a bit more straightforward, and can be useful. Later, we shall also see that its value is in no way the value of the $\sigma_L + \sigma_{T_1} + \sigma_{T_2}$, which could be in some possible experiments a measurable quantity.

Finally, to give a flavour of the results, we write here the expression of $T^{\mu\mu'} \varepsilon_{T_1,\mu} \varepsilon^\star_{T_1\mu'}$, which is by far the simplest one:

$$\frac{4\,(-m_\pi^2\, m_q^2 + m_\pi^2\, Q^2 + m_\pi^2\, t - m_q^4 + m_q^2\, Q^2 + m_q^2\, s + 2\, m_q^2\, t - Q^2\, t - s\, t - t^2)}{m_q^4 - 2\, m_q^2\, t + t^2}$$

6.2.4 Performing the Integration

For the sake of completeness, we explain in this section how we proceed to the integration with or without cut-off. Besides, we show that the crossed-diagrams contribution are higher-twists as announced.

First of all, the integration was simply undertaken by MATHEMATICA using analytical (command `Integrate[..]`) primitivation over t. The latter generates a logarithm of $t_{\min}$ and $t_{\max}$, or of the cut-off[5] when the kinematic limits are less strict than the one coming from the cut-off. On the other hand, the integration over x_B, *e.g.* to get F_1 and F_2, were performed numerically (command `NIntegrate[..]`) only considering the real part of the result.

[3] $\lambda(x, y, z) \equiv x^2 + y^2 + z^2 - 2xy - 2xz - 2yz$

[4] As a complement of information the code source of either REDUCE and MATHEMATICA– used for the integration– programs are given in the appendices B & C .

[5] Cut-off on t and not on the relative momentum; both can be linked to the size of the pion.

Cut-off and Higher-twists

Irrespective of the factors arising in the extraction of the structure functions (see section (6.3.2)), we can simply convince ourselves that in the presence of a cut-off the contribution of the crossed diagrams (the first photon hits a quark(antiquark) and the second an antiquark (quark)) are higher-twists, *i.e.* they disappear as $\frac{1}{Q^2}$ relative to the direct diagrams, by plotting the ratio of these two contributions as a function of Q^2. The suppression is clear on Fig. 6.4 whatever the value of the cut-off.

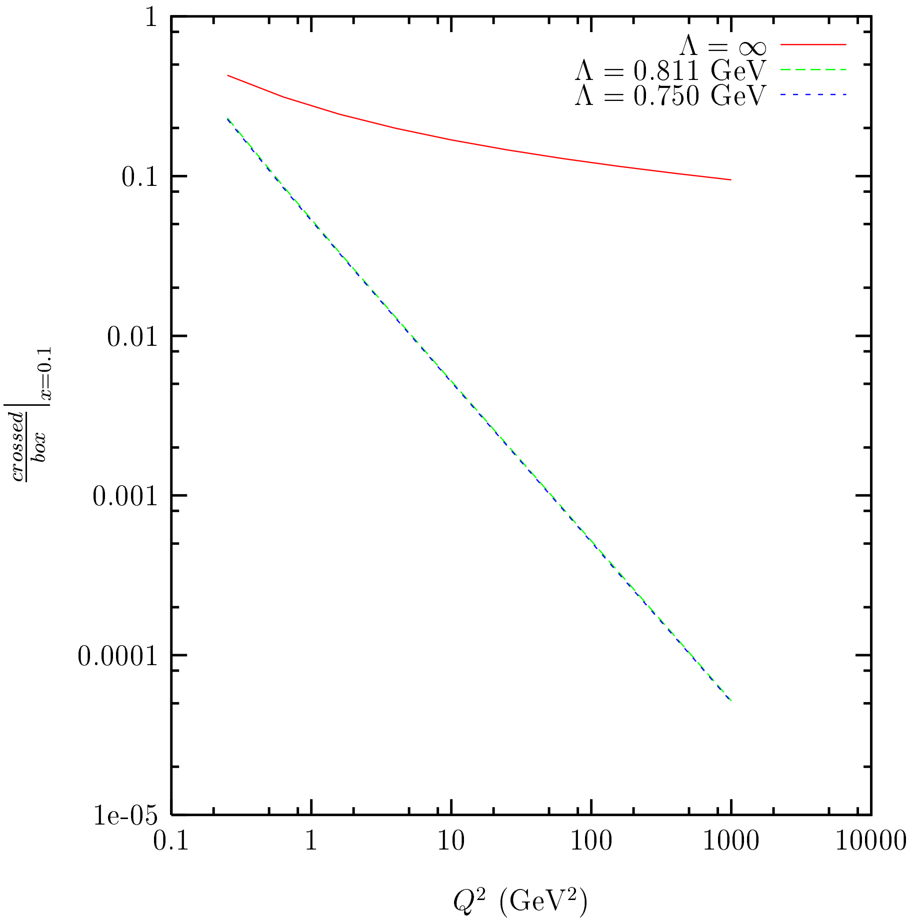

Figure 6.4: Ratio of the direct contributions to the crossed contributions to the cross-section for $\gamma^{\star}\pi^0 \to q\bar{q}$ at $x_B = 0.1$ and for three values of the cut-off Λ.

As we already said, in order to get a physical interpretation of our results –in terms of structure functions–, we needed the crossed diagram contributions to be suppressed. The presence of a cut-off, which is not a regulator in the studied process, is thus now fully justified and not only as a consequence of the pion size.

Cut-off and Gauge Invariance

In most cases, the presence of a cut-off implies the breaking of gauge invariance. This is the main reason why one commonly uses other regularization methods as Pauli-Villars or dimensional regularization. In the context of an effective theory, the two first have the critical advantage that the regularization parameter (which is kept to a finite value) can be interpreted as a physical one. In the case of dimensional regularization, the signification of fractional dimensional space is not at all clear.

Nevertheless, in our model and in the case of the study of *diagonal* structure functions, as the intermediate states in $\gamma^\star\pi^0 \to \gamma^\star\pi^0$ are on-shell, the cut-off on the internal loop momentum[6] is a cut-off on a physical observable, that is t of the process $\gamma^\star\pi^0 \to q\bar{q}$ [7]. The conclusion is thus staightforward: this cut-off does not break gauge invariance.

Let us now explain more precisely how we introduced the cut-off in our calculations. As we have previously explained, a cut-off on the relative momentum is equivalent to a cut-off on t. The procedure is thus obvious: instead of using $t_{\min}$ and $t_{\max}$ as boundary values for the integral over t, we used $Max\{t_{\min}, \Lambda_t\}$ and $t_{\max}$ (when $\Lambda_t < t_{\max}$, otherwise the result is zero)[8].

This procedure would have been fully right if we had only one pion vertex, and thus one condition to implement. But we have two vertices with two different expressions for the relative momenta. To keep gauge invariance, the cut-off on t must be on the overall cross-section as the physical observable is the full cross-section (the square of the sum of the two diagrams) at a given t.

To keep the constraint coming from the pion size, we should have imposed two conditions on the cross-section to be integrated over t. However, this would have given zero. As a makeshift we imposed one condition or the other.

Even if the physical interpretation is not so direct, we thus kept gauge invariance, information from the pion size, suppressed the crossed diagrams and hence obtained the interpretation in terms of structure functions.

6.3 $\sigma_{\gamma^\star\pi_0\to q\bar{q}}$, W_1, W_2, F_1 and F_2

At this stage we have obtained the polarised cross-sections and we should be able to link them to the wanted structure functions for neutral pion. Before doing this, we shall nevertheless recall some mandatory formulae derived from the analysis of deep inelastic proton scattering.

[6] which corresponds, up to some constants, to a cut-off on the relative mometum between the two quarks at the $\pi^0 q\bar{q}$ vertex.

[7] This is clear if we extract the structure functions from $\gamma^\star\pi^0 \to q\bar{q}$ as we have exposed in this report, it is a bit less evident although if we work with $\gamma^\star\pi^0 \to \gamma^\star\pi^0$.

[8] Recall that $t < 0$.

6.3.1 Classical Formulae

As already discussed, unlike the case of the scattering of point particles –typically the leptons– when compound particles are involved, we have to turn to tensorial analysis to introduce expressions which describe the overall interaction of the components. For deep inelastic electron-proton scattering, we can write the cross-section in the following way:

$$\mathrm{d}\sigma \propto L^{\mu\nu} W_{\mu\nu}, \tag{6.22}$$

with $L^{\mu\nu}$, the well-known electromagnetic tensor (see *e.g.* [20] p. 90) and $W_{\mu\nu}$, the hadronic tensor, which can be written (excluding C-violating contributions):

$$W_{\mu\nu}(p,q) = (-g_{\mu\nu} - \frac{q_\mu q_\nu}{Q^2})W_1(Q^2,\nu) + [p_\mu + (\frac{p\cdot q}{Q^2})q_\mu][p_\nu + (\frac{p\cdot q}{Q^2})q_\nu]\frac{W_2(Q^2,\nu)}{M^2}, \tag{6.23}$$

with M, the hadron mass.

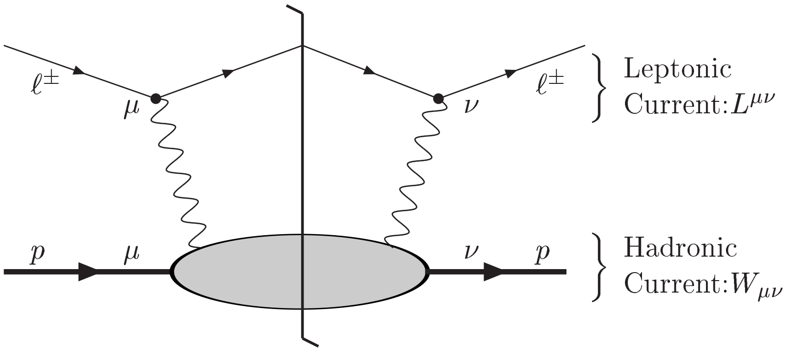

Figure 6.5: Illustration of the signification of $L^{\mu\nu}$ & $W_{\mu\nu}$.

In the expresion (6.23), $W_1(Q^2,\nu)$ and $W_2(Q^2,\nu)$ are called the structure functions and are the degrees of freedom left when all the constraints upon $W_{\mu\nu}(p,q)$ have been applied, such as current conservation, covariance, etc.

Let us now introduce the Bjorken variable x,

$$\begin{aligned} \nu &\equiv p\cdot q, \\ x &\equiv \frac{Q^2}{2\nu}. \end{aligned} \tag{6.24}$$

If we want to analyse the deep structure of the hadron, we have somehow to sharpen the probe. Physically, this corresponds to an increase of the energy of the exchanged photon, and thus to the Bjorken limit,

$$\begin{aligned} &Q^2 \to \infty, \\ &\nu \to \infty \text{ with } x \text{ kept fixed.} \end{aligned} \tag{6.25}$$

In this limit, the structure functions **scale**, becoming dependent only on x,

$$\begin{aligned} MW_1(Q^2,\nu) &\to F_1(x), \\ \frac{\nu}{M}W_2(Q^2,\nu) &\to F_2(x). \end{aligned} \tag{6.26}$$

This is, in fact, the sign of the compositeness of the hadrons.

Supposing that the hadron is constituted only of spin one-half partons, it can be shown (see p. 95-96 [20]) that we have (Callan-Gross [21]):

$$2xF_1(x) = F_2(x). \tag{6.27}$$

Conversely, the fact that experimentally, we have $2xF_1(x) = F_2(x)$ is a proof that the parton are spin one-half particles.

In the same spirit as the definition of the cross-section of $\gamma^\star p \to X$ (see p. 95 [20]), we define the polarised cross-sections for $\gamma^\star\pi_0 \to X$ by [9]:

$$\sigma_\lambda(\gamma^\star\pi_0 \to X) = \frac{4\pi^2\alpha}{K}\varepsilon_\lambda^{\star\mu}\varepsilon_\lambda^\nu W_{\mu\nu}, \forall\lambda = x, y, z, \tag{6.28}$$

with the equivalence

$$\begin{aligned} \varepsilon_x &\equiv \varepsilon_{T_1}, \\ \varepsilon_z &\equiv \varepsilon_L, \\ \varepsilon_y &\equiv \varepsilon_{T_2} \end{aligned} \tag{6.29}$$

and the flux factor $K = \frac{1}{2}\frac{\sqrt{\lambda(s,-Q^2,m_\pi^2)}}{m_\pi}$.

Defining longitudinal and transverse cross-sections through

$$\begin{aligned} \sigma_T &\equiv \frac{1}{2}(\sigma_x + \sigma_y) \text{ and} \\ \sigma_L &\equiv \sigma_z, \end{aligned} \tag{6.30}$$

we can easily show that:

$$\sigma_T = \frac{4\pi^2\alpha}{K}W_1, \tag{6.31}$$

$$\sigma_L = \frac{4\pi^2\alpha}{K}\left[(1 + \frac{\nu}{2xm_\pi^2})W_2 - W_1\right]. \tag{6.32}$$

These last two formulae are the ones required to link the functions W_1 and W_2 to previously calculated polarised cross-sections for $\gamma^\star\pi_0 \to q\bar{q}$.

[9] This definition is independent of the hadron spin because, on the one hand, we have to sum the contributions coming from the different polarisations and on the other hand, we have a spin factor arising in the relation between $W_{\mu\nu}$ and the hadronic current.

Besides we would like to stress that one has to be cautious if one wants to consider non-polarised processes. Usually, a simple contraction of the amplitude for a given helicity with the expression,

$$-g^{\mu\nu} + \frac{q^\mu q^\nu}{M^2} \tag{6.33}$$

seems to be the most convenient way to proceed, instead of considering separately the different polarisations. This is in most cases licit because

$$\sum_\lambda \varepsilon_\lambda^{\star\mu}\varepsilon_\lambda^\nu = -g^{\mu\nu} + \frac{q^\mu q^\nu}{M^2}, \tag{6.34}$$

for massive particles, and thus the –strict– sum over polarisations gives the *good* tensor.

For virtual particles, nevertheless, we have the following normalisations

$$\begin{aligned} \varepsilon_T \cdot \varepsilon_T &= -1, \\ \varepsilon_L \cdot \varepsilon_L &= +1. \end{aligned} \tag{6.35}$$

Therefore, the following relation –which indeed reduce to (6.34) for massive particles for which (6.35) does not hold–,

$$\sum_\lambda \frac{\varepsilon_\lambda^{\star\mu}\varepsilon_\lambda^\nu}{\varepsilon_\lambda \cdot \varepsilon_\lambda} = g^{\mu\nu} + \frac{q^\mu q^\nu}{Q^2} \tag{6.36}$$

leads, in this case, to

$$\sigma_{contr.} = \frac{4\pi^2\alpha}{K}\left(g^{\mu\nu} + \frac{q^\mu q^\nu}{Q^2}\right) W_{\mu\nu} = \sigma_L - 2\sigma_T \tag{6.37}$$

but not to

$$\sigma_L + 2\sigma_T \; ! \tag{6.38}$$

6.3.2 Expression of W_1 and W_2 from $\sigma_{\gamma^\star\pi_0\to q\bar{q},i}$

With all these tools, we can now extract the functions W_1 and W_2. Nonetheless, we have at our disposal several means to proceed. Each of them are not strictly equivalent, and some are better than others for the determination of either W_1 or W_2.

Here are the descriptions of these:

Direct extraction of W_1 from σ_T

The simplest way to extract W_1 is to use the relation (6.31). This gives

$$\begin{aligned} W_1 =& \frac{\sqrt{\lambda}}{8\pi^2 m_\pi \alpha}\sigma_T \\ =& \frac{\sqrt{\lambda}}{8\pi^2 m_\pi \alpha}\frac{1}{16\pi\lambda}3g^2 4\pi\alpha(\frac{1}{9}+\frac{4}{9})\int \mathrm{d}t\frac{1}{2}\sum_i \left(T_i^{\mu\mu'}\varepsilon_{T_1,\mu}\varepsilon^\star_{T_1\mu'} + T_i^{\mu\mu'}\varepsilon_{T_2,\mu}\varepsilon^\star_{T_2\mu'}\right), \end{aligned} \tag{6.39}$$

where the sum upon i refers to the different diagrams.

We then get F_1 and F_2 as usual taking account of the scaling relations and of the Callan-Gross relation. This extraction is exact for W_1.

Extraction of W_2 from σ_L and σ_T.

Given that $\sigma_L + \sigma_T = \frac{8\pi^2 m_\pi \alpha}{\sqrt{\lambda}}(1+\frac{\nu}{2xm_\pi^2})W_2$,

$$W_2 = \frac{\sqrt{\lambda}}{8\pi^2 m_\pi \alpha}\frac{2xm_\pi^2}{\nu + 2xm_\pi^2}(\sigma_L + \sigma_T). \tag{6.40}$$

This allows the extraction of F_2 without the need of the Callan-Gross relation and is exact for W_2. This requires however the knowledge of all the polarised cross-sections.

Extraction of W_2 from $\sigma_{contr.}$, the scaling and the Callan-Gross relations

The simplest way to obtain an approximate extraction of the structure functions is the following one. It is based on the approximate identity[10] $W_1 \approx \frac{\nu W_2}{2xm_\pi^2}$.

Recalling that $\sigma_{contr.} = \sigma_L - 2\sigma_T = \frac{8\pi^2 m_\pi \alpha}{\sqrt{\lambda}}\left[(1+\frac{\nu}{2xm_\pi^2})W_2 - 3W_1\right]$, we can immediately write that

$$W_2 = \frac{\sqrt{\lambda}}{8\pi^2 m_\pi \alpha}\frac{xm_\pi^2}{xm_\pi^2 - \nu}\sigma_{contr.}. \tag{6.41}$$

We eventually obtain F_2 by means of the second scaling relation (see Eq. (6.26)). Similarly, we could have expressed W_1 instead of W_2 in terms of $\sigma_{contr.}$ in Eq. (6.41).

Extraction of W_1 from $\sigma_{contr.}$ and σ_L

As $\sigma_{contr.} - \sigma_L = -2\sigma_T$ and using Eqs. (6.32) & (6.31), we get in the same way,

$$W_1 = \frac{\sqrt{\lambda}}{8\pi^2 m_\pi \alpha}\frac{\sigma_L - \sigma_{contr.}}{2}. \tag{6.42}$$

This is totally equivalent to the first method but avoids the calculation of σ_T.

[10]This comes from the following relations : $m_\pi W_1 \to F_1 \simeq \frac{F_2}{2x} \to \frac{\nu W_2}{2xm_\pi}$.

6.3.3 Sum Rules

The first rule comes from the fact that in a pion the total number of quarks plus antiquarks is two. In order to impose this condition on F_1 and F_2, we first express the latter in terms of quarks distribution in the following way:

$$\begin{aligned} F_2 =& x_B\left(\frac{4}{9}u_v(x_B)+\frac{4}{9}\bar{u}_v(x_B)+\frac{1}{9}d_v(x_B)+\frac{1}{9}\bar{d}_v(x_B)\right), \\ F_1 =& \frac{F_2}{2x_B}. \end{aligned} \tag{6.43}$$

In our model, the u and d quarks are degenerate and differ only by their charges, hence we can define a generic valence parton distribution $v(x_B)$ such that:

$$v(x_B)=u_v(x_B)=\bar{u}_v(x_B)=d_v(x_B)=\bar{d}_v(x_B), \tag{6.44}$$

with the condition

$$\int_0^1 v(x_B)dx_B=\frac{1}{2}. \tag{6.45}$$

We can thus derive the following condition upon F_1:

$$\int_0^1 F_1(x_B)dx_B=\frac{5}{18}. \tag{6.46}$$

The other rule is relative to the fraction momentum $(= 2\langle x_B\rangle)$carried by the partons. Generically, we can state that this fraction, denoted by $\mathcal{F}$, is given by

$$\mathcal{F}=4\int_0^1 x_B F_1(x_B)dx_B=\frac{18}{5}\int_0^1 F_2(x_B)dx_B. \tag{6.47}$$

A sensible range of values for $\mathcal{F}$ is between 0.5 and 0.6. This condition and Eq. (6.47) gives us the sum rule on F_2.

6.3.4 Plots and Results

In this section, we show different plots of F_1, F_2 and their moments as functions of either x_B or Q^2 obtained, first without cut-off and with g fixed without any considerations on the normalisation. Then are presented the final results, with cut-off and with the value of g obtained with our procedure of normalisation thanks to the quark sum rule.

Preliminary results without cut-off

Here we present four plots obtained with the different methods exposed above. In the following, we will only put plots for the extraction from $\sigma_{contr.}$ as all give the same results.

The different curves in a plot correspond to different values of the quark mass (recall that the u and d quarks are degenerate in our model). The purpose of these plots is to illustrate the evolution of the results when the quark mass changes. The value of the parameter (for $\Lambda = \infty$, g fixed) are given in the Tab. 6.1:

m_q(GeV)	0.15	0.2	0.25	0.3	0.35	0.35	0.4	0.45
m_π (MeV)	138	138	138	138	138	138	138	138
g	3.2	3.2	3.2	3.2	3.2	3.2	3.2	3.2
m_q(GeV)	0.50	0.55	0.60	0.65	0.70	0.75	0.80	
m_π (MeV)	138	138	138	138	138	138	138	
g	3.2	3.2	3.2	3.2	3.2	3.2	3.2	

Table 6.1: Values of the parameters for the six following plots.

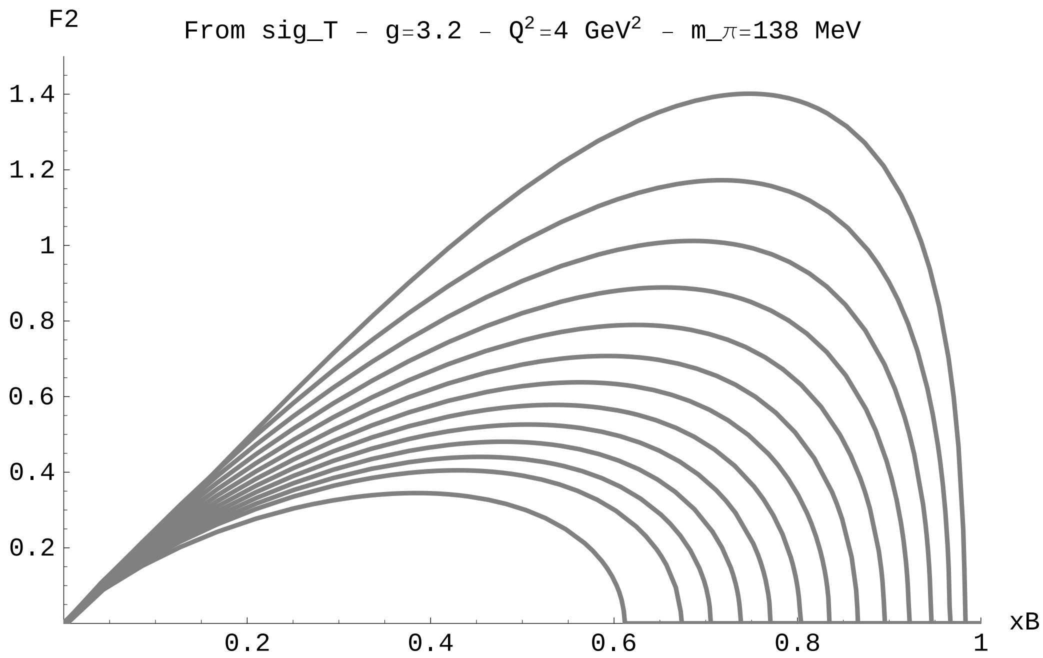

Figure 6.6: F_2 from the direct extraction of W_1 from σ_T and for the values of m_q given in Tab. 6.1.

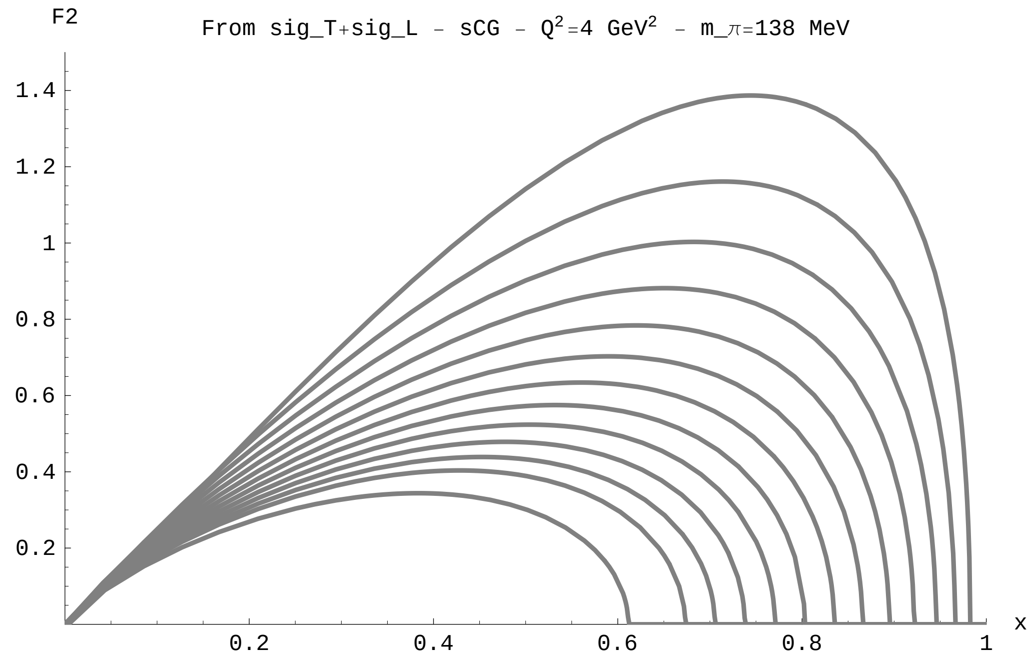

Figure 6.7: F_2 from the extraction of W_2 from σ_L and σ_T and for the values of m_q given in Tab. 6.1.

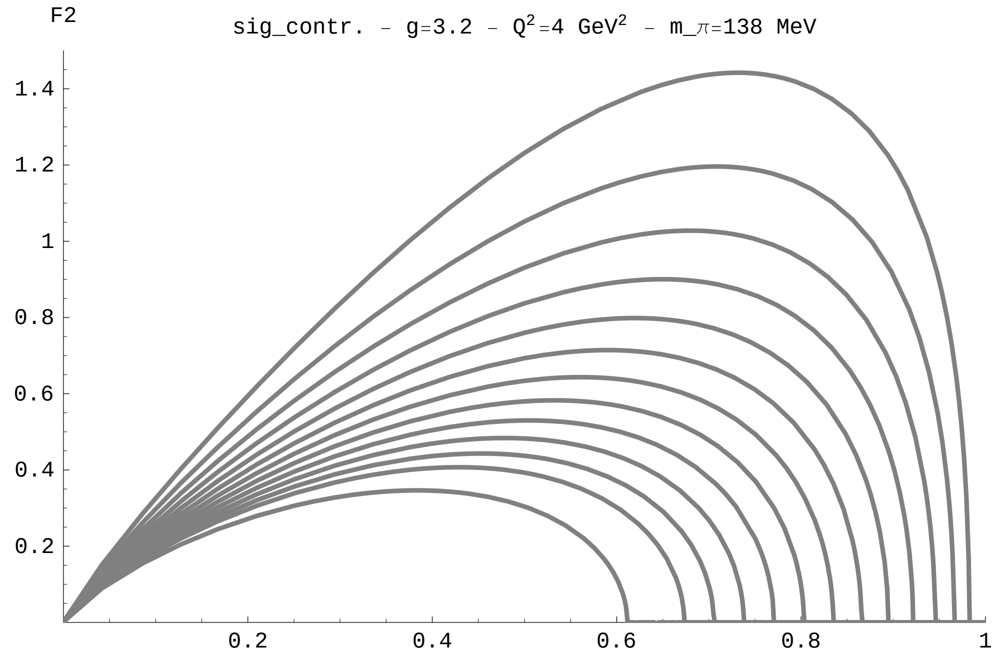

Figure 6.8: F_2 from the extraction of W_2 from $\sigma_{contr.}$, the scaling and the Callan-Gross relations and for the values of m_q given in Tab. 6.1.

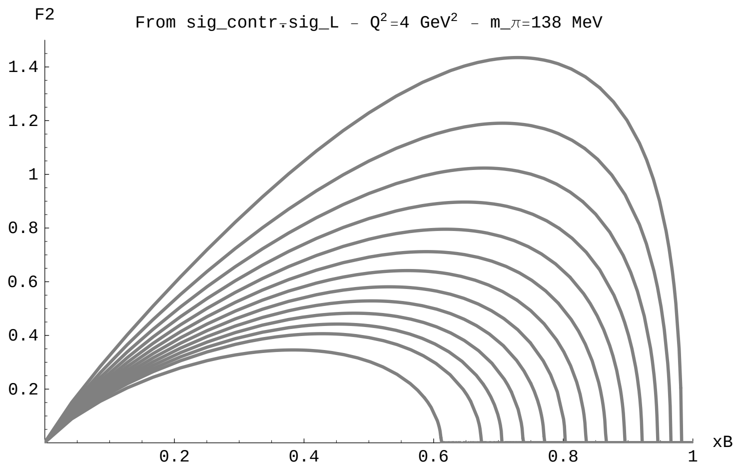

Figure 6.9: F_2 from the extraction of W_1 from $\sigma_{contr.}$ and σ_L and for the values of m_q given in Tab. 6.1.

As we have seen on the plots, the curve for F_2 as a function of x_B reaches zero before x_B is 1. This is due to a kinematical threshold: if we fix Q^2, increasing the value of x_B corresponds to lowering s. Hence, it is natural to reach a value of x_B such that the energy in the CM frame is not sufficient to produce two on-shell quarks as required in the process $\gamma^\star\pi^0 \to q\bar{q}$ or equivalently to put on their mass shell the two intermediate quarks in $\gamma^\star\pi^0 \to \gamma^\star\pi^0$ in order to get this time an imaginary part to the amplitude from which will arise the structure functions. It is thus clear why, when m_q increases, the x_B range gets smaller. We can also foresee the same dependence for the moments of F_1 relative to m_q.

Beside the plot for F_2, we can plot F_1 –Fig. 6.10 corresponds to Fig. 6.8.

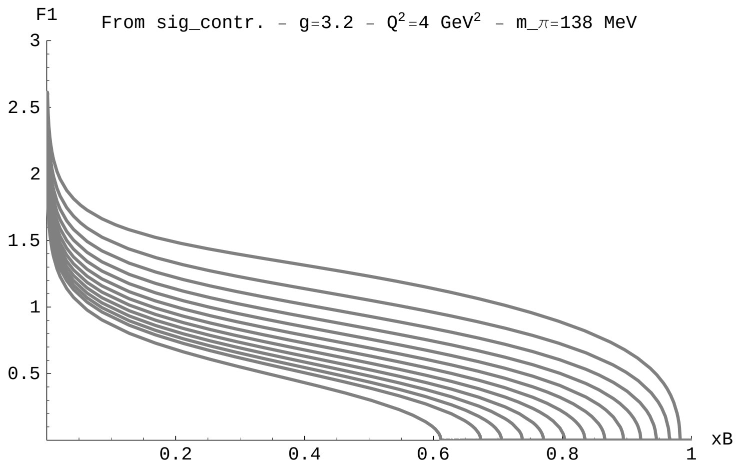

Figure 6.10: F_1 from the extraction of W_2 from $\sigma_{contr.}$, the scaling and the Callan-Gross relations and for the values of m_q given in Tab. 6.1.

With a simple[11] cut-off

As we have seen in section 6.2.4, the presence of a cut-off is a necessity as it simulates the size of the pion and, as a consequence makes the crossed diagram contributions higher-twists. Let us now analyze its effect on the evolution of F_2 as a function of x_B at a given Q^2. We recall that, from now on, only the extraction from the contracted cross-section is plotted (see Fig. 6.11).

We thus see that the cut-off tends to reduce, on the one hand, the value of $F_2(x_B)$ and on the other hand the range where it is non-vanishing. This reduction of the range corresponds to the cases where x_B, Q^2 and Λ_t are such that the kinematical limit t_{max} is lower than Λ_t : the set $[\Lambda_t, t_{max}]$ is thus empty. The reduction of F_2 is then when we have only $t_{min} < \Lambda_t < t_{max}$.

We can also observe a discontinuity in the first derivative of F_2 due to the cut-off. This is why we shall only consider our results as valid in the region where Q^2 is much larger than the cut-off; this restriction is anyway required for Bjorken scaling. Another argument in favour of this restriction will be exposed in the next section.

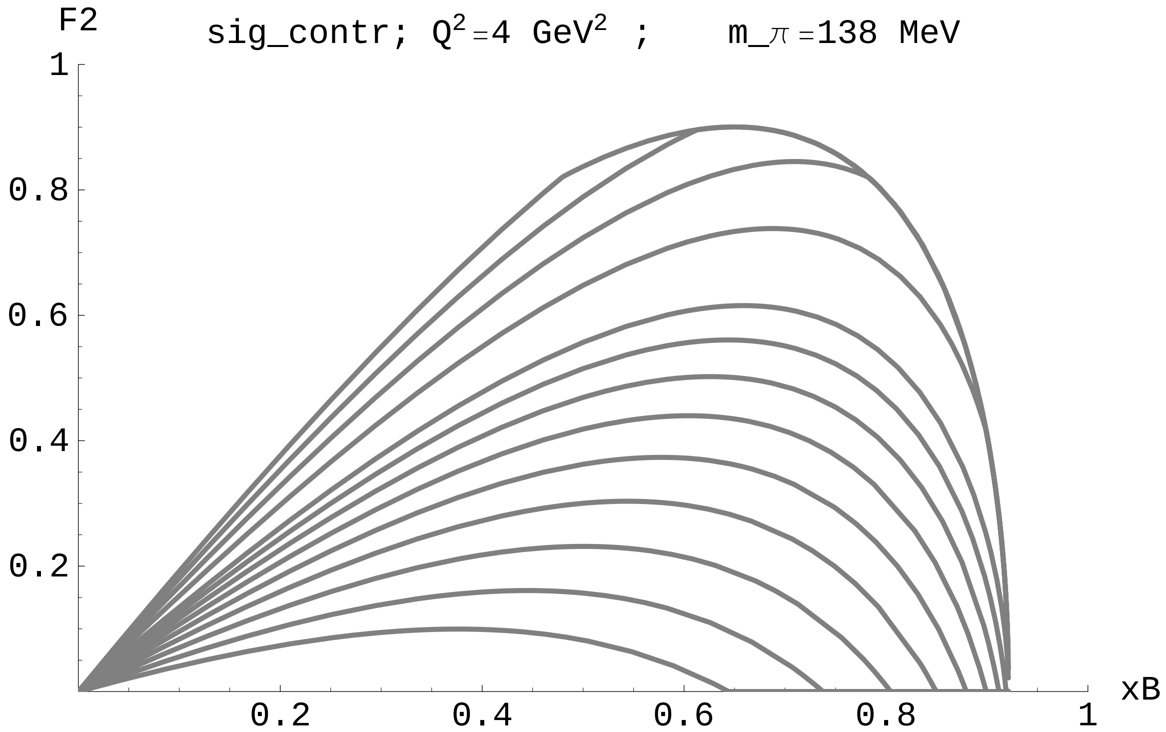

Figure 6.11: Evolution of F_2 for Λ_t from -8 GeV to -0.16 GeV.

[11] In this example, we apply the cut-off only for one vertex; but the following interpretations are similar when the procedure explained above is applied.

Final Results with Cut-off and Normalisation

Here are the plots obtained with a cut-off and the normalisation from the quark sum rule.

First we show the dependence of the coupling constant on Q^2 for four sets of m_q and Λ (which is here the maximum relative momentum allowed).

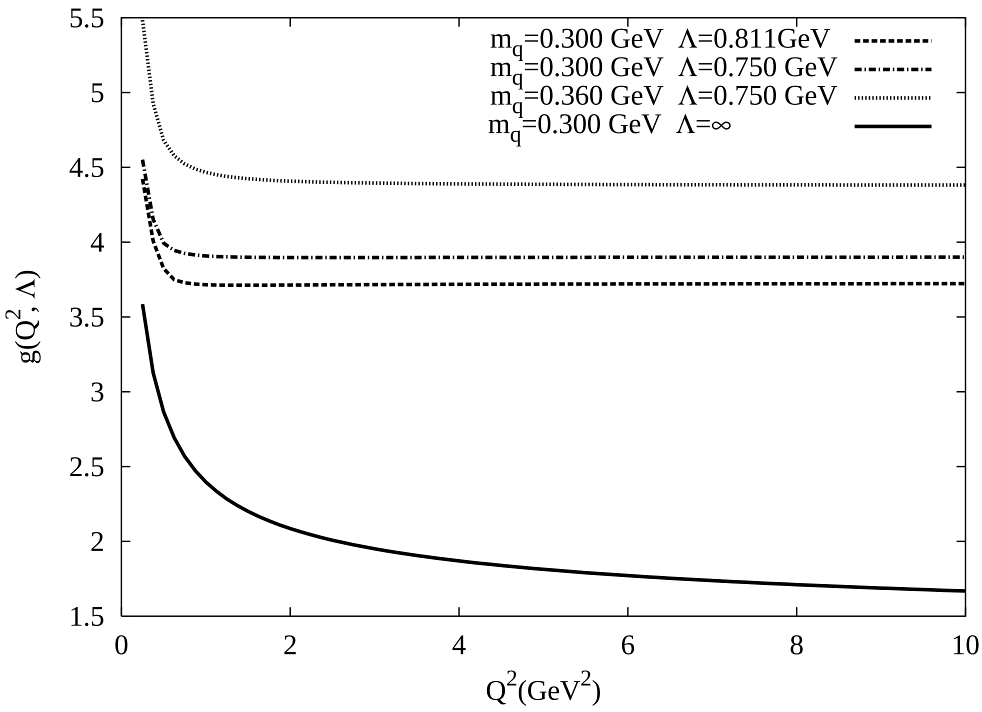

Figure 6.12: Plot of g as a function of Q^2 and for different values of Λ .

The important point to notice is that the coupling constant becomes independent of Q^2 when the latter is much greater than Λ; this is due to a sort of saturation, in the sense that an additional increase of energy has no effect because of the cut-off (this effect of course does not appear for an infinite cut-off). Moreover we notice that a bigger value for the cut-off implies a smaller value for g. This is normal as the cut-off reduces the structure functions; hence to keep the sum rule satisfied, g must increase.

We also observe that the influence of the quark mass can be significant, at least for the value of g. As we will see later, its effect on the momentum fraction ($2\langle x_B \rangle = \frac{18}{5}\int F_2(x)dx$) is less significant.

Let us now consider the evolution of $g_\infty(= \lim\limits_{Q^2\to\infty} g(\Lambda, Q^2))$ as a function of Λ. As we have just said, when Λ increases, g and thus g_∞ decreases. The results we obtained by plotting $g_\infty(\Lambda)$ are shown in Fig. 6.13.

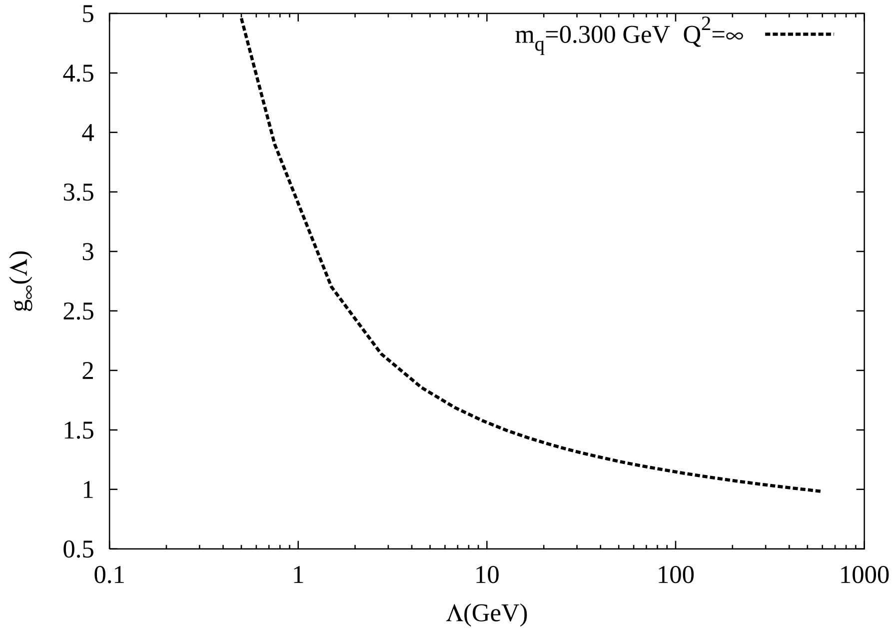

Figure 6.13: Plot of g_∞ as a function of Λ.

The value of g being determined by our normalisation procedure, we can obtained $F_2(x_B)$. We plot it for $Q^2 = 10$ GeV^2 for the reasons exposed in the previous section and also because we want to stay in the region where the coupling constant becomes independent of Q^2.

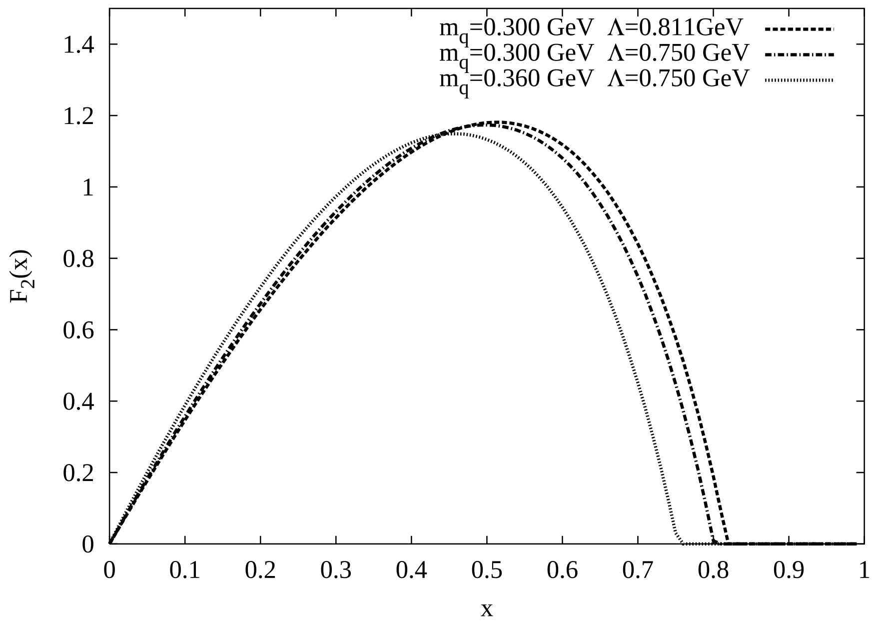

Figure 6.14: Plot of F_2 at $Q^2 = 10$ GeV^2.

From $F_2(x_B)$, we may also obtain the momentum fraction of the partons (here the two constituent quarks). Once again, we reach constant values for large values of Q^2, except for an infinite cut-off in which case $2\langle x_B\rangle$ tends to 1 for infinitely large Q^2.

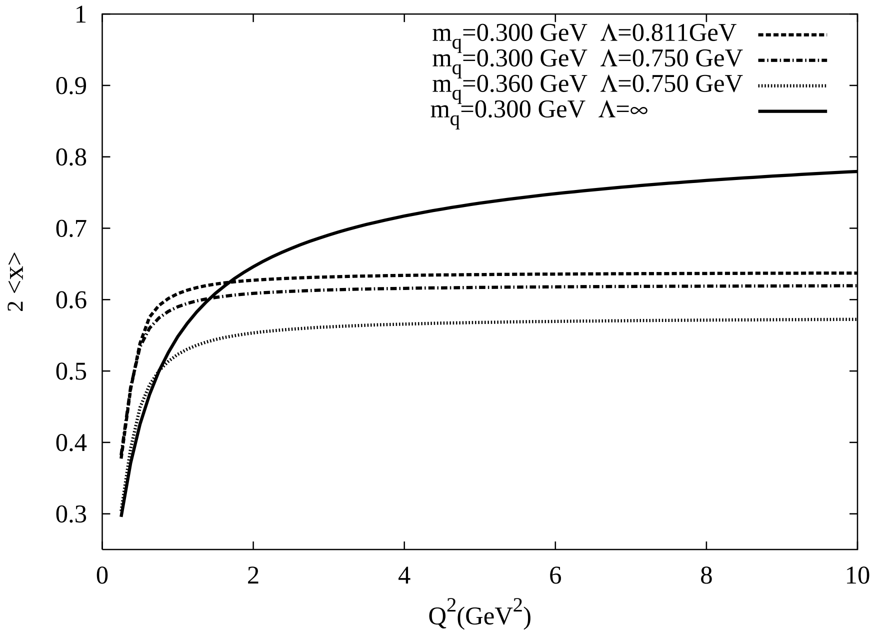

Figure 6.15: Plot of $2\langle x_B\rangle$ as a function of Q^2 and for different values of Λ

An essential point to notice is that for sensible values of the cut-off, we get momentum fractions fully compatible with results given in the literature. The values for g are also compatible with the ones obtained within the context of the NJL model (compare Fig. 6.1 and Fig. 6.13).

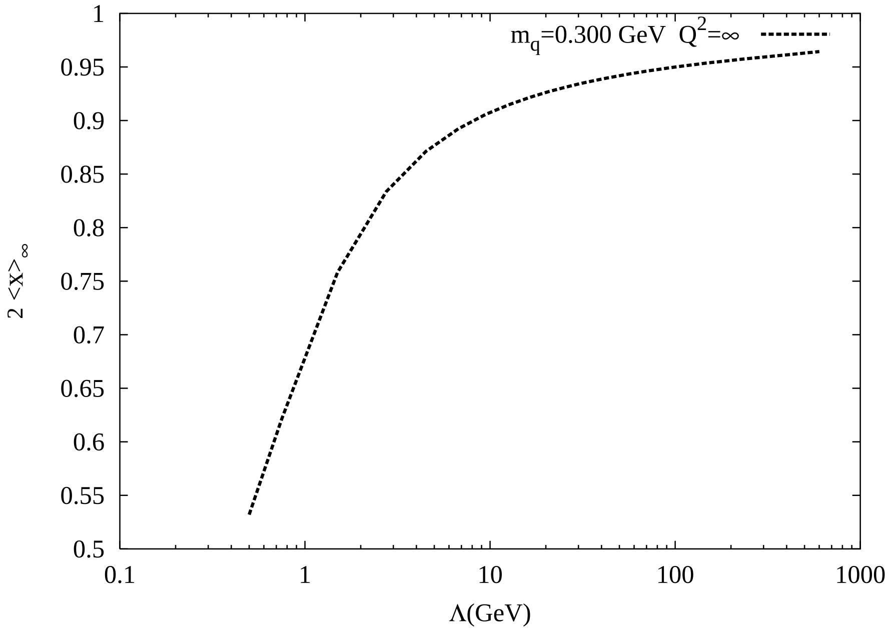

Figure 6.16: Plot of $2\langle x_B\rangle_\infty$ as a function of Λ.

Chapter 7

Structure Functions of a Scalar Particle

In this Chapter, we extend our calculation to the case of a scalar particle. This extension is valid as long as the particle considered has a mass lower than twice the mass of its constituent quarks.

If we choose a quark constituent mass to be 500 MeV (as some authors do in NJL applications), mesons such $a_0(980)$ and $f_0(980)$ are likely to satisfy this condition and our calculation becomes applicable. As we shall consider only scalar isoscalar particles here, our main application will be the $f_0(980)$ state.

7.1 Which Differences Compared to the Pion Case ?

As all calculations will be based on the considerations of the previous Chapter, let us analyse the common points and the differences that are likely to appear.

In fact the situation is quite clear: if we consider the same quark content as for the pion, the one and only difference between the two calculations comes from the vertex factor.

For the neutral pion, we saw that the vertex factor was:

$$ig_{\pi qq}\gamma^5, \tag{7.1}$$

now, for a scalar particle, we simply have (see Appendix A):

$$g_{\sigma qq}, \tag{7.2}$$

with the generic name σ for the scalar (independently of the identification of the studied scalar with the so-called sigma particle).

The kinematics is absolutely identical, as well as the way we shall obtain the structure functions from the polarised cross-sections. Therefore we directly focus on their calculation.

7.1.1 Amplitude Calculation

Analytical Expression

As in the previous case, we apply Feynman rules for the process shown in Fig. 7.1 and we directly obtain the analytical expression of the squared amplitude. For a given polarisation of the virtual photon, $i = L, T_1, T_2$, and with our conventions (see Appendix A) we have the following expression for the direct contribution to the squared amplitude,

$$|\mathcal{M}_i|^2 = 3g_{\sigma qq}^2(e_u^2 + e_d^2)\mathrm{Tr}\left((-\not{k}_4 + m)\frac{\not{k}_3 - \not{q} + m}{(k_3-q)^2 - m^2}\gamma^{\mu'}\right. \\ \left.(\not{k}_3 + m)\gamma^{\mu}\frac{\not{k}_3 - \not{q} + m}{(k_3-q)^2 - m^2}\right)\varepsilon_{i\mu}\varepsilon^{\star}_{i\mu'}. \tag{7.3}$$

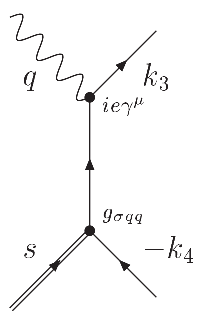

Figure 7.1: One of the two Feynman diagrams for the process $\gamma^{\star}\sigma \to q\bar{q}$.

As all the other kinematical quantities, the polarisation vectors keep the same form (see section 6.2.2). We just recall here the expressions for the polarised cross-sections:

$$\begin{aligned} \sigma_{T_1} &= \frac{1}{16\pi\lambda}3g^2(e_u^2 + e_d^2)\int \mathrm{d}t\ T^{\mu\mu'}\varepsilon_{T_1,\mu}\varepsilon^{\star}_{T_1\mu'} \\ \sigma_{T_2} &= \frac{1}{16\pi\lambda}3g^2(e_u^2 + e_d^2)\int \mathrm{d}t\ T^{\mu\mu'}\varepsilon_{T_2,\mu}\varepsilon^{\star}_{T_2\mu'} \\ \sigma_{L} &= \frac{1}{16\pi\lambda}3g^2(e_u^2 + e_d^2)\int \mathrm{d}t\ T^{\mu\mu'}\varepsilon_{L,\mu}\varepsilon^{\star}_{L\mu'} \\ \sigma_{contr.} &= \frac{1}{16\pi\lambda}3g^2(e_u^2 + e_d^2)\int \mathrm{d}t\ T^{\mu\mu'}(g_{\mu\mu'} + \frac{q_\mu q_{\mu'}}{Q^2}). \end{aligned} \tag{7.4}$$

7.1.2 Integration, t, Cut-off and all that Stuff...

The integration was done in exactly the same way, only the results from REDUCE trace calculations were modified. The cut-off was applied as well in the same way as for the pion case. The discussion about the gauge invariance is also obviously valid here.

7.2 The Results

As the effect of the quark mass and the cut-off are the same, we directly show the final results, with the cut-off and the normalisation from the quark sum rule. Hence we first show the dependence of the coupling constant on Q^2 for four sets of m_q and Λ.

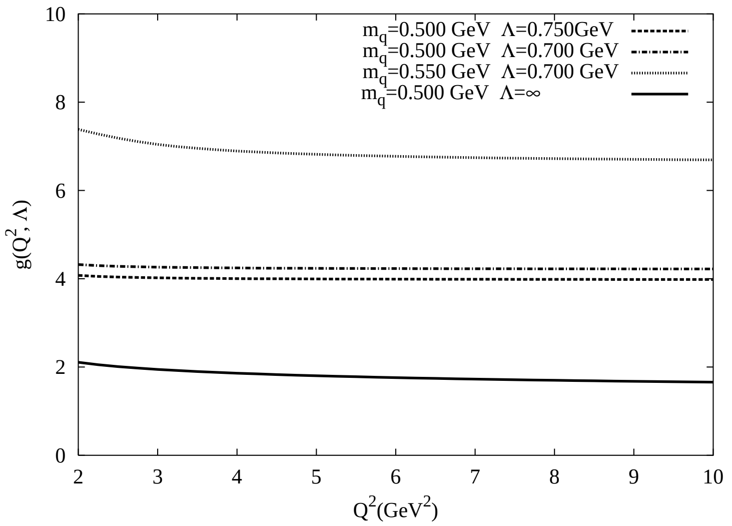

Figure 7.2: Plot of g as a function of Q^2 and for different values of Λ .

Now let us consider the evolution of $g_\infty (= \lim_{Q^2 \to \infty} g(\Lambda, Q^2))$ as a function of Λ. Here is what we obtained for $g_\infty(\Lambda)$:

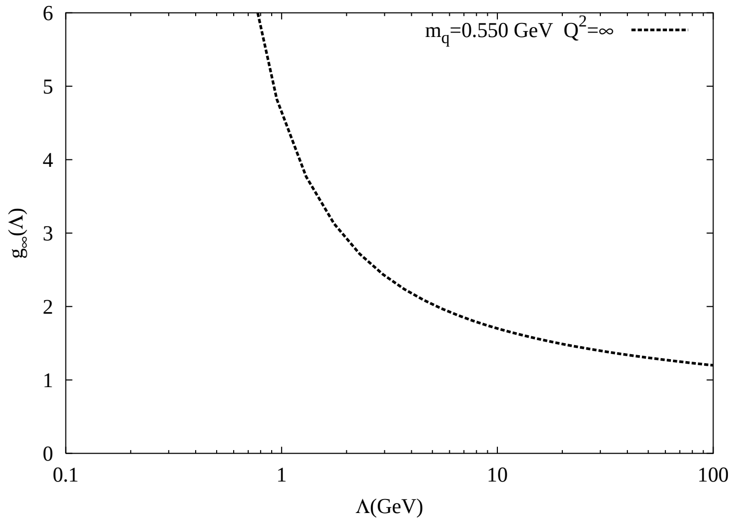

Figure 7.3: Plot of g_∞ as a function of Λ.

We plot here $F_2(x_B)$ for $Q^2 = 10$ GeV^2 (10 GeV^2 is chosen for the same reasons as in the pion case).

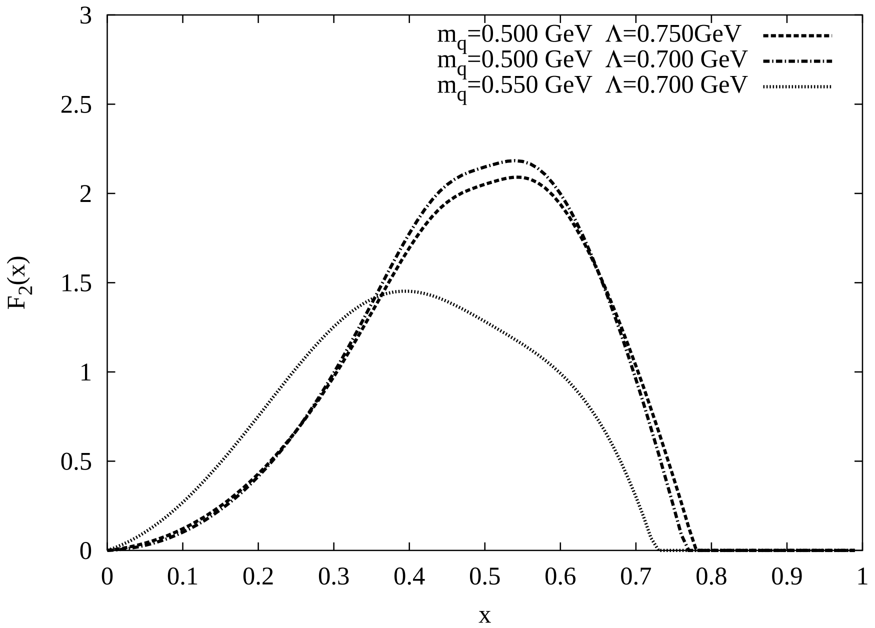

Figure 7.4: Plot of F_2 at $Q^2 = 10$ GeV.

From $F_2(x_B)$, we also obtain the momentum fraction of the partons.

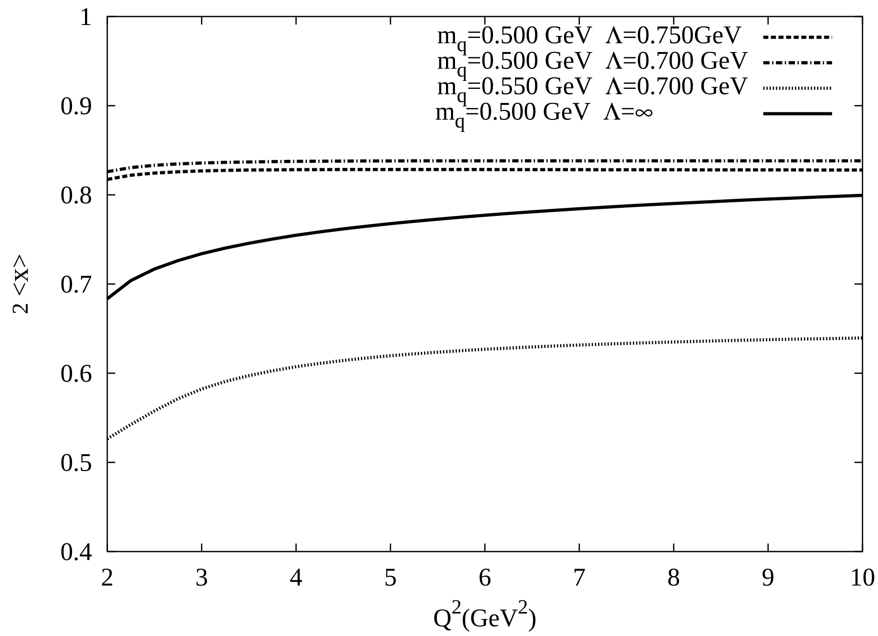

Figure 7.5: Plot of $2\langle x_B \rangle$ as a function of Q^2 and for different values of Λ

We get momentum fractions somehow larger than for the pion. On the other hand, the values for g are just a bit higher, but the variations seem to depend strongly on the quark mass which may vary significantly when we consider different mesons within the context of NJL models. The principal conclusion is therefore that the behaviour is the same as for the pion. The coupling constant and the momentum fraction reach a plateau when the cut-off procedure is applied, and the values of g are sensible and compatible with other normalisation conditions.

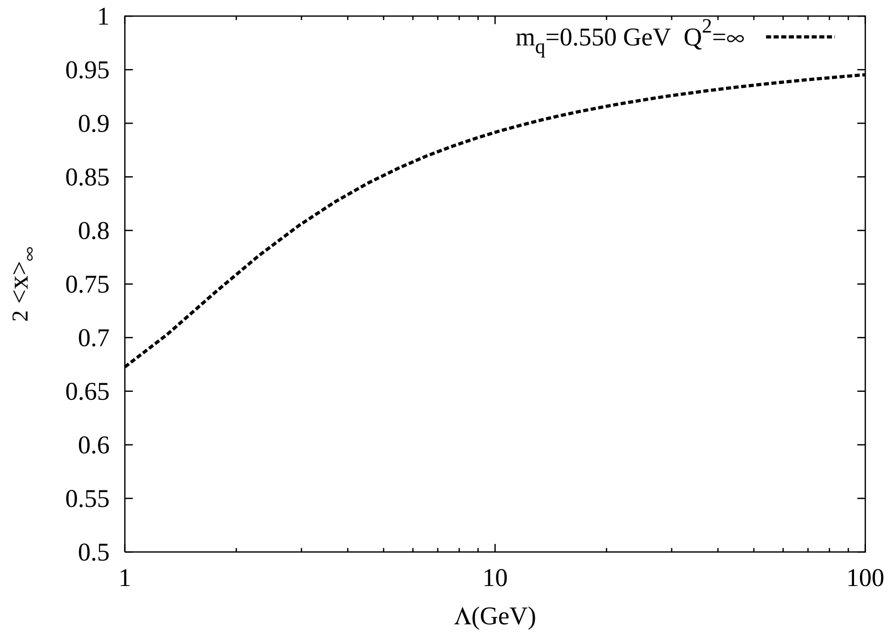

Figure 7.6: Plot of $2\left\langle x_B \right\rangle_\infty$ as a function of Λ.

Chapter 8

Conclusion and Outlook

From a simple model describing neutral pions and scalar particles, we have obtained the corresponding structure functions. This simple model initially introduced the finite size of the pion at the level of the vertex factor. Technically, this was realized by imposing a cut-off on the relative momentum of the quarks at the meson-quark-antiquark vertex.

However, a re-interpretation of this cut-off enabled us to obtain the structure functions, directly and in a gauge invariant way, through $\gamma^\star$-meson forward elastic-scattering cross-section. From this we could then extract the two functions W_1 and W_2 describing the hadronic current. The effect of the cut-off was to make the crossed diagram contributions, contained in the amplitude of the latter process, disappear linearly as Q^2 increases.

Therefore, for sufficiently large Q^2, we could obtain a direct relation between the –gauge invariant– cross-section for $\gamma^\star$-meson forward elastic-scattering and the wanted functions. Using the Bjorken scaling relations, which apply when the energy in the system is sufficient, we eventually obtained the two structure functions F_1 and F_2. We also obtained that the latter were linked by the Callan-Gross relation, as predicted for spin one-half constituents –the quarks here.

Concerning the structure of the vertex, we normalised the coupling constant imposing the quark sum rule, constraining the integral of F_1 by imposing that the number of quarks and antiquarks within the meson was two. This way of normalising the vertex coupling constant is justified by the presence of a cut-off in the problem which allows a probabilistic interpretation. If we had performed the normalisation by the means of the form factors, we would have introduced gauge dependent quantities in our calculations. This would have been annoying as all the other ingredients were gauge invariant since our cut-off was just a limitation on an observable of the problem, *i.e.* the Mandelstam variable t for $\gamma^\star$meson $\to q\bar{q}$.

On the other hand, depending on the meson, we described its scalar or pseudoscalar character through the introduction of the right tensorial structure at the vertex, *i.e.* 1 for the scalar particle and the γ^5 Dirac matrix for the pion.

Finally the numerical results we obtained showed clear signs of saturation of the system for large Q^2 (compared to the cut-off), which in terms of g and –longitudinal– momentum fraction $\langle 2x_B \rangle$ induces the appearance of plateaus for these quantities.

Having now at our disposal the diagonal structure functions for either neutral pions (or more generally neutral pseudoscalar particles) or scalar particles, we hope to get a better understanding of off-forward structure functions of these particles.

A first step in this direction would be to *off-diagonalise* the kinematics, allowing the final photon and meson to have a different momentum from the initial ones but still imposing the intermediate quarks to be on-shell or equivalently considering only the imaginary part of the amplitude. Then we shall perhaps have more precise ideas concerning the essential properties of the different contributions, and hence be able to initiate the study of the real part of the amplitude within an off-diagonal kinematics.

Appendix A

Feynman Rules, Color, Spin and Isospin Space

A.1 Vertex Factors

The factor for the vertex pion-quark-antiquark (see Fig. A.1) is

$$g_{\pi q\bar{q}} i\gamma_5 \vec{\tau}_i, \;\; i = 1, 2, 3, \tag{A.1}$$

for scalar-quark-antiquark it is then[1]

$$g_{\sigma q\bar{q}}, \tag{A.2}$$

and for the photon, we have

$$i\varepsilon^{\mu}(k)\hat{Q}\gamma_{\mu}. \tag{A.3}$$

These factors correspond to the choice of a Dirac scalar pure isoscalar (the σ particle) and of a Dirac pseudoscalar pure isovector (*i.e.* the three pions).

More precisely, this gives, for the three pion states, π^-, π^0, π^+, for the σ and for the photon, the following matrix factors for the isospin space:

- π^-: $\begin{pmatrix} 0 & 0 \\ \sqrt{2} & 0 \end{pmatrix}$
- π^0: $\begin{pmatrix} 1 & 0 \\ 0 & -1 \end{pmatrix}$
- π^+: $\begin{pmatrix} 0 & \sqrt{2} \\ 0 & 0 \end{pmatrix}$

[1] The fact that we have i in pseudoscalar vertex factor and not in the scalar one, can be understood from the form of the Lagrangian: $\mathcal{L}_{\text{int}} = -\bar{\psi}\mathbf{M}\psi$ with $\mathbf{M} = g_\sigma\phi_\sigma + ig_\pi\gamma^5\phi_\pi$ (ϕ_σ and ϕ_π are 2×2 hermitian matrix fields). For further discussions, see [16] and references therein, *e.g.* [24].

- σ: $\begin{pmatrix} 1 & 0 \\ 0 & 1 \end{pmatrix}$
- γ: $\begin{pmatrix} e_u & 0 \\ 0 & e_d \end{pmatrix}$

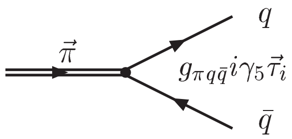

Figure A.1: Feynman rule for the vertex $\vec{\pi} \rightarrow q\bar{q}$

A.2 A First Example: $\pi^0 \rightarrow \gamma\gamma$

Let us consider the decay of the neutral pion into two photons. In term of Feynman diagrams, we have two contributions:

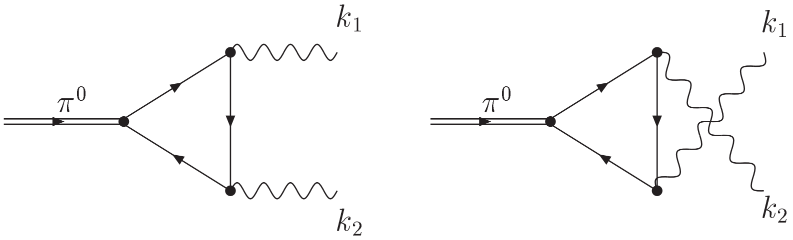

Figure A.2: Feynman graphs of the π^0 decay into two photons.

The internal lines represent the quarks u or d.

A.2.1 Isospin Space

According to the rules given in section A.1, we have the following contribution from the isospin space trace:

$$\mathrm{Tr}\left\{\begin{pmatrix} 1 & 0 \\ 0 & -1 \end{pmatrix}\begin{pmatrix} e_u & 0 \\ 0 & e_d \end{pmatrix}\begin{pmatrix} e_u & 0 \\ 0 & e_d \end{pmatrix}\right\} = \mathrm{Tr}\begin{pmatrix} e_u^2 & 0 \\ 0 & -e_d^2 \end{pmatrix} = e_u^2 - e_d^2 \tag{A.4}$$

Note here that the corresponding trace for $\pi^\pm$ decay in two photons is fortunately zero, in agreement with charge conservation.

A.2.2 Color Space

The color being conserved at either a pion-quark-antiquark or a photon-quark-antiquark, we simply put a kronecker symbol δ^{ab} imposing that color of the quark a is the same as the color of the antiquark b.

Therefore, the trace upon the product of factor for each vertex function gives simply N_c, *i.e.* 3.

A.2.3 Spin Space

Remembering the pseudoscalar nature of the π^0, we put a γ^5 Dirac matrix at the pion-quark-antiquark vertex (cf. Eq. (A.1)) and as usual a γ^μ Dirac matrix at photon vertices (cf. Eq. (A.3)). Thus for the first diagram of Fig.A.2, we get the following trace to calculate for the direct contribution:

$$\mathrm{Tr}\left(\gamma^5 \frac{\not{q}_1 + m}{q_1^2 - m^2}\gamma^{\mu'} \frac{\not{q}_2 + m}{q_2^2 - m^2}\gamma^{\mu} \frac{\not{q}_3 + m}{q_3^2 - m^2}\right) \varepsilon^\star_{i\mu}\varepsilon^\star_{i\mu'}, \tag{A.5}$$

with q_1, q_2 and q_3 the momenta of the three internal quark lines.

A.3 Another Example: $\gamma^\star\pi^0 \to q\bar{q}$

As this calculation is exposed in section 6.2.2, we simply describe in a few lines how the flavour factor in Eq. (6.15) is obtained.

Still according to the rules given in section A.1, we have the following contribution from the isospin space trace:

$$\begin{aligned}&\mathrm{Tr}\left\{\begin{pmatrix}1 & 0\\ 0 & -1\end{pmatrix}\begin{pmatrix}e_u & 0\\ 0 & e_d\end{pmatrix}\begin{pmatrix}e_u & 0\\ 0 & e_d\end{pmatrix}\begin{pmatrix}1 & 0\\ 0 & -1\end{pmatrix}\right\} = \\ &\mathrm{Tr}\begin{pmatrix}e_u^2 & 0\\ 0 & e_d^2\end{pmatrix} = e_u^2 + e_d^2\end{aligned} \tag{A.6}$$

Let us analyse the difference with the previous process. First the sign between the squared charge is different; secondly, if we had considered the case of the π^+ or of the π^-, we could have seen that this time the result was not zero because the charge is conserved in such processes.

Appendix B

REDUCE codes used

B.1 Pion Case

```
on div,gcd;

vector k3,k4,q,p,epsl,epst1,epst2;

% Calcul de produits scalaires de epsl avec les autres 4-vect.

% déf des vecteurs de polarisation.
let epsl.q=0;
let epst1.q=0;
let epst2.q=0;
let epsl.epsl=1;
let epst1.epst1=-1;
let epst2.epst2=-1;

% PRODUITS SCALAIRES AVEC epsl:
%______________________________

% Expression de epsl.p (Syst du CM):
% epl=1/sqrt(Q2)*(q_z,0,0,q_0)
% p=(E_pi,0,0,-q_z)
% Rappel: sqrt(s)=E+E_pi
let epsl.p=1/sqrt(Q2)*sqrt(En**2+Q2)*sqrt(s);


% Expression de epsl.k3 (Syst du CM):
%k3=(sqrt(s)/2,0,-|k3|*sin(theta),|k3|*cos(theta))
%k4=(sqrt(s)/2,0,|k3|*sin(theta),-|k3|*cos(theta))
%t=(k3-q)**2=(k4-p)**2=m**2+mp**2-sqrt(s)/2*(En-sqrt(s))+2|k3|cos(theta)
%Avec En=(s-mp**2-Q2)/(2*sqrt(s))
% => |k3|*cos(theta)= (t-mq**2-mp**2/2+s/2+Q2/2)/(2*sqrt(En**2+Q2))
% =>
let epsl.k3= 1/sqrt(Q2)*(sqrt(En**2+Q2)*sqrt(s)/2-
En*(t-mq**2-mp**2/2+s/2+Q2/2)/(2*sqrt(En**2+Q2)));

let En=(s-mp**2-Q2)/(2*sqrt(s));


% PRODUITS SCALAIRES AVEC epsti:
%______________________________

% Expression de epst.p (Syst du CM):
% epst1=(0,1,0,0)
% epst2=(0,0,1,0)
```

```
% p=(E_pi,0,0,-q_z)
let epst1.p=0;
let epst2.p=0;


% Expression de epsti.k3 (Syst du CM):
% |k3|*sin(theta)=|k3|*sqrt(1-(t-mq**2-mp**2/2+s/2+Q2/2)**2
%/(2*sqrt(En**2+Q2)*sqrt(s/4-mq**2)**2))
let epst1.k3=0;
let epst2.k3=sqrt(s/4-mq**2)*sqrt(1-(t-mq**2-mp**2/2+s/2+Q2/2)**2
/(2*sqrt(En**2+Q2)*sqrt(s/4-mq**2)**2));

%REMARQUE: Pourrait faire apparaitre des sqrt(t), mais dans le cas de notre
% amplitude, seul (epst.k3)**2 apparaît

% AUTRES PRODUITS SCALAIRES :
%____________________________


let
p.p=mp**2,
q.q=-Q2,
k3.k3=mq**2,
k4=p+q-k3,
% k4.k4=mq**2
k3.p=(mp**2-Q2)/2+p.q-k3.q,
%p.q=nu,
p.q=(s+Q2-mp**2)/2,
k3.q=(mq**2-Q2-t)/2;

let sqrt(1/s)=1/sqrt(s);
let abs(mp**2 + Q2 + s)=mp**2 + Q2 + s;

pause;

% Calcul des traces;


% Diagrammes box.


% facteur "2" car 2 diagrammes (le photon frappe le quark ou l'anti-quark)
%de meme contribution
% facteur "4": facteur dû à REDUCE.


%directs & cas où le photon frappe le quark
2*4*G(l1,a)*(-G(l1,k4)+mq)*G(l1,a)*(G(l1,k3-q)+mq)*G(l1,MUP)*(G(l1,k3)+mq)*
G(l1,MU)*(G(l1,k3-q)+mq)*(MU.MUP+(q.MU*q.MUP)/Q2)$
trace1_tot:=ws;
%croisés & cas où le photon frappe l'antiquark --ça change rien anyway--
2*4*G(l2,a)*(G(l2,-k3+q)+mq)*G(l2,MU)*(-G(l2,k3)+mq)*G(l2,a)*(G(l2,k4-q)+mq)*
G(l2,MUP)*(G(l2,k4)+mq)*(MU.MUP+(q.MU*q.MUP)/Q2)$
trace2_tot:=ws;
index MU,MUP;



%Amplitude longitudinale:
%_________________________

%directs
2*4*G(l1,a)*(-G(l1,k4)+mq)*G(l1,a)*(G(l1,k3-q)+mq)*G(l1,epsl)*(G(l1,k3)+mq)*
G(l1,epsl)*(G(l1,k3-q)+mq)$
trace1_L:=ws;
```

```
%croisés
2*4*G(l2,a)*(G(l2,-k3+q)+mq)*G(l2,epsl)*(-G(l2,k3)+mq)*G(l2,a)*(G(l2,k4-q)+mq)*
G(l2,epsl)*(G(l2,k4)+mq)$
trace2_L:=ws;


%Amplitudes transverses :
%_________________________

% 1)

%directs
2*4*G(l1,a)*(-G(l1,k4)+mq)*G(l1,a)*(G(l1,k3-q)+mq)*G(l1,epst1)*(G(l1,k3)+mq)*
G(l1,epst1)*(G(l1,k3-q)+mq)$
trace1_T1:=ws;

%croisés
2*4*G(l2,a)*(G(l2,-k3+q)+mq)*G(l2,epst1)*(-G(l2,k3)+mq)*G(l2,a)*(G(l2,k4-q)+mq)*
G(l2,epst1)*(G(l2,k4)+mq)$
trace2_T1:=ws;

% 2)

%directs
2*4*G(l1,a)*(-G(l1,k4)+mq)*G(l1,a)*(G(l1,k3-q)+mq)*G(l1,epst2)*(G(l1,k3)+mq)*
G(l1,epst2)*(G(l1,k3-q)+mq)$
trace1_T2:=ws;

%croisés
2*4*G(l2,a)*(G(l2,-k3+q)+mq)*G(l2,epst2)*(-G(l2,k3)+mq)*G(l2,a)*(G(l2,k4-q)+mq)*
G(l2,epst2)*(G(l2,k4)+mq)$
trace2_T2:=ws;



on factor;
propagateurs1:=1/((k3-q).(k3-q)-mq**2)**2;

propagateurs2:=1/((k3-q).(k3-q)-mq**2)*1/((k4-q).(k4-q)-mq**2);

off nat;
amplitude1_tot:=trace1_tot*propagateurs1;
amplitude2_tot:=trace2_tot*propagateurs2;

ampl_tot:=amplitude1_tot+amplitude2_tot;

amplitude1_L:=trace1_L*propagateurs1;
amplitude2_L:=trace2_L*propagateurs2;

ampl_L=amplitude1_L+amplitude2_L;

amplitude1_T1:=trace1_T1*propagateurs1;
amplitude2_T1:=trace2_T1*propagateurs2;


amplitude1_T2:=trace1_T2*propagateurs1;
amplitude2_T2:=trace2_T2*propagateurs2;


%ne mélange pas les prop (meilleur pour intégrer,
% si on ne veut pas intégrer tout en un)
ampltitude1_T:=amplitude1_T1+amplitude1_T2;
ampltitude2_T:=amplitude2_T1+amplitude2_T2;
```

```
end;
```

B.2 Scalar Case

```
on div,gcd;

vector k3,k4,q,p,epsl,epst1,epst2;

% Calcul de produits scalaires de epsl avec les autres 4-vect.

% déf des vecteurs de polarisation.
let epsl.q=0;
let epst1.q=0;
let epst2.q=0;
let epsl.epsl=1;
let epst1.epst1=-1;
let epst2.epst2=-1;

% PRODUITS SCALAIRES AVEC epsl:
%______________________________

% Expression de epsl.p (Syst du CM):
% epl=1/sqrt(Q2)*(q_z,0,0,q_0)
% p=(E_pi,0,0,-q_z)
% Rappel: sqrt(s)=E+E_pi
let epsl.p=1/sqrt(Q2)*sqrt(En**2+Q2)*sqrt(s);



% Expression de epsl.k3 (Syst du CM):
%k3=(sqrt(s)/2,0,-|k3|*sin(theta),|k3|*cos(theta))
%k4=(sqrt(s)/2,0,|k3|*sin(theta),-|k3|*cos(theta))
%t=(k3-q)**2=(k4-p)**2=m**2+mp**2-sqrt(s)/2*(En-sqrt(s))+2|k3|cos(theta)
%Avec En=(s-mp**2-Q2)/(2*sqrt(s))
% => |k3|*cos(theta)= (t-mq**2-mp**2/2+s/2+Q2/2)/(2*sqrt(En**2+Q2))
% =>
let epsl.k3= 1/sqrt(Q2)*(sqrt(En**2+Q2)*sqrt(s)/2
-En*(t-mq**2-mp**2/2+s/2+Q2/2)/(2*sqrt(En**2+Q2)));

let En=(s-mp**2-Q2)/(2*sqrt(s));


% PRODUITS SCALAIRES AVEC epsti:
%______________________________

% Expression de epst.p (Syst du CM):
% epst1=(0,1,0,0)
% epst2=(0,0,1,0)
% p=(E_pi,0,0,-q_z)
let epst1.p=0;
let epst2.p=0;

% Expression de epsti.k3 (Syst du CM):
% |k3|*sin(theta)=|k3|*sqrt(1-(t-mq**2-mp**2/2+s/2+Q2/2)**2
%/(2*sqrt(En**2+Q2)*sqrt(s/4-mq**2)**2))
let epst1.k3=0;
let epst2.k3=sqrt(s/4-mq**2)*sqrt(1-(t-mq**2-mp**2/2+s/2+Q2/2)**2
/(2*sqrt(En**2+Q2)*sqrt(s/4-mq**2)**2));

%REMARQUE: Pourrait faire apparaitre des sqrt(t), mais dans le cas de notre
% amplitude, seul (epst.k3)**2 apparaît
```

```
% AUTRES PRODUITS SCALAIRES :
%____________________________


let
p.p=mp**2,
q.q=-Q2,
k3.k3=mq**2,
k4=p+q-k3,
% k4.k4=mq**2
k3.p=(mp**2-Q2)/2+p.q-k3.q,
%p.q=nu,
p.q=(s+q2-mp**2)/2,
k3.q=(mq**2-Q2-t)/2;

let sqrt(1/s)=1/sqrt(s);
let abs(mp**2 + Q2 + s)=mp**2 + Q2 + s;


% Calcul des traces;

%Amplitude contractée avec (MU.MUP+(q.MU*q.MUP)/Q2):
%__________________________________________________

% facteur "2" car 2 diagrammes (le photon frappe le quark ou l'anti-quark)
%de meme contribution
% facteur "4": facteur dû à REDUCE.

%Matrice de Dirac au vertex scalaire-quark-antiquark.
dirac:=1;

%directs
2*4*dirac*(-G(l1,k4)+mq)*dirac*(G(l1,k3-q)+mq)*G(l1,MUP)*(G(l1,k3)+mq)*
G(l1,MU)*(G(l1,k3-q)+mq)*(MU.MUP+(q.MU*q.MUP)/Q2)$
trace1_contr:=ws;
%croisés
2*4*dirac*(G(l2,-k3+q)+mq)*G(l2,MU)*(-G(l2,k3)+mq)*dirac*(G(l2,k4-q)+mq)*
G(l2,MUP)*(G(l2,k4)+mq)*(MU.MUP+(q.MU*q.MUP)/Q2)$
trace2_contr:=ws;
index MU,MUP;



%Amplitude longitudinale:
%_________________________

%directs
2*4*dirac*(-G(l1,k4)+mq)*dirac*(G(l1,k3-q)+mq)*G(l1,epsl)*(G(l1,k3)+mq)*
G(l1,epsl)*(G(l1,k3-q)+mq)$
trace1_L:=ws;

%croisés
2*4*dirac*(G(l2,-k3+q)+mq)*G(l2,epsl)*(-G(l2,k3)+mq)*dirac*(G(l2,k4-q)+mq)*
G(l2,epsl)*(G(l2,k4)+mq)$
trace2_L:=ws;


%Amplitudes transverses :
%_________________________

% 1)
```

```
%directs
2*4*dirac*(-G(l1,k4)+mq)*dirac*(G(l1,k3-q)+mq)*G(l1,epst1)*(G(l1,k3)+mq)*
G(l1,epst1)*(G(l1,k3-q)+mq)$
trace1_T1:=ws;

%croisés
2*4*dirac*(G(l2,-k3+q)+mq)*G(l2,epst1)*(-G(l2,k3)+mq)*dirac*(G(l2,k4-q)+mq)*
G(l2,epst1)*(G(l2,k4)+mq)$
trace2_T1:=ws;

% 2)

%directs
2*4*dirac*(-G(l1,k4)+mq)*dirac*(G(l1,k3-q)+mq)*G(l1,epst2)*(G(l1,k3)+mq)*
G(l1,epst2)*(G(l1,k3-q)+mq)$
trace1_T2:=ws;

%croisés
2*4*dirac*(G(l2,-k3+q)+mq)*G(l2,epst2)*(-G(l2,k3)+mq)*dirac*(G(l2,k4-q)+mq)*
G(l2,epst2)*(G(l2,k4)+mq)$
trace2_T2:=ws;


on factor;
propagateurs1:=1/((k3-q).(k3-q)-mq**2)**2;

propagateurs2:=1/((k3-q).(k3-q)-mq**2)*1/((k4-q).(k4-q)-mq**2);

off nat;
amplitude1_contr:=trace1_contr*propagateurs1;
amplitude2_contr:=trace2_contr*propagateurs2;

ampl_contr:=amplitude1_contr+amplitude2_contr;

amplitude1_L:=trace1_L*propagateurs1;
amplitude2_L:=trace2_L*propagateurs2;

ampl_L=amplitude1_L+amplitude2_L;

amplitude1_T1:=trace1_T1*propagateurs1;
amplitude2_T1:=trace2_T1*propagateurs2;


amplitude1_T2:=trace1_T2*propagateurs1;
amplitude2_T2:=trace2_T2*propagateurs2;


%ne mélange pas les prop (meilleur pour intégrer,
% si on ne veut pas intégrer tout en un)
ampltitude1_T:=amplitude1_T1+amplitude1_T2;
ampltitude2_T:=amplitude2_T1+amplitude2_T2;

end;
```

Appendix C

MATHEMATICA codes used

C.1 Pion Case

```
<< Graphics`MultipleListPlot`
<< Graphics`Legend`

tmin[mp_, q2_, s_, mq_] =
  Re[-1 / 2 * Sqrt[(mp^4 + 2 * mp^2 * q2 - 2 * mp^2 * s + q2^2 + 2 * q2 * s + s^2) / s] *
      Sqrt[-4 * mq^2 + s] + 1 / 2 * mp^2 + mq^2 - 1 / 2 * q2 - 1 / 2 * s];
tmax[mp_, q2_, s_, mq_] = Re[1 / 2 * Sqrt[
       (mp^4 + 2 * mp^2 * q2 - 2 * mp^2 * s + q2^2 + 2 * q2 * s + s^2) / s] *
      Sqrt[-4 * mq^2 + s] + 1 / 2 * mp^2 + mq^2 - 1 / 2 * q2 - 1 / 2 * s];

lambda = (s^2 + q2^ 2 + mp^4  + 2 * s * q2  + 2 * q2 * mp^2 - 2 * s * mp^2);
```

Expression du premier cut−offsur t: t>−2*lambdaNJL^2−mq^2+mp^2/2

```
C1[co_, mp_, mq_] = -2 * co^2  - mq^2 + mp^2 / 2 ;
```

Expression du second cut−offsur t: t<2*lambdaNJL^2+3mq^2+mp^2/2 −s−q2

```
C2[co_, mp_, mq_, q2_, s_] = 2 * co^2  + 3 * mq^2 + mp^2 / 2 - s - q2 ;


cutoffsurt = -1000 * cutoff^2  - mq^2 + mp^2 / 2
```

```
AMPLITUDE Contractée avec g_ {mu nu} + q_mu q_nu / Q2 :


Int1Prim[t_, mp_, mq_, q2_, s_] = Simplify[1 / (16 * Pi * lambda) * Integrate[
      8 * (3 * mp^4 * mq^2 - mp^4 * q2 - mp^4 * t + mp^2 * mq^4 -
          4 * mp^2 * mq^2 * q2 - 3 * mp^2 * mq^2 * s - 2 * mp^2 * mq^2 * t + mp^2 * q2^2 +
          mp^2 * q2 * s + 2 * mp^2 * q2 * t + mp^2 * s * t + mp^2 * t^2 - mq^4 * q2 -
          mq^4 * s + mq^2 * q2^2 + 2 * mq^2 * q2 * s + 2 * mq^2 * q2 * t + mq^2 * s^2 +
          2 * mq^2 * s * t - q2^2 * t - 2 * q2 * s * t - q2 * t^2 - s^2 * t - s * t^2) *
       (mp^2 + mq^2 - q2 - s - t) ^ (-1) * (mq^2 - t) ^ (-2), t], TimeConstraint → 10];

Int1cutoff = Simplify[1 / (16 * Pi * lambda) * Integrate[
     8 * (3 * mp^4 * mq^2 - mp^4 * q2 - mp^4 * t + mp^2 * mq^4 - 4 * mp^2 * mq^2 * q2 -
         3 * mp^2 * mq^2 * s - 2 * mp^2 * mq^2 * t + mp^2 * q2^2 + mp^2 * q2 * s + 2 * mp^2 * q2 * t +
         mp^2 * s * t + mp^2 * t^2 - mq^4 * q2 - mq^4 * s + mq^2 * q2^2 + 2 * mq^2 * q2 * s +
         2 * mq^2 * q2 * t + mq^2 * s^2 + 2 * mq^2 * s * t - q2^2 * t - 2 * q2 * s * t - q2 * t^2 -
         s^2 * t - s * t^2) * (mp^2 + mq^2 - q2 - s - t) ^ (-1) * (mq^2 - t) ^ (-2)
     , {t, Max[cutoffsurt, tmin], tmax}], TimeConstraint → 10]
```

AMPLITUDE LONGITUDINALE:
sig_L: 1 → diagrammes box; 2→ diagrammes croisés

Intégration:

$$\texttt{IntL1Prim[t\_, mp\_, mq\_, q2\_, s\_] = FullSimplify}\Big[\,1 / (16 * \texttt{Pi} * \texttt{lambda}) *$$

$$\texttt{Integrate}\left[\frac{4\,s\,\left((q2+s)\,(mq^2-t)+mp^2\,(-mq^2+2\,q2+t)\right)^2}{q2\,\left(mp^4+2\,mp^2\,(q2-s)+(q2+s)^2\right)\,(mq^2-t)^2},\,t\right],\ \texttt{TimeConstraint} \to 10\Big]$$

$$\frac{s\left(\frac{4\,mp^4\,q2^2}{mq^2-t}-(-mp^2+q2+s)^2\,(mq^2-t)+4\,mp^2\,q2\,(mp^2-q2-s)\,\mathrm{Log}[mq^2-t]\right)}{4\,\pi\,q2\,\left(mp^4+2\,mp^2\,(q2-s)+(q2+s)^2\right)^2}$$

```
IntL2Prim[t_, mp_, mq_, q2_, s_] = FullSimplify[1 / (16 * Pi * lambda) * Integrate[
    - (4 s ((q2 + s) (mq^2 - t) + mp^2 (-mq^2 + 2 q2 + t))
        (mp^4 + mp^2 (mq^2 - 2 s - t) + (q2 + s) (-mq^2 + q2 + s + t))) /
     (q2 (mp^4 + 2 mp^2 (q2 - s) + (q2 + s)^2) (mq^2 - t) (-mp^2 - mq^2 + q2 + s + t))
    , t], TimeConstraint → 10]
```

$$-\left(s\left(-\left(mp^2-q2-s\right)^3 t+2\,mp^2\,q2\left(mp^4-2\,mp^2\,s+\left(q2+s\right)^2\right)\left(-\mathrm{Log}\left[-mq^2+t\right]+\mathrm{Log}\left[-mp^2-mq^2+q2+s+t\right]\right)\right)\right)\Big/\left(4\,\pi\,q2\left(-mp^2+q2+s\right)\left(mp^4+2\,mp^2\left(q2-s\right)+\left(q2+s\right)^2\right)^2\right)$$

AMPLITUDE TRANSVERSE:
sig_T: 1 → diagrammes box; 2→ diagrammes croisés
Facteur 1/2: cf. sig_T=1/2*(sig_T1+sig_T2)

```
IntT1Prim[t_, mp_, mq_, q2_, s_] = 1 / 2 * FullSimplify[1 / (16 * Pi * lambda) * Integrate[
      -4 * (((q2 + s) ^ 2 + mp ^ 4 + 2 * mp ^ 2 * q2 - 2 * mp ^ 2 * s) / s) ^ ((-1) / 2) *
        (Sqrt[((q2 + s) ^ 2 + mp ^ 4 + 2 * mp ^ 2 * q2 - 2 * mp ^ 2 * s) / s] *
            ((mp ^ 2 + mq ^ 2 - t) * (mq ^ 2 - q2 - s - t) + 4 * mq ^ 2 * mp ^ 2) +
          (2 * mq ^ 2 + mp ^ 2 - q2 - s - 2 * t) ^ 2 * mp ^ 2 -
          Sqrt[((q2 + s) ^ 2 + mp ^ 4 + 2 * mp ^ 2 * q2 - 2 * mp ^ 2 * s) / s] *
            ((q2 + t - mq ^ 2) * mp ^ 2 - (mq ^ 2 - q2 - s - t) * (mq ^ 2 - t))) * (mq ^ 2 - t) ^ (-2)
      , t], TimeConstraint →
     5];

IntT1cutoff = 1 / 2 * Simplify[1 / (16 * Pi * lambda) * Integrate[
      -4 * (((q2 + s) ^ 2 + mp ^ 4 + 2 * mp ^ 2 * q2 - 2 * mp ^ 2 * s) / s) ^ ((-1) / 2) *
        (Sqrt[((q2 + s) ^ 2 + mp ^ 4 + 2 * mp ^ 2 * q2 - 2 * mp ^ 2 * s) / s] *
            ((mp ^ 2 + mq ^ 2 - t) * (mq ^ 2 - q2 - s - t) + 4 * mq ^ 2 * mp ^ 2) +
          (2 * mq ^ 2 + mp ^ 2 - q2 - s - 2 * t) ^ 2 * mp ^ 2 -
          Sqrt[((q2 + s) ^ 2 + mp ^ 4 + 2 * mp ^ 2 * q2 - 2 * mp ^ 2 * s) / s] *
            ((q2 + t - mq ^ 2) * mp ^ 2 - (mq ^ 2 - q2 - s - t) * (mq ^ 2 - t))) * (mq ^ 2 - t) ^ (-2)
      , {t, Max[cutoffsurt, tmin], tmax}], TimeConstraint → 5];

IntT2Prim[t_, mp_, mq_, q2_, s_] = 1 / 2 * FullSimplify[1 / (16 * Pi * lambda) * Integrate[
      4 * (((q2 + s) ^ 2 + mp ^ 4 + 2 * mp ^ 2 * q2 - 2 * mp ^ 2 * s) / s) ^ ((-1) / 2) *
        (Sqrt[((q2 + s) ^ 2 + mp ^ 4 + 2 * mp ^ 2 * q2 - 2 * mp ^ 2 * s) / s] *
            ((mp ^ 2 + mq ^ 2 - t) * (mq ^ 2 - q2 - s - t) + 4 * mq ^ 2 * mp ^ 2) +
          (2 * mq ^ 2 + mp ^ 2 - q2 - s - 2 * t) ^ 2 * mp ^ 2 -
          Sqrt[((q2 + s) ^ 2 + mp ^ 4 + 2 * mp ^ 2 * q2 - 2 * mp ^ 2 * s) / s] *
            ((q2 + t - mq ^ 2) * mp ^ 2 - (mq ^ 2 - q2 - s - t) * (mq ^ 2 - t))) *
        (mq ^ 2 - q2 - s - t + mp ^ 2) ^ (-1) * (mq ^ 2 - t) ^ (-1)
      , t], TimeConstraint → 5];

IntT2cutoff = 1 / 2 * Simplify[1 / (16 * Pi * lambda) * Integrate[
      4 * (((q2 + s) ^ 2 + mp ^ 4 + 2 * mp ^ 2 * q2 - 2 * mp ^ 2 * s) / s) ^ ((-1) / 2) *
        (Sqrt[((q2 + s) ^ 2 + mp ^ 4 + 2 * mp ^ 2 * q2 - 2 * mp ^ 2 * s) / s] *
            ((mp ^ 2 + mq ^ 2 - t) * (mq ^ 2 - q2 - s - t) + 4 * mq ^ 2 * mp ^ 2) +
          (2 * mq ^ 2 + mp ^ 2 - q2 - s - 2 * t) ^ 2 * mp ^ 2 -
          Sqrt[((q2 + s) ^ 2 + mp ^ 4 + 2 * mp ^ 2 * q2 - 2 * mp ^ 2 * s) / s] *
            ((q2 + t - mq ^ 2) * mp ^ 2 - (mq ^ 2 - q2 - s - t) * (mq ^ 2 - t))) *
        (mq ^ 2 - q2 - s - t + mp ^ 2) ^ (-1) * (mq ^ 2 - t) ^ (-1)
      , {t, Max[cutoffsurt, tmin], tmax}], TimeConstraint → 5];
```

q2=2*xB*nu
s=mp^2-2*xB*nu+2*nu

```
IntTPrim[t_, mp_, mq_, q2_, s_] =
  IntT1Prim[t, mp, mq, q2, s] + IntT2Prim[t, mp, mq, q2, s];
```

```
IntT[co_, mp_, mq_, q2_, s_] =
  If[C1[co, mp, mq] < C2[co, mp, mq, q2, s],
   IntTPrim[tmax[mp, q2, s, mq], mp, mq, q2, s] -
    IntTPrim[tmin[mp, q2, s, mq], mp, mq, q2, s],
   If[C1[co, mp, mq] > tmax[mp, q2, s, mq], 0,
     IntTPrim[tmax[mp, q2, s, mq], mp, mq, q2, s] -
      IntTPrim[C1[co, mp, mq], mp, mq, q2, s]
    ] +
    If[C2[co, mp, mq, q2, s] < tmin[mp, q2, s, mq], 0,
     IntTPrim[C2[co, mp, mq, q2, s], mp, mq, q2, s] -
      IntTPrim[tmin[mp, q2, s, mq], mp, mq, q2, s]
    ]
  ];

IntT1[co_, mp_, mq_, q2_, s_] =
  If[C1[co, mp, mq] < C2[co, mp, mq, q2, s],
   IntT1Prim[tmax[mp, q2, s, mq], mp, mq, q2, s] -
    IntT1Prim[tmin[mp, q2, s, mq], mp, mq, q2, s],
   If[C1[co, mp, mq] > tmax[mp, q2, s, mq], 0,
     IntT1Prim[tmax[mp, q2, s, mq], mp, mq, q2, s] -
      IntT1Prim[C1[co, mp, mq], mp, mq, q2, s]
    ] +
    If[C2[co, mp, mq, q2, s] < tmin[mp, q2, s, mq], 0,
     IntT1Prim[C2[co, mp, mq, q2, s], mp, mq, q2, s] -
      IntT1Prim[tmin[mp, q2, s, mq], mp, mq, q2, s]
    ]
  ];

IntT2[co_, mp_, mq_, q2_, s_] =
  If[C1[co, mp, mq] < C2[co, mp, mq, q2, s],
   IntT2Prim[tmax[mp, q2, s, mq], mp, mq, q2, s] -
    IntT2Prim[tmin[mp, q2, s, mq], mp, mq, q2, s],
   If[C1[co, mp, mq] > tmax[mp, q2, s, mq], 0,
     IntT2Prim[tmax[mp, q2, s, mq], mp, mq, q2, s] -
      IntT2Prim[C1[co, mp, mq], mp, mq, q2, s]
    ] +
    If[C2[co, mp, mq, q2, s] < tmin[mp, q2, s, mq], 0,
     IntT2Prim[C2[co, mp, mq, q2, s], mp, mq, q2, s] -
      IntT2Prim[tmin[mp, q2, s, mq], mp, mq, q2, s]
    ]
  ];

IntT[co_, mp_, mq_, q2_, s_] = IntTPrim[tmax[mp, q2, s, mq], mp, mq, q2, s] -
   IntTPrim[tmin[mp, q2, s, mq], mp, mq, q2, s];
```

```
Int1cutoff=Simplify[Int1cutoff,mp>0&& mq>0 && nu >0 && 0<xB<1,TimeConstraint → 10]
```

```
Int1[co_, mp_, mq_, q2_, s_] =
  If[C1[co, mp, mq] < C2[co, mp, mq, q2, s],
   Int1Prim[tmax[mp, q2, s, mq], mp, mq, q2, s] -
    Int1Prim[tmin[mp, q2, s, mq], mp, mq, q2, s],
   If[C1[co, mp, mq] > tmax[mp, q2, s, mq], 0,
     Int1Prim[tmax[mp, q2, s, mq], mp, mq, q2, s] -
      Int1Prim[C1[co, mp, mq], mp, mq, q2, s]
    ] +
    If[C2[co, mp, mq, q2, s] < tmin[mp, q2, s, mq], 0,
     Int1Prim[C2[co, mp, mq, q2, s], mp, mq, q2, s] -
      Int1Prim[tmin[mp, q2, s, mq], mp, mq, q2, s]
    ]
  ];

Int1[co_, mp_, mq_, q2_, s_] = Int1Prim[tmax[mp, q2, s, mq], mp, mq, q2, s] -
   Int1Prim[tmin[mp, q2, s, mq], mp, mq, q2, s];
```

```
IntLPrim[t_, mp_, mq_, q2_, s_] =
  IntL1Prim[t, mp, mq, q2, s] + IntL2Prim[t, mp, mq, q2, s];
```

```
IntL[co_, mp_, mq_, q2_, s_] =
  If[C1[co, mp, mq] < C2[co, mp, mq, q2, s],
   IntLPrim[tmax[mp, q2, s, mq], mp, mq, q2, s] -
    IntLPrim[tmin[mp, q2, s, mq], mp, mq, q2, s],
   If[C1[co, mp, mq] > tmax[mp, q2, s, mq], 0,
     IntLPrim[tmax[mp, q2, s, mq], mp, mq, q2, s] -
      IntLPrim[C1[co, mp, mq], mp, mq, q2, s]
    ] +
    If[C2[co, mp, mq, q2, s] < tmin[mp, q2, s, mq], 0,
     IntLPrim[C2[co, mp, mq, q2, s], mp, mq, q2, s] -
      IntLPrim[tmin[mp, q2, s, mq], mp, mq, q2, s]
    ]
  ];

IntL[co_, mp_, mq_, q2_, s_] = IntLPrim[tmax[mp, q2, s, mq], mp, mq, q2, s] -
   IntLPrim[tmin[mp, q2, s, mq], mp, mq, q2, s];
```

```
IntL=Simplify[(IntL1buffer+IntL2buffer),mp>0&&mq>0 && nu >0 && 0<xB<1,TimeConstraint → 10]

IntT=Simplify[(IntT1buffer+IntT2buffer),mp>0&&mq>0 && nu >0 && 0<xB<1,TimeConstraint → 5];

 IntTcutoff=Simplify[(IntT1cutoff+IntT2cutoff),mp>0&&mq>0 && nu >0 && 0<xB<1,TimeConstraint → 5];
```

NOTE: Pas de besoin de mettre des facteurs pour l'évaluation du rapport des contributions croisées–box
Ils disparaissent évidemment dans le rapport !!!

```
IntRapport[co_, mp_, mq_, q2_, s_] = IntT1[co, mp, mq, q2, s] / IntT2[co, mp, mq, q2, s];
```

```
IntRapport=Simplify[IntT2cutoff/(IntT1cutoff),mp>0&&mq>0 && nu >0 && 0<xB<1,TimeConstraint → 5]
```

En mettant les facteurs de couleurs: 3; Pas de 1/Sqrt[3]: on considère le pion comme un photon
Facteur 1/2 enlevé:supposé etre le facteur d'isospin

```
K = 1 / 2 * 1 / mp * Sqrt[lambda];
e = Sqrt[4 * Pi * 1 / 137];
facteur = 3 * g^2 * e^2 * ((1 / 3)^2 + (2 / 3)^2);

xlim[q2_, mp_, mq_] = q2 / (q2 - mp^2 + 4 mq^2);
```

W1 par IntT en utilisant Callan–Gross

```
W1a=Simplify[K/(4*Pi^    2*1/137)*IntNew[tmin,tmax,C1,C2]*facteur,ComplexityFunction→(Count[{#1},-
Log,∞]&),TimeConstraint → 10]
```

```
W1a[co_, mp_, mq_, q2_, xB_] = K / (4 * Pi^ 2 * 1 / 137) * IntT[co, mp, mq, q2, s] * facteur
   /. s → (mp^2 - q2 + q2 / xB);

F1a[co_, mp_, mq_, q2_, xB_] = mp * W1a[co, mp, mq, q2, xB];

F2a[co_, mp_, mq_, q2_, xB_] = 2 * xB * F1a[co, mp, mq, q2, xB];

Export["/home/lansberg/mathematica/out.dat", {{5.7, 4.3}, {-1.2, 7.8}}]
```

```
Plot3D[Re[F2a[co, 0.138, 0.3, q2, 0.5] / (2 * 0.5) /. g → 1], {q2, 1, 100}, {co, 0.5, 10}]
```

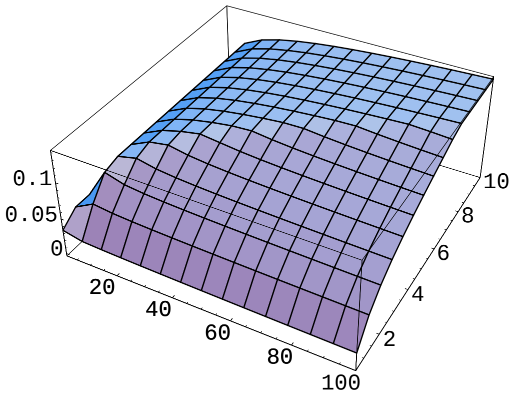


```
- SurfaceGraphics -
```

```
Plot[Evaluate[Table[Re[F1a[0.7, 0.138, 0.3, q2, xB] /. g → 1], {q2, 1, 20, 2}]],
 {xB, 0.000001, 1}]
```

Rapport des contributions: IL FAUT METTRE LE CUT-OFF!!!!!!

```
Rapport = IntRapport /. mp → 0.138 /. mq → 0.3 /. cutoff → 0.8
```

W2 par (IntL+IntT) sans utiliser Callan-Gross

```
W2sCG[co_, mp_, mq_, q2_, xB_] =
  K / (4 * Pi ^ 2 * 1 / 137) * facteur * (2 * xB * mp ^ 2) / (2 * xB * mp ^ 2 + q2 / (2 * xB)) *
    (IntL[co, mp, mq, q2, s] + IntT[co, mp, mq, q2, s]) /. s → (mp ^ 2 - q2 + q2 / xB);

F2sCG[co_, mp_, mq_, q2_, xB_] = q2 / (2 * xB * mp) * W2sCG[co, mp, mq, q2, xB];
```

```
Plot3D[Re[F2sCG[co, 0.138, 0.3, q2, 0.5] / (2 * 0.5) /. g → 1],
 {q2, 1, 100}, {co, 0.5, 10}]
```

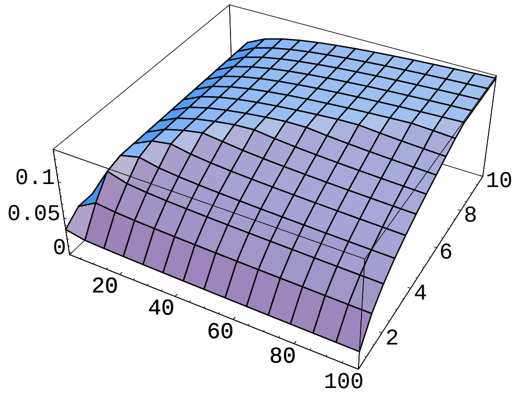


```
- SurfaceGraphics -
```

```
Plot[
 Evaluate[Table[Re[F2sCG[0.7, 0.138, 0.3, q2, xB] / (2 * xB) /. g → 1], {q2, 1, 20, 2}]],
 {xB, 0.000001, 1}]
```

W2 par Int1 en utilisant Callan−Grosspour relier W1 & W2 (déjà à la 1ère equation)

```
W2c[co_, mp_, mq_, q2_, xB_] =
  K / (4 * Pi ^ 2 * 1 / 137) * (xB * mp ^ 2) / (xB * mp ^ 2 - q2 / (2 * xB)) *
    Int1[co, mp, mq, q2, s] * facteur /. s → (mp ^ 2 - q2 + q2 / xB) ;

F2c[co_, mp_, mq_, q2_, xB_] = q2 / (2 * xB * mp) * W2c[co, mp, mq, q2, xB];

Plot3D[Re[F2c[co, 0.138, 0.3, q2, 0.5] / (2 * 0.5) /. g → 1], {q2, 1, 100}, {co, 0.5, 10}]
```

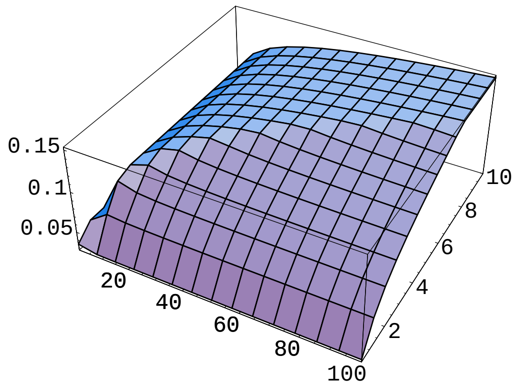


```
- SurfaceGraphics -
```

```
Plot[
 Evaluate[Table[Re[F2c[0.7, 0.138, 0.3, q2, xB] / (2 * xB) /. g → 1], {q2, 1, 20, 2}]],
 {xB, 0.000001, 1}, FrameLabel → {"xB", "F1/g^2", "", ""},
 Frame -> True, Axes → False, RotateLabel → False]
```

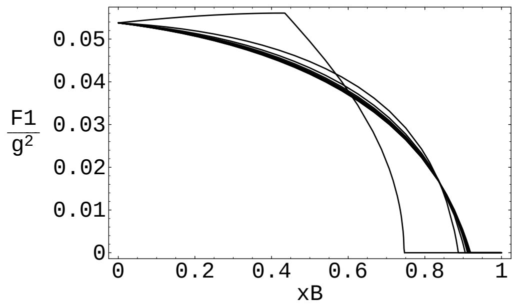

- Graphics -

```
Plot[Evaluate[Table[Re[F2c[0.4, 0.138, 0.3, q2, xB] /. g → 1], {q2, 0.4, 10, 0.2}]],
 {xB, 0.000001, 1}, FrameLabel → {"xB", "F2/g^2", "", ""},
 Frame -> True, Axes → False, RotateLabel → False]
```

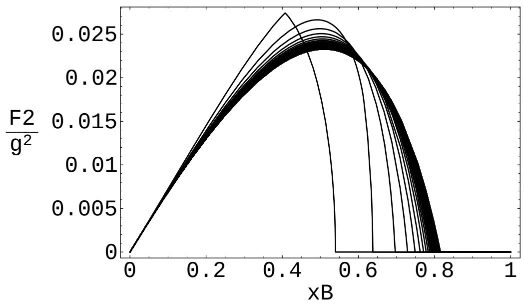

- Graphics -

W1 par (Int1-IntL)en utilisant Callan-Gross(3ème équation)

```
W1d[co_, mp_, mq_, q2_, xB_] =
  K / (-8 * Pi ^ 2 * 1 / 137) * (Int1[co, mp, mq, q2, s] - IntL[co, mp, mq, q2, s]) * facteur /.
   s → (mp ^ 2 - q2 + q2 / xB) ;

F1d[co_, mp_, mq_, q2_, xB_] = mp * W1d[co, mp, mq, q2, xB];

F2d[co_, mp_, mq_, q2_, xB_] = 2 * xB * F1d[co, mp, mq, q2, xB];
```

```
Plot3D[Re[F1d[co, 0.138, 0.3, q2, 0.5] /. g → 1], {q2, 1, 100}, {co, 0.5, 10}]

- SurfaceGraphics -

Plot[Evaluate[Table[Re[F1d[0.7, 0.138, 0.3, q2, xB] /. g → 1], {q2, 1, 20, 2}]],
 {xB, 0.000001, 1} Axes → False, FrameLabel → {"Q^2 (GeV^2)", "g^2", "", ""}]
```

W1 par IntTcutoff en utilisant Callan–Gross

```
W1cutoffa = K / (4 * Pi ^ 2 * 1 / 137) * IntTcutoff * facteur;

F1cutoffa = mp * W1cutoffa /. mp → 0.138

F1cutoffa = mp * W1cutoffa /. mp → 0.138 /. nu → (4 / 2 / xB);

F2cutoffa = 2 * xB * F1cutoffa /. mp → 0.138 /. nu → (4 / 2 / xB);
```

W2 par Int1 en utilisant Callan–Grosspour relier W1 &W2 (déjà à la 1ère equation)

```
W2cutoffc = K / (4 * Pi ^ 2 * 1 / 137) * (xB * mp ^ 2) / (xB * mp ^ 2 - nu) * Int1cutoff * facteur

F2cutoffc = nu / mp * W2cutoffc /. mp → 0.138 /. nu → (4 / 2 / xB)
```

Courbes en fonctions de Q^2.

Domaine de variation sur Q^2: Q^2=a+b*(i−1),avec i variant de 1 à 20 par pas de 1.

```
a = 0.25;
b = 0.125;
Listdesco = {0.764 / 2};
Listdescoetm = {{0.27, 0.872}, {0.29, 0.828},
   {0.3, 0.811}, {0.32, 0.784}, {0.34, 0.764}, {0.36, 0.75}};

Listdescoetmwanted = {{0.3, 10000000000000000000000000000000000000000000000000},
   {0.3, 0.811}, {0.3, 0.75}, {0.36, 0.75}};

Listdesg2 =
  Table[{a + b * (ii - 1), 5 / 18 / NIntegrate[Re[F2c[Listdescoetm[[j]][[2]] / 2, 0.138,
          Listdescoetm[[j]][[1]], a + b * (ii - 1), xB] / (2 * xB) /. g → 1] *
       UnitStep[Re[F2c[Listdescoetm[[j]][[2]] / 2, 0.138, Listdescoetm[[j]][[1]],
           a + b * (ii - 1), xB] / (2 * xB) /. g → 1]],
      {xB, 0.00000001, xlim[a + b * (ii - 1), 0.138, Listdescoetm[[j]][[1]]]}]},
   {j, 1, 6}, {ii, 1, 10, 1}];

Listdesgwanted = Table[{a + b * (ii - 1),
     Sqrt[5 / 18 / NIntegrate[Re[F2c[Listdescoetmwanted[[j]][[2]] / 2, 0.138,
             Listdescoetmwanted[[j]][[1]], a + b * (ii - 1), xB] / (2 * xB) /. g → 1] *
         UnitStep[Re[F2c[Listdescoetmwanted[[j]][[2]] / 2, 0.138,
              Listdescoetmwanted[[j]][[1]], a + b * (ii - 1), xB] / (2 * xB) /. g → 1]],
        {xB, 0.00000001, xlim[a + b * (ii - 1), 0.138, Listdescoetmwanted[[j]][[1]]]}]]},
   {j, 1, 4}, {ii, 1, 80, 1}];


A Q ^ 2 infini :

qdeux = 2000000;
aa = 0.5;
bb = 0.25;
```

```
Plot[Evaluate[Table[Re[F1d[0.7, 0.138, 0.3, q2, xB] /. g → 1], {q2, 1, 20, 2}]],
 {xB, 0.000001, 1}]
```

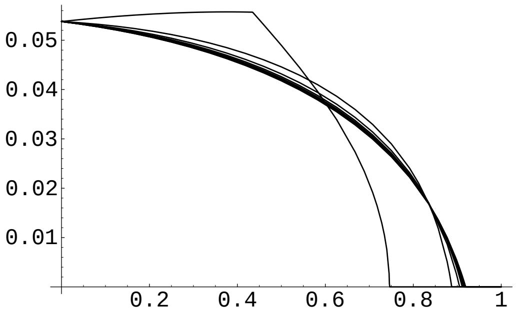


```
- Graphics -
```

W1 par IntTcutoff en utilisant Callan−Gross

```
W1cutoffa = K / (4 * Pi ^ 2 * 1 / 137) * IntTcutoff * facteur;

F1cutoffa = mp * W1cutoffa /. mp → 0.138

F1cutoffa = mp * W1cutoffa /. mp → 0.138 /. nu → (4 / 2 / xB);

F2cutoffa = 2 * xB * F1cutoffa /. mp → 0.138 /. nu → (4 / 2 / xB);
```

W2 par Int1 en utilisant Callan−Grosspour relier W1 &W2 (déjà à la 1ère equation)

```
W2cutoffc = K / (4 * Pi ^ 2 * 1 / 137) * (xB * mp ^ 2) / (xB * mp ^ 2 - nu) * Int1cutoff * facteur

F2cutoffc = nu / mp * W2cutoffc /. mp → 0.138 /. nu → (4 / 2 / xB)
```

Courbes en fonctions de Q^2.

Domaine de variation sur Q^2: Q^2=a+b*(i−1),avec i variant de 1 à 20 par pas de 1.

```
In[169]:= a = 1;
          b = 0.25;
          Listdesco = {0.2, 0.4, 0.6, 0.8, 1.2};
          Listdescoetmwanted =
            {{0.5, 1000000000000000000000000000000000000000000000000000},
             {0.5, 0.75}, {0.5, 0.7}, {0.55, 0.7}};

        Listdesg2 = Table[{a + b * (ii - 1), 5 / 18 / NIntegrate[Re[
                F2c[Listdesco[[j]], 0.138, 0.3, a + b * (ii - 1), xB] / (2 * xB) /. g → 1] * UnitStep[
                Re[F2c[Listdesco[[j]], 0.138, 0.3, a + b * (ii - 1), xB] / (2 * xB) /. g → 1]],
            {xB, 0.00000001, xlim[a + b * (ii - 1), 0.138, 0.3]}]}, {j, 1, 5}, {ii, 1, 40, 1}];
        MultipleListPlot[Listdesg2, Frame → True, Background -> RGBColor[0.8, 0.9, 0.8],
         PlotJoined → True, PlotLabel → "∫F1dx= 5/18 → g^2  - m_π=138 MeV- m_q=300 MeV",
         Axes → False, FrameLabel → {"Q^2 (GeV^2)", "g^2", "", ""}, RotateLabel → False,
         PlotRange → {3, 25}, PlotLegend → {"0.6", "0.75", "0.9", "1.05"},
         LegendLabel → "Cut-Off", LegendPosition → {0.9, -0.4}, LegendTextSpace → 1,
         LegendLabelSpace → .1, LegendOrientation → Vertical, LegendShadow → {.02, -.04}]
        Sqrt[Listdesg2];
        Listdesg2;
```

```
MultipleListPlot[Listdesg2, Frame → True, PlotJoined → True,
 PlotLabel → "∫F1dx= 5/18 → g²  - m_π=138 MeV", Axes → False,
 FrameLabel → {"Q² (GeV²)", "g²", "", ""}, RotateLabel → False,
 PlotRange → {10, 25}, PlotLegend → {".872", ".828", ".811", ".784", ".764", ".750"},
 LegendLabel → "Cut-Off", LegendPosition → {0.925, -0.4}, LegendTextSpace → 1.25,
 LegendLabelSpace → .1, LegendOrientation → Vertical, LegendShadow → {.02, -.04}]
Sqrt[Listdesg2];
Listdesg2;
```

```
- Graphics -
```

```
TableForm[Transpose[Sqrt[Listdesg2]]]

Mlist = Table[{a + b * (i - 1), Listdesg2[[j]][[i]][[2]] * 18 / 5 *
    NIntegrate[Re[F2c[Listdescoetm[[j]][[2]] / 2, 0.138, Listdescoetm[[j]][[1]],
         a + b * (i - 1), xB] /. g → 1] * UnitStep[Re[F2c[Listdescoetm[[j]][[2]] / 2,
          0.138, Listdescoetm[[j]][[1]], a + b * (i - 1), xB] /. g → 1]], {xB, 0.01,
      xlim[a + b * (i - 1), 0.138, Listdescoetm[[j]][[1]]]}]}, {j, 1, 6}, {i, 1, 10, 1}];

Mlistwanted =
  Table[{a + b * (i - 1), Listdesgwanted[[j]][[i]][[2]] ^2 * 18 / 5 * NIntegrate[Re[
        F2c[Listdescoetmwanted[[j]][[2]] / 2, 0.138, Listdescoetmwanted[[j]][[1]], a +
           b * (i - 1), xB] /. g → 1] * UnitStep[Re[F2c[Listdescoetmwanted[[j]][[2]] / 2,
           0.138, Listdescoetmwanted[[j]][[1]], a + b * (i - 1), xB] /. g → 1]],
      {xB, 0.01, xlim[a + b * (i - 1), 0.138, Listdescoetmwanted[[j]][[1]]]}]},
   {j, 1, 4}, {i, 1, 80, 1}];

Mlistwantedb = Table[{aa + bb * (i - 1) ^2, Listdesgwantedb[[i]][[2]] ^2 * 18 / 5 *
    NIntegrate[Re[F2c[(aa + bb * (i - 1) ^2) / 2, 0.138, 0.3, qdeux, xB] /. g → 1] *
      UnitStep[Re[F2c[(aa + bb * (i - 1) ^2) / 2, 0.138, 0.3, qdeux, xB] /. g → 1]],
     {xB, 0.01, xlim[qdeux, 0.138, 0.3]}]}, {i, 1, 50, 1}];

MultipleListPlot[Mlist, Frame → True, PlotJoined → True,
  PlotLabel → "~M^tum f^tion  - m_π=138 MeV- m_q=300 MeV", Axes → False,
  FrameLabel → {"Q² (GeV²)", " 18/5 ∫F2(Q²)dx", "", ""}, RotateLabel → False,
  PlotLegend → {".872", ".828", ".811", ".784", ".764", ".750"},
  LegendLabel → "Cut-Off", LegendPosition → {0.175, -0.35},
  LegendTextSpace → 1, LegendLabelSpace → .1, LegendOrientation → Horizontal,
  LegendShadow → {.02, -.04}, PlotRange → {0.2, 0.8}];

Export["/home/lansberg/mathematica/mf_co_inf_m_300.dat", Mlistwanted[[1]]];
Export["/home/lansberg/mathematica/mf_co_811_m_300.dat", Mlistwanted[[2]]];
Export["/home/lansberg/mathematica/mf_co_750_m_300.dat", Mlistwanted[[3]]];
Export["/home/lansberg/mathematica/mf_co_750_m_360.dat", Mlistwanted[[4]]];

Export["/home/lansberg/mathematica/mf_q2_inf_m_300.dat", Mlistwantedb];

TableForm[Transpose[Mlist]]
```

Plot de F2 à Q^2= 10 GeV^2

```
ouch1 = {0.00001 + 0.01 * (i - 1), 0, 0, 0, 0}
ouch2 = {0, 1, 1, 1, 1}
```

```
{0.00001 + 0.01 (-1 + i), 0, 0, 0, 0}

{0, 1, 1, 1, 1}
```

```
gq210

{3.72279, 3.89966, 4.38151}

F2listwanted = Table[Table[ouch1[[j]] +
    ouch2[[j]] * gq210[[j]]^2 * 18 / 5 * Re[F2c[Listdescoetmwanted[[j]][[2]] / 2, 0.138,
        Listdescoetmwanted[[j]][[1]], 10, 0.00001 + 0.01 * (i - 1)] /. g → 1] * UnitStep[
      Re[F2c[Listdescoetmwanted[[j]][[2]] / 2, 0.138, Listdescoetmwanted[[j]][[1]],
         10, 0.00001 + 0.01 * (i - 1)] /. g → 1]], {j, 1, 4}], {i, 1, 100, 1}];


Export["/home/lansberg/mathematica/F2_xB.dat", F2listwanted];

F2listwanted[[1]]

{{0.00001, {0.0000360914, 0.0000396023, 0.0000499936}},
 {0.00001, {0.0000339808, 0.0000372863, 0.00004707}},
 {0.00001, {0.0000297028, 0.0000325923, 0.0000411442}}}
```

Plot en fonction de Q^2 de l’intégrale sur x du rapport des contributions des deux types de diagrammes.

```
ListPlot[Table[{a + b * (i - 1),
   Listdesg2[[i, 2]] * NIntegrate[Re[IntRapport[0.8, 0.138, 0.3, a + b * (i - 1), xB]] *
      UnitStep[Re[IntRapport[0.8, 0.138, 0.3, a + b * (i - 1), xB]]],
     {xB, 0.01, xlim[a + b * (i - 1), 0.138, 0.3]}]}, {i, 1, 40, 1}],
 Frame → True, Background → RGBColor[0.8, 0.9, 0.8],
 PlotJoined → True,
 PlotLabel → "Λ=800 MeV - Rapport - m_π=138 MeV- m_q=300 MeV",
 Axes → False, FrameLabel → {"Q² (GeV²)", "Int1/Int2", "", ""},
 RotateLabel → False]

- Graphics -
```

Création d'une liste de fonction (à plotter) en fonction de la valeur de la masse du quark.

```
F1lista = {F1a /. mq → 0.15, F1a /. mq → 0.2, F1a /. mq → 0.25, F1a /. mq → 0.3,
   F1a /. mq → 0.35, F1a /. mq → 0.4, F1a /. mq → 0.45, F1a /. mq → 0.5, F1a /. mq → 0.55,
   F1a /. mq → 0.60, F1a /. mq → 0.65, F1a /. mq → 0.70, F1a /. mq → 0.80};

F2lista = {F2a /. mq → 0.15, F2a /. mq → 0.2, F2a /. mq → 0.25, F2a /. mq → 0.3,
  F2a /. mq → 0.35, F2a /. mq → 0.4, F2a /. mq → 0.45, F2a /. mq → 0.5, F2a /. mq → 0.55,
  F2a /. mq → 0.60, F2a /. mq → 0.65, F2a /. mq → 0.70, F2a /. mq → 0.80}

F2listsCG = {F2sCG /. mq → 0.15, F2sCG /. mq → 0.2,
  F2sCG /. mq → 0.25, F2sCG /. mq → 0.3, F2sCG /. mq → 0.35,
  F2sCG /. mq → 0.4, F2sCG /. mq → 0.45, F2sCG /. mq → 0.5, F2sCG /. mq → 0.55,
  F2sCG /. mq → 0.60, F2sCG /. mq → 0.65, F2sCG /. mq → 0.70, F2sCG /. mq → 0.8}

F2listc = {F2c /. mq → 0.15, F2c /. mq → 0.2, F2c /. mq → 0.25, F2c /. mq → 0.3,
  F2c /. mq → 0.35, F2c /. mq → 0.4, F2c /. mq → 0.45, F2c /. mq → 0.5, F2c /. mq → 0.55,
  F2c /. mq → 0.60, F2c /. mq → 0.65, F2c /. mq → 0.70, F2c /. mq → 0.80}

F2listd = {F2d /. mq → 0.15, F2d /. mq → 0.2, F2d /. mq → 0.25, F2d /. mq → 0.3,
  F2d /. mq → 0.35, F2d /. mq → 0.4, F2d /. mq → 0.45, F2d /. mq → 0.5, F2d /. mq → 0.55,
  F2d /. mq → 0.60, F2d /. mq → 0.65, F2d /. mq → 0.70, F2d /. mq → 0.80}

F2listcutoffa = {F2cutoffa /. mq → 0.3 /. cutoff → 0.2,
   F2cutoffa /. mq → 0.3 /. cutoff → 0.3, F2cutoffa /. mq → 0.3 /. cutoff → 0.4,
   F2cutoffa /. mq → 0.3 /. cutoff → 0.5, F2cutoffa //. mq → 0.3 /. cutoff → 0.6,
   F2cutoffa /. mq → 0.3 /. cutoff → 0.7, F2cutoffa /. mq → 0.3 /. cutoff → 0.8,
   F2cutoffa /. mq → 0.3 /. cutoff → 0.9, F2cutoffa /. mq → 0.3 /. cutoff → 1.0,
   F2cutoffa /. mq → 0.3 /. cutoff → 1.25, F2cutoffa /. mq → 0.3 /. cutoff → 1.5,
   F2cutoffa /. mq → 0.3 /. cutoff → 1.75, F2cutoffa /. mq → 0.3 /. cutoff → 2.0};


F1listcutoffa = {F1cutoffa /. mq → 0.3 /. cutoff → 0.2,
   F1cutoffa /. mq → 0.3 /. cutoff → 0.3, F1cutoffa /. mq → 0.3 /. cutoff → 0.4,
   F1cutoffa /. mq → 0.3 /. cutoff → 0.5, F1cutoffa /. mq → 0.3 /. cutoff → 0.6,
   F1cutoffa /. mq → 0.3 /. cutoff → 0.7, F1cutoffa /. mq → 0.3 /. cutoff → 0.8,
   F1cutoffa /. mq → 0.3 /. cutoff → 0.9, F1cutoffa /. mq → 0.3 /. cutoff → 1.0,
   F1cutoffa /. mq → 0.3 /. cutoff → 1.25, F1cutoffa /. mq → 0.3 /. cutoff → 1.5,
   F1cutoffa /. mq → 0.3 /. cutoff → 1.75, F1cutoffa /. mq → 0.3 /. cutoff → 2.0};

F2listcutoffc = {F2cutoffc /. mq → 0.3 /. cutoff → 0.2,
  F2cutoffc /. mq → 0.3 /. cutoff → 0.3, F2cutoffc /. mq → 0.3 /. cutoff → 0.4,
  F2cutoffc /. mq → 0.3 /. cutoff → 0.5, F2cutoffc /. mq → 0.3 /. cutoff → 0.6,
  F2cutoffc /. mq → 0.3 /. cutoff → 0.7, F2cutoffc /. mq → 0.3 /. cutoff → 0.8,
  F2cutoffc /. mq → 0.3 /. cutoff → 0.9, F2cutoffc /. mq → 0.3 /. cutoff → 1.0,
  F2cutoffc /. mq → 0.3 /. cutoff → 1.25, F2cutoffc /. mq → 0.3 /. cutoff → 1.5,
  F2cutoffc /. mq → 0.3 /. cutoff → 1.75, F2cutoffc /. mq → 0.3 /. cutoff → 2.0}

Plot[Evaluate[Re[F1lista]], {xB, 0.001, 1}, AxesLabel → {"xB", "F1"},
 PlotLabel → "From sig_T - g=3.2 - Q²=4 GeV² - m_π=138 MeV",
 PlotStyle → {{Thickness[0.005], GrayLevel[0.5]}},
 Background -> RGBColor[0.8, 0.9, 0.8], PlotRange → {0, 2}]

Re[F2listcutoffNew]

Plot[Evaluate[Re[F2lista]], {xB, 0.001, 1}, AxesLabel → {"xB", "F2"},
 PlotLabel → "From sig_T - g=3.2 - Q²=4 GeV² - m_π=138 MeV",
 PlotStyle → {{Thickness[0.005], GrayLevel[0.5]}},
 Background -> RGBColor[0.8, 0.9, 0.8]]
```

```
ListPlot[Table[{i,
   Re[NIntegrate[Evaluate[Re[F1cutoffa /. nu → (i / 2 / xB) /. mq → 0.3 /. cutoff → 0.8] *
       UnitStep[Re[F1cutoffa /. mq → 0.3 /. cutoff → 0.8 /. nu → (i / 2 / xB)]]],
     {xB, 0.01, 0.8}]]}, {i, 0.5, 100.0, 10.0}], AxesLabel → {"Q^2 (GeV^2)", "∫F1dx"},
 PlotLabel → "Λ=800 MeV g=3.2 m_quark=300 MeV m_π=138 MeV",
 Background -> RGBColor[0.8, 0.9, 0.8],
 PlotJoined → True]

Plot[Evaluate[Re[F2listsCG]], {xB, 0.001, 1}, AxesLabel → {"xB", "F2"},
 PlotLabel → "From sig_T+sig_L - sCG - Q^2=4 GeV^2 - m_π=138 MeV",
 PlotStyle → {{Thickness[0.005], GrayLevel[0.5]}},
 Background -> RGBColor[0.8, 0.9, 0.8]]

Plot[Evaluate[F2listc], {xB, 0.001, 1}, AxesLabel → {"xB", "F2"},
 PlotLabel → "sig_false - g=3.2 - Q^2=4 GeV^2 - m_π=138 MeV",
 PlotStyle → {{Thickness[0.005], GrayLevel[0.5]}},
 Background -> RGBColor[0.8, 0.9, 0.8]]

Plot[Evaluate[Re[F2listd]], {xB, 0.001, 1}, AxesLabel → {"xB", "F2"},
 PlotLabel → "From sig_false-sig_L - Q^2=4 GeV^2 - m_π=138 MeV",
 PlotStyle → {{Thickness[0.005], GrayLevel[0.5]}},
 Background -> RGBColor[0.8, 0.9, 0.8]]

TableForm[Table[{i, Re[[F2sCG /. mq = 0.3] /. xB → i]}, {i, 0.05, 0.9, 0.05}]]

Plot[Evaluate[F2a /. mq → 0.3], {xB, 0.001, 1}, AxesLabel → {"xB", "F2"},
 PlotLabel → "A partir de sig_T; Q^2=4 GeV^2; M_quark=300 MeV, M_pion=138 MeV",
 PlotStyle → {{Thickness[0.005], GrayLevel[0.5]}}]

Plot[Evaluate[Re[F1listcutoffa] * UnitStep[Re[F1listcutoffa]]],
 {xB, 0.001, 1}, FrameLabel → {"xB", "F2", "F2", "F2"},
 PlotLabel → "sig_T - Q^2=4 GeV^2 - M_π=138 MeV",
 PlotStyle → {{Thickness[0.005], GrayLevel[0.5]}},
 Frame → True, Background -> RGBColor[0.8, 0.9, 0.8]]


Plot[Evaluate[Re[F2listcutoffc] * UnitStep[Re[F2listcutoffc]]], {xB, 0.001, 1},
 AxesLabel → {"xB", "F2"}, PlotLabel → "sig_false; Q^2=4 GeV^2; M_pion=138 MeV",
 PlotStyle → {{Thickness[0.005], GrayLevel[0.5]}}]


Plot[Evaluate[Re[F1listcutoffa] * UnitStep[Re[F1listcutoffa]]], {xB, 0.001, 1},
 AxesLabel → {"xB", "F2"}, PlotLabel → "sig_false; Q^2=100 GeV^2; M_pion=138 MeV",
 PlotStyle → {{Thickness[0.005], GrayLevel[0.5]}}]

Re[NIntegrate[Evaluate[F2lista], {xB, 0.00, 1}]]

Re[NIntegrate[Evaluate[F2listsCG], {xB, 0.00, 1}]]

Re[NIntegrate[Evaluate[F2listc], {xB, 0.00, 1}]]

Re[NIntegrate[Evaluate[F2listd], {xB, 0.00, 1}]]

TableForm[Transpose[{Listedescutoff,
   Re[NIntegrate[Evaluate[Re[F2listcutoffa] * UnitStep[Re[F2listcutoffa]]],
     {xB, 0.01, 0.92}]], Re[NIntegrate[
     Evaluate[Re[F2listcutoffc] * UnitStep[Re[F2listcutoffc]]], {xB, 0.01, 0.92}]]}]]

TableForm[Transpose[{Listedescutoff, Re[NIntegrate[
     Evaluate[Re[F2listcutoffa] * UnitStep[Re[F2listcutoffa]]], {xB, 0.01, 0.92}]]}]]

TableForm[Transpose[{Listedescutoff, Re[NIntegrate[
     Evaluate[Re[F1listcutoffa] * UnitStep[Re[F1listcutoffa]]], {xB, 0.01, 0.92}]]}]]
```

C.2 Scalar Case

```
In[1]:= << Graphics`MultipleListPlot`
        << Graphics`Legend`

In[3]:= tmin[mp_, q2_, s_, mq_] =
          Re[-1/2*Sqrt[(mp^4 + 2*mp^2*q2 - 2*mp^2*s + q2^2 + 2*q2*s + s^2)/s]*
             Sqrt[-4*mq^2 + s] + 1/2*mp^2 + mq^2 - 1/2*q2 - 1/2*s];
        tmax[mp_, q2_, s_, mq_] = Re[1/2*Sqrt[
              (mp^4 + 2*mp^2*q2 - 2*mp^2*s + q2^2 + 2*q2*s + s^2)/s]*
             Sqrt[-4*mq^2 + s] + 1/2*mp^2 + mq^2 - 1/2*q2 - 1/2*s];

In[5]:= lambda = (s^2 + q2^ 2 + mp^4  + 2*s*q2  + 2*q2*mp^2 - 2*s*mp^2);
```

Expression du premier cut−offsur t: t>−2*lambdaNJL^2−mq^2+mp^2/2

```
In[6]:= C1[co_, mp_, mq_] = -2*co^2  - mq^2 + mp^2/2;
```

Expression du second cut−offsur t: t<2*lambdaNJL^2+3mq^2+mp^2/2 −s−q2

```
In[7]:= C2[co_, mp_, mq_, q2_, s_] = 2*co^2  + 3*mq^2 + mp^2/2 - s - q2;


        cutoffsurt = -1000*cutoff^2  - mq^2 + mp^2/2
```

$$-1000\,\text{cutoff}^2 + \frac{\text{mp}^2}{2} - \text{mq}^2$$

AMPLITUDE Contractée avec g_{mu nu} + q_mu q_nu / Q2 :

```
In[8]:= Int1Prim[t_, mp_, mq_, q2_, s_] =
          Simplify[-1/(16*Pi*lambda)*Integrate[-8*(3*mp^4*mq^2 - mp^4*q2 - mp^4*t -
                5*mp^2*mq^4 - 3*mp^2*mq^2*s - 4*mp^2*mq^2*t + mp^2*q2^2 + mp^2*q2*s +
                2*mp^2*q2*t + mp^2*s*t + mp^2*t^2 + 4*mq^6 + mq^4*q2 + mq^4*s -
                8*mq^4*t - 3*mq^2*q2^2 - 2*mq^2*q2*s + 8*mq^2*q2*t + mq^2*s^2 +
                8*mq^2*s*t + 4*mq^2*t^2 - q2^2*t - 2*q2*s*t - q2*t^2 - s^2*t - s*t^2)*
              (mp^2 + mq^2 - q2 - s - t)^(-1)*(mq^2 - t)^(-2), t], TimeConstraint → 10];

        Int1cutoff = Simplify[-1/(16*Pi*lambda)*Integrate[
            8*(3*mp^4*mq^2 - mp^4*q2 - mp^4*t + mp^2*mq^4 - 4*mp^2*mq^2*q2 -
               3*mp^2*mq^2*s - 2*mp^2*mq^2*t + mp^2*q2^2 + mp^2*q2*s + 2*mp^2*q2*t +
               mp^2*s*t + mp^2*t^2 - mq^4*q2 - mq^4*s + mq^2*q2^2 + 2*mq^2*q2*s +
               2*mq^2*q2*t + mq^2*s^2 + 2*mq^2*s*t - q2^2*t - 2*q2*s*t - q2*t^2 -
               s^2*t - s*t^2)*(mp^2 + mq^2 - q2 - s - t)^(-1)*(mq^2 - t)^(-2)
            , {t, Max[cutoffsurt, tmin], tmax}], TimeConstraint → 10]
```

AMPLITUDE LONGITUDINALE:

sig_L: 1 → diagrammes box; 2→ diagrammes croisés

Intégration:

```
IntL1Prim[t_, mp_, mq_, q2_, s_] = FullSimplify[ -1 / (16 * Pi * lambda) * Integrate[
    4 * (((2 * (2 * mp^2 * mq^4 - 4 * mp^2 * mq^2 * q2 + 2 * mp^2 * q2 * s + 4 * mp^2 * q2 * t +
                4 * mq^4 * q2 - 4 * mq^4 * s - 8 * mq^2 * q2^2 + mq^2 * q2 * s - 8 * mq^2 * q2 * t +
                6 * q2^2 * s + 8 * q2^2 * t - 2 * q2 * s^2 - 2 * q2 * s * t + 4 * q2 * t^2 +
                (mp^2 - 2 * s) * (s + 2 * t) * t) - (mp^2 - 2 * s) * (s + 8 * t) * mq^2) * mq^2 -
          ((2 * q2 + t) * mp^2 - 2 * (q2 + s) * t) * (2 * q2 + t) * s) * mp^2 +
       (4 * mq^4 * q2^2 - 8 * mq^4 * q2 * s + 4 * mq^4 * s^2 - 8 * mq^2 * q2^3 - mq^2 * q2^2 * s -
          4 * mq^2 * q2^2 * t + 6 * mq^2 * q2 * s^2 + 8 * mq^2 * q2 * s * t - mq^2 * s^3 -
          4 * mq^2 * s^2 * t + q2^2 * s * t + 2 * q2 * s^2 * t + s^3 * t) * (mq^2 - t)) *
     ((mp^2 + 2 * q2 - 2 * s) * mp^2 + (q2 + s)^2)^(-1) *
     (mq^2 - t)^(-2) *
     q2^(-1)
    , t], TimeConstraint → 10]
```

```
(- (4 mp^2 (mp^2 - 4 mq^2) q2^2 s)/(mq^2 - t) +
   (mp^4 (4 mq^2 - s) + 4 mq^2 (q2 - s)^2 - s (q2 + s)^2 + 2 mp^2 (4 mq^2 (q2 - s) + s (q2 + s))) t +
   4 q2 (2 mq^2 (mp^2 + q2)^2 + mp^2 (-mp^2 + q2) s + (mp^2 - 2 mq^2) s^2) Log[-mq^2 + t]) /
 (4 π q2 (mp^4 + 2 mp^2 (q2 - s) + (q2 + s)^2)^2)
```

```
IntL2Prim[t_, mp_, mq_, q2_, s_] = FullSimplify[
  -1 / (16 * Pi * lambda) * Integrate[-4 * (((4 * mp^4 * mq^2 - 4 * mp^4 * q2 - mp^4 * s -
              4 * mp^4 * t + 4 * mp^2 * mq^4 + 4 * mp^2 * mq^2 * q2 - 13 * mp^2 * mq^2 * s -
              8 * mp^2 * mq^2 * t - 12 * mp^2 * q2^2 + 7 * mp^2 * q2 * s - 4 * mp^2 * q2 * t +
              3 * mp^2 * s^2 + 14 * mp^2 * s * t + 4 * mp^2 * t^2 + 8 * mq^4 * q2 - 8 * mq^4 * s -
              4 * mq^2 * q2^2 - 6 * mq^2 * q2 * s - 16 * mq^2 * q2 * t + 14 * mq^2 * s^2 +
              16 * mq^2 * s * t - 12 * q2^3 + 5 * q2^2 * s + 4 * q2^2 * t - 2 * q2 * s^2 +
              4 * q2 * s * t + 8 * q2 * t^2 - (3 * s^2 + 16 * s * t + 8 * t^2) * s) * mq^2 +
           (2 * q2 + t) * mp^4 * s + (2 * q2^2 + 2 * q2 * s + 3 * q2 * t + 3 * s * t + 2 * t^2) *
            (q2 + s) * s - ((4 * s + 3 * t) * q2 + (3 * s + t) * t) * mp^2 * s) * mp^2 +
        (4 * mq^4 * q2^2 - 8 * mq^4 * q2 * s + 4 * mq^4 * s^2 - 4 * mq^2 * q2^3 +
           3 * mq^2 * q2^2 * s - 8 * mq^2 * q2^2 * t + 2 * mq^2 * q2 * s^2 + 16 * mq^2 * q2 * s * t -
           4 * q2^4 - 11 * q2^3 * s + 4 * q2^3 * t - 9 * q2^2 * s^2 - 2 * q2^2 * s * t +
           4 * q2^2 * t^2 - q2 * s^3 - 8 * q2 * s * t^2 - (5 * s + 8 * t) * mq^2 * s^2 +
           (s^2 + 6 * s * t + 4 * t^2) * s^2) * mq^2 - (q2 + s + t) * (q2 + s)^2 * s * t) *
      ((mp^2 + 2 * q2 - 2 * s) * mp^2 + (q2 + s)^2)^(-1) *
      (mq^2 - q2 - s - t + mp^2)^(-1) *
      (mq^2 - t)^(-1) *
     q2^(-1)
    , t], TimeConstraint → 10]
```

$$-\Big((mp^2 - q2 - s)\,\big(-4\,mq^2\,(q2 - s)^2 + mp^4\,(-4\,mq^2 + s) + s\,(q2 + s)^2 - 2\,mp^2\,(4\,mq^2\,(q2 - s) + s\,(q2 + s))\big)\,t + 2\,q2\,\big(mp^6\,(2\,mq^2 - s) + 2\,mq^2\,(q2 + s)^3 + 2\,mp^4\,(mq^2\,(3\,q2 - s) + s^2) + mp^2\,(-s\,(q2 + s)^2 + 2\,mq^2\,(q2 - s)\,(3\,q2 + s))\big)\,\big(-\mathrm{Log}[-mq^2 + t] + \mathrm{Log}[-mp^2 - mq^2 + q2 + s + t]\big)\Big)\Big/\Big(4\,\pi\,q2\,(-mp^2 + q2 + s)\,\big(mp^4 + 2\,mp^2\,(q2 - s) + (q2 + s)^2\big)^2\Big)$$

AMPLITUDE TRANSVERSE:

sig_T: 1 → diagrammes box; 2→ diagrammes croisés

Facteur 1/2: cf. sig_T=1/2*(sig_T1+sig_T2)

```
IntT1Prim[t_, mp_, mq_, q2_, s_] = 1 / 2 * FullSimplify[-1 / (16 * Pi * lambda) *
     Integrate[-4 * (((q2 + s)^2 + mp^4 + 2 * mp^2 * q2 - 2 * mp^2 * s) / s)^((-1) / 2) *
       (Sqrt[((q2 + s)^2 + mp^4 + 2 * mp^2 * q2 - 2 * mp^2 * s) / s] *
          ((5 * mq^2 - q2 - s - t) * (3 * mq^2 + t) - 5 * mp^2 * mq^2) -
         (mp^2 + 2 * mq^2 - q2 - s - 2 * t)^2 * (mp + 2 * mq) * (mp - 2 * mq) +
         Sqrt[((q2 + s)^2 + mp^4 + 2 * mp^2 * q2 - 2 * mp^2 * s) / s] * (s + t + q2) * mp^2 -
         Sqrt[((q2 + s)^2 + mp^4 + 2 * mp^2 * q2 - 2 * mp^2 * s) / s] *
          ((mq^2 + 3 * q2 - (s + 2 * t)) * mq^2 + (s + t + q2) * t -
             (q2 + t - mq^2) * mp^2)) * (mq^2 - t)^(-2)
      , t], TimeConstraint →
     5];

IntT1cutoff = 1 / 2 * Simplify[-1 / (16 * Pi * lambda) * Integrate[
      , {t, Max[cutoffsurt, tmin], tmax}], TimeConstraint → 5];


IntT2Prim[t_, mp_, mq_, q2_, s_] = 1 / 2 * FullSimplify[-1 / (16 * Pi * lambda) *
     Integrate[4 * (((q2 + s)^2 + mp^4 + 2 * mp^2 * q2 - 2 * mp^2 * s) / s)^((-1) / 2) *
       (Sqrt[((q2 + s)^2 + mp^4 + 2 * mp^2 * q2 - 2 * mp^2 * s) / s] *
          ((5 * mq^2 - q2 - s - t) * (3 * mq^2 + t) - 5 * mp^2 * mq^2) -
         (mp^2 + 2 * mq^2 - q2 - s - 2 * t)^2 * (mp + 2 * mq) * (mp - 2 * mq) +
         Sqrt[((q2 + s)^2 + mp^4 + 2 * mp^2 * q2 - 2 * mp^2 * s) / s] * (s + t + q2) * mp^2 -
         Sqrt[((q2 + s)^2 + mp^4 + 2 * mp^2 * q2 - 2 * mp^2 * s) / s] *
          ((mq^2 + 3 * q2 - (s + 2 * t)) * mq^2 + (s + t + q2) * t - (q2 + t - mq^2) * mp^2)) *
       (mq^2 - q2 - s - t + mp^2)^(-1) * (mq^2 - t)^(-1)
      , t], TimeConstraint → 5];

IntT2cutoff = 1 / 2 * Simplify[-1 / (16 * Pi * lambda) * Integrate[
      , {t, Max[cutoffsurt, tmin], tmax}], TimeConstraint → 5];
```

q2=2*xB*nu

s=mp^2-2*xB*nu+2*nu

```
IntTPrim[t_, mp_, mq_, q2_, s_] =
  IntT1Prim[t, mp, mq, q2, s] + IntT2Prim[t, mp, mq, q2, s];

IntT[co_, mp_, mq_, q2_, s_] =
  If[C1[co, mp, mq] < C2[co, mp, mq, q2, s],
   IntTPrim[tmax[mp, q2, s, mq], mp, mq, q2, s] -
    IntTPrim[tmin[mp, q2, s, mq], mp, mq, q2, s],
   If[C1[co, mp, mq] > tmax[mp, q2, s, mq], 0,
     IntTPrim[tmax[mp, q2, s, mq], mp, mq, q2, s] -
      IntTPrim[C1[co, mp, mq], mp, mq, q2, s]
    ] +
    If[C2[co, mp, mq, q2, s] < tmin[mp, q2, s, mq], 0,
     IntTPrim[C2[co, mp, mq, q2, s], mp, mq, q2, s] -
      IntTPrim[tmin[mp, q2, s, mq], mp, mq, q2, s]
    ]
  ];

IntT1[co_, mp_, mq_, q2_, s_] =
  If[C1[co, mp, mq] < C2[co, mp, mq, q2, s],
   IntT1Prim[tmax[mp, q2, s, mq], mp, mq, q2, s] -
    IntT1Prim[tmin[mp, q2, s, mq], mp, mq, q2, s],
   If[C1[co, mp, mq] > tmax[mp, q2, s, mq], 0,
     IntT1Prim[tmax[mp, q2, s, mq], mp, mq, q2, s] -
      IntT1Prim[C1[co, mp, mq], mp, mq, q2, s]
    ] +
    If[C2[co, mp, mq, q2, s] < tmin[mp, q2, s, mq], 0,
     IntT1Prim[C2[co, mp, mq, q2, s], mp, mq, q2, s] -
      IntT1Prim[tmin[mp, q2, s, mq], mp, mq, q2, s]
    ]
  ];

IntT2[co_, mp_, mq_, q2_, s_] =
  If[C1[co, mp, mq] < C2[co, mp, mq, q2, s],
   IntT2Prim[tmax[mp, q2, s, mq], mp, mq, q2, s] -
    IntT2Prim[tmin[mp, q2, s, mq], mp, mq, q2, s],
   If[C1[co, mp, mq] > tmax[mp, q2, s, mq], 0,
     IntT2Prim[tmax[mp, q2, s, mq], mp, mq, q2, s] -
      IntT2Prim[C1[co, mp, mq], mp, mq, q2, s]
    ] +
    If[C2[co, mp, mq, q2, s] < tmin[mp, q2, s, mq], 0,
     IntT2Prim[C2[co, mp, mq, q2, s], mp, mq, q2, s] -
      IntT2Prim[tmin[mp, q2, s, mq], mp, mq, q2, s]
    ]
  ];

IntT[co_, mp_, mq_, q2_, s_] = IntTPrim[tmax[mp, q2, s, mq], mp, mq, q2, s] -
   IntTPrim[tmin[mp, q2, s, mq], mp, mq, q2, s];
```

Int1cutoff=Simplify[Int1cutoff,mp>0&& mq>0 && nu >0 && 0<xB<1,TimeConstraint → 10]

```
In[9]:= Int1[co_, mp_, mq_, q2_, s_] =
  If[C1[co, mp, mq] < C2[co, mp, mq, q2, s],
   Int1Prim[tmax[mp, q2, s, mq], mp, mq, q2, s] -
    Int1Prim[tmin[mp, q2, s, mq], mp, mq, q2, s],
   If[C1[co, mp, mq] > tmax[mp, q2, s, mq], 0,
     Int1Prim[tmax[mp, q2, s, mq], mp, mq, q2, s] -
      Int1Prim[C1[co, mp, mq], mp, mq, q2, s]
    ] +
    If[C2[co, mp, mq, q2, s] < tmin[mp, q2, s, mq], 0,
     Int1Prim[C2[co, mp, mq, q2, s], mp, mq, q2, s] -
      Int1Prim[tmin[mp, q2, s, mq], mp, mq, q2, s]
    ]
  ];

Int1[co_, mp_, mq_, q2_, s_] = Int1Prim[tmax[mp, q2, s, mq], mp, mq, q2, s] -
   Int1Prim[tmin[mp, q2, s, mq], mp, mq, q2, s];
```

```
IntLPrim[t_, mp_, mq_, q2_, s_] =
  IntL1Prim[t, mp, mq, q2, s] + IntL2Prim[t, mp, mq, q2, s];

IntL[co_, mp_, mq_, q2_, s_] =
  If[C1[co, mp, mq] < C2[co, mp, mq, q2, s],
   IntLPrim[tmax[mp, q2, s, mq], mp, mq, q2, s] -
    IntLPrim[tmin[mp, q2, s, mq], mp, mq, q2, s],
   If[C1[co, mp, mq] > tmax[mp, q2, s, mq], 0,
     IntLPrim[tmax[mp, q2, s, mq], mp, mq, q2, s] -
      IntLPrim[C1[co, mp, mq], mp, mq, q2, s]
    ] +
    If[C2[co, mp, mq, q2, s] < tmin[mp, q2, s, mq], 0,
     IntLPrim[C2[co, mp, mq, q2, s], mp, mq, q2, s] -
      IntLPrim[tmin[mp, q2, s, mq], mp, mq, q2, s]
    ]
  ];

IntL[co_, mp_, mq_, q2_, s_] = IntLPrim[tmax[mp, q2, s, mq], mp, mq, q2, s] -
   IntLPrim[tmin[mp, q2, s, mq], mp, mq, q2, s];
```

IntL=Simplify[(IntL1buffer+IntL2buffer),mp>0&&mq>0 && nu >0 && 0<xB<1,TimeConstraint → 10]

IntT=Simplify[(IntT1buffer+IntT2buffer),mp>0&&mq>0 && nu >0 && 0<xB<1,TimeConstraint → 5];

IntTcutoff=Simplify[(IntT1cutoff+IntT2cutoff),mp>0&&mq>0 && nu >0 && 0<xB<1,TimeConstraint → 5];

NOTE: Pas de besoin de mettre des facteurs pour l'évaluation du rapport des contributions croisées–box
Ils disparaissent évidemment dans le rapport !!!

```
IntRapport[co_, mp_, mq_, q2_, s_] = IntT1[co, mp, mq, q2, s] / IntT2[co, mp, mq, q2, s];
```

IntRapport=Simplify[IntT2cutoff/(IntT1cutoff),mp>0&&mq>0 && nu >0 && 0<xB<1,TimeConstraint → 5]

En mettant les facteurs de couleurs: 3; Pas de 1/Sqrt[3]: on considère le pion comme un photon
Facteur 1/2 enlevé:supposé etre le facteur d'isospin

```
In[10]:= K = 1 / 2 * 1 / mp * Sqrt[lambda];
         e = Sqrt[4 * Pi * 1 / 137];
         facteur = 3 * g^2 * e^2 * ((1 / 3) ^2 + (2 / 3) ^2);

In[13]:= xlim[q2_, mp_, mq_] = q2 / (q2 - mp^2 + 4 mq^2);
```

W1 par IntT en utilisant Callan–Gross

W1a=Simplify[K/(4*Pi^ 2*1/137)*IntNew[tmin,tmax,C1,C2]*facteur,ComplexityFunction→(Count[{#1},_Log,∞]&),TimeConstraint → 10]

```
W1a[co_, mp_, mq_, q2_, xB_] = K / (4 * Pi^ 2 * 1 / 137) * IntT[co, mp, mq, q2, s] * facteur
   /. s → (mp^2 - q2 + q2 / xB);

F1a[co_, mp_, mq_, q2_, xB_] = mp * W1a[co, mp, mq, q2, xB];

F2a[co_, mp_, mq_, q2_, xB_] = 2 * xB * F1a[co, mp, mq, q2, xB];

Export["/home/lansberg/mathematica/out.dat", {{5.7, 4.3}, {-1.2, 7.8}}]

Re[F1a[0.7, 0.138, 0.3, 10, 0.5] /. g → 1]

-0.0677694
```

```
Plot3D[Re[F2a[co, 0.138, 0.3, q2, 0.5] / (2 * 0.5) /. g → 1], {q2, 1, 100}, {co, 0.5, 10}]
```

- SurfaceGraphics -

```
Plot[Evaluate[Table[Re[F2a[0.7, 0.138, 0.3, q2, xB] /. g → 1], {q2, 1, 20, 2}]],
 {xB, 0.000001, 1}]
```

- Graphics -

Rapport des contributions: IL FAUT METTRE LE CUT−OFF!!!!!!

```
Rapport = IntRapport /. mp → 0.138 /. mq → 0.3 /. cutoff → 0.8
```

W2 par (IntL+IntT) sans utiliser Callan−Gross

```
W2sCG[co_, mp_, mq_, q2_, xB_] =
  K / (4 * Pi ^ 2 * 1 / 137) * facteur * (2 * xB * mp ^ 2) / (2 * xB * mp ^ 2 + q2 / (2 * xB)) *
    (IntL[co, mp, mq, q2, s] + IntT[co, mp, mq, q2, s]) /. s → (mp ^ 2 - q2 + q2 / xB);

F2sCG[co_, mp_, mq_, q2_, xB_] = q2 / (2 * xB * mp) * W2sCG[co, mp, mq, q2, xB];

Plot3D[Re[F2sCG[co, 0.138, 0.3, q2, 0.5] / (2 * 0.5) /. g → 1],
 {q2, 1, 100}, {co, 0.5, 10}]
```

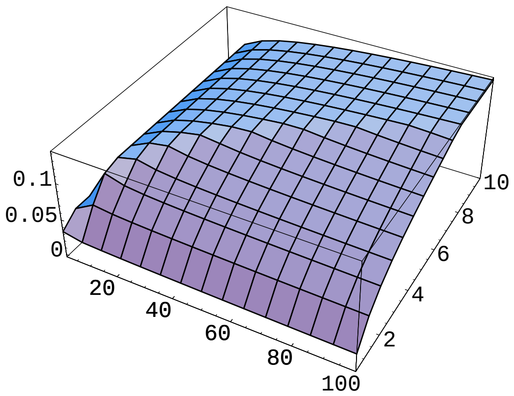

- SurfaceGraphics -

```
Plot[
 Evaluate[Table[Re[F2sCG[0.7, 0.138, 0.3, q2, xB] / (2 * xB) /. g → 1], {q2, 1, 20, 2}]],
 {xB, 0.000001, 1}]
```

- Graphics -

W2 par Int1 en utilisant Callan−Grosspour relier W1 & W2 (déjà à la 1ère equation)

```
In[14]:= W2c[co_, mp_, mq_, q2_, xB_] =
           K / (4 * Pi ^ 2 * 1 / 137) * (xB * mp ^ 2) / (xB * mp ^ 2 - q2 / (2 * xB)) *
             Int1[co, mp, mq, q2, s] * facteur /. s → (mp ^ 2 - q2 + q2 / xB) ;

         F2c[co_, mp_, mq_, q2_, xB_] = q2 / (2 * xB * mp) * W2c[co, mp, mq, q2, xB];
```

```
Plot3D[Re[F2c[co, 0.980, 0.5, q2, 0.5] / (2 * 0.5) /. g → 1], {q2, 1, 100}, {co, 0.5, 10}]
```

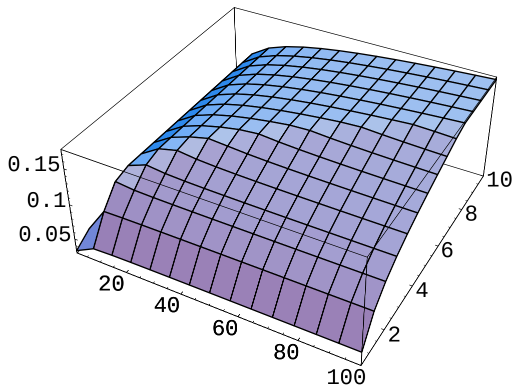


```
Out[78]= - SurfaceGraphics -
```

```
Plot[
 Evaluate[Table[Re[F2c[0.7, 0.980, 0.5, q2, xB] / (2 * xB) /. g → 1], {q2, 2, 20, 2}]],
 {xB, 0.000001, 1}, PlotRange → {{0, 1} , {0, 0.07}}]
```

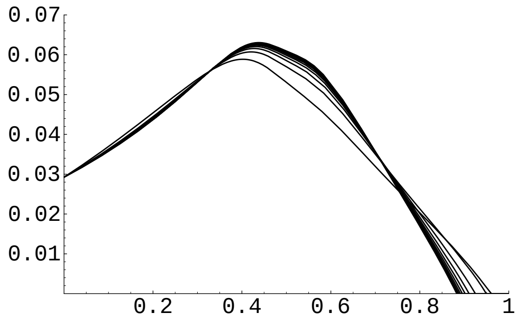


```
Out[89]= - Graphics -
```

W1 par (Int1−IntL)en utilisant Callan−Gross(3ème équation)

```
W1d[co_, mp_, mq_, q2_, xB_] =
  K / (-8 * Pi^ 2 * 1 / 137) * (Int1[co, mp, mq, q2, s] - IntL[co, mp, mq, q2, s]) * facteur /.
   s → (mp^2 - q2 + q2 / xB) ;

F1d[co_, mp_, mq_, q2_, xB_] = mp * W1d[co, mp, mq, q2, xB];

F2d[co_, mp_, mq_, q2_, xB_] = 2 * xB * F1d[co, mp, mq, q2, xB];
```

```
Plot3D[Re[F1d[co, 0.138, 0.3, q2, 0.5] /. g → 1], {q2, 1, 100}, {co, 0.5, 10}]
```

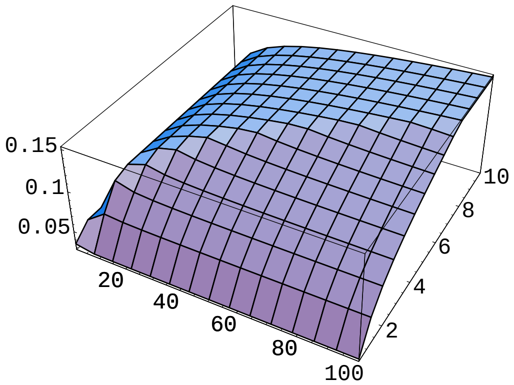


```
- SurfaceGraphics -
```

```
Plot[Evaluate[Table[Re[F1d[0.7, 0.138, 0.3, q2, xB] /. g → 1], {q2, 1, 20, 2}]],
 {xB, 0.000001, 1}]
```

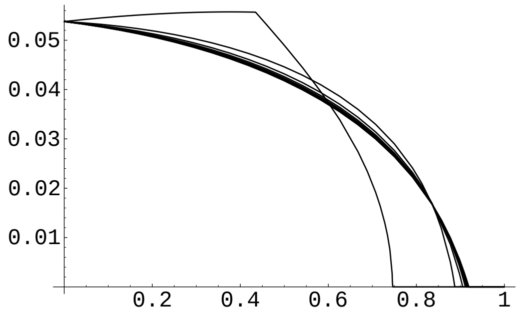


```
- Graphics -
```

W1 par IntTcutoff en utilisant Callan−Gross

```
W1cutoffa = K / (4 * Pi ^ 2 * 1 / 137) * IntTcutoff * facteur;

F1cutoffa = mp * W1cutoffa /. mp → 0.138

F1cutoffa = mp * W1cutoffa /. mp → 0.138 /. nu → (4 / 2 / xB);

F2cutoffa = 2 * xB * F1cutoffa /. mp → 0.138 /. nu → (4 / 2 / xB);
```

W2 par Int1 en utilisant Callan−Grosspour relier W1 &W2 (déjà à la 1ère equation)

```
W2cutoffc = K / (4 * Pi ^ 2 * 1 / 137) * (xB * mp ^2) / (xB * mp ^2 - nu) * Int1cutoff * facteur

F2cutoffc = nu / mp * W2cutoffc /. mp → 0.138 /. nu → (4 / 2 / xB)
```

Courbes en fonctions de Q^2.

Domaine de variation sur Q^2: Q^2=a+b*(i−1),avec i variant de 1 à 20 par pas de 1.

```
In[169]:= a = 1;
          b = 0.25;
          Listdesco = {0.2, 0.4, 0.6, 0.8, 1.2};
          Listdescoetmwanted =
            {{0.5, 1000000000000000000000000000000000000000000000000},
             {0.5, 0.75}, {0.5, 0.7}, {0.55, 0.7}};

Listdesg2 = Table[{a + b * (ii - 1), 5 / 18 / NIntegrate[Re[
        F2c[Listdesco[[j]], 0.138, 0.3, a + b * (ii - 1), xB] / (2 * xB) /. g → 1] * UnitStep[
        Re[F2c[Listdesco[[j]], 0.138, 0.3, a + b * (ii - 1), xB] / (2 * xB) /. g → 1]],
      {xB, 0.00000001, xlim[a + b * (ii - 1), 0.138, 0.3]}]}, {j, 1, 5}, {ii, 1, 40, 1}];
MultipleListPlot[Listdesg2, Frame → True, Background -> RGBColor[0.8, 0.9, 0.8],
 PlotJoined → True, PlotLabel → "∫F1dx= 5/18 → g^2  - m_π=138 MeV- m_q=300 MeV",
 Axes → False, FrameLabel → {"Q^2 (GeV^2)", "g^2", "", ""}, RotateLabel → False,
 PlotRange → {3, 25}, PlotLegend → {"0.6", "0.75", "0.9", "1.05"},
 LegendLabel → "Cut-Off", LegendPosition → {0.9, -0.4}, LegendTextSpace → 1,
 LegendLabelSpace → .1, LegendOrientation → Vertical, LegendShadow → {.02, -.04}]
Sqrt[Listdesg2];
Listdesg2;
```

```
In[173]:= Listdesgwanted = Table[{a + b * (ii - 1),
              Sqrt[5 / 18 / NIntegrate[Re[F2c[Listdescoetmwanted[[j]][[2]] / 2, 0.98,
                     Listdescoetmwanted[[j]][[1]], a + b * (ii - 1), xB] / (2 * xB) /. g → 1] *
                 UnitStep[Re[F2c[Listdescoetmwanted[[j]][[2]] / 2, 0.98,
                      Listdescoetmwanted[[j]][[1]], a + b * (ii - 1), xB] / (2 * xB) /. g → 1]],
                {xB, 0.00000001, xlim[a + b * (ii - 1), 0.98,
                  Listdescoetmwanted[[j]][[1]]]}]]}, {j, 1, 4}, {ii, 1, 80, 1}];
```

A Q^2 infini :

```
In[195]:= qdeux = 2000000;
          aa = 0.5;
          bb = 0.05;
```

```
In[202]:= Listdesgwantedb =
            Table[{aa + bb * (ii - 1) ^2 , Sqrt[5 / 18 / NIntegrate[Re[F2c[(aa + bb * (ii - 1) ^2) / 2,
                     0.98, 0.55, qdeux, xB] / (2 * xB) /. g → 1] * UnitStep[
                  Re[F2c[(aa + bb * (ii - 1) ^2) / 2 , 0.98, 0.55, qdeux, xB] / (2 * xB) /. g → 1]],
                {xB, 0.00000001, xlim[qdeux, 0.98, 0.55]}]]}, {ii, 1, 50, 1}];
```

```
In[132]:=
          MultipleListPlot[Listdesgwanted, Frame → True, PlotJoined → True,
           PlotLabel → "∫F1dx= 5/18 → g^2  - m_π=138 MeV", Axes → False,
           FrameLabel → {"Q^2 (GeV^2)", "g^2", "", ""}, RotateLabel → False,
           PlotRange → {0, 10}, PlotLegend → {"Infini", ".811", ".750", ".750"},
           LegendLabel → "Cut-Off", LegendPosition → {0.925, -0.4}, LegendTextSpace → 1.25,
           LegendLabelSpace → .1, LegendOrientation → Vertical, LegendShadow → {.02, -.04}]
          Sqrt[Listdesg];
          Listdesg;
          TableForm[Transpose[Listdesgwanted]];

Out[132]= - Graphics -
```

```
In[178]:= Export["/home/lansberg/mathematica/g_co_inf_m_500_scal.dat",
            Listdesgwanted[[1]]];
          Export["/home/lansberg/mathematica/g_co_750_m_500_scal.dat",
            Listdesgwanted[[2]]];
          Export["/home/lansberg/mathematica/g_co_700_m_500_scal.dat",
            Listdesgwanted[[3]]];
          Export["/home/lansberg/mathematica/g_co_700_m_550_scal.dat",
            Listdesgwanted[[4]]];
```

```
In[203]:= Export["/home/lansberg/mathematica/g_q2_inf_m_550_scal.dat", Listdesgwantedb];
```

Valeur des g à Q^2=10 GeV (le deuxieme parametre "b" dans Listdesgwanted[[a]][[b]][[c]] doit etre plus petit que la valeur max atteinte par i (quand on genères les valeurs de Q^2) et correspond "normalement" à la valeur de i telle que Q^2=10 GeV^ 2.

```
In[183]:= gq210 = {0, Listdesgwanted[[2]][[79]][[2]], Listdesgwanted[[3]][[79]][[2]]
            , Listdesgwanted[[4]][[79]][[2]]}

Out[183]= {0, 3.97754, 4.21531, 6.63795}

In[184]:= Mlistwanted = Table[{a + b * (i - 1), Listdesgwanted[[j]][[i]][[2]] ^2 *
               18 / 5 * NIntegrate[Re[F2c[Listdescoetmwanted[[j]][[2]] / 2, 0.98,
                    Listdescoetmwanted[[j]][[1]], a + b * (i - 1), xB] /. g → 1] *
                 UnitStep[Re[F2c[Listdescoetmwanted[[j]][[2]] / 2, 0.98,
                     Listdescoetmwanted[[j]][[1]], a + b * (i - 1), xB] /. g → 1]],
                {xB, 0.01, xlim[a + b * (i - 1), 0.98, Listdescoetmwanted[[j]][[1]]]}]},
            {j, 1, 4}, {i, 1, 80, 1}];

In[204]:= Mlistwantedb = Table[{aa + bb * (i - 1) ^2, Listdesgwantedb[[i]][[2]] ^2 * 18 / 5 *
               NIntegrate[Re[F2c[(aa + bb * (i - 1) ^2) / 2, 0.98, 0.55, qdeux, xB] /. g → 1] *
                 UnitStep[Re[F2c[(aa + bb * (i - 1) ^2) / 2, 0.98, 0.55, qdeux, xB] /. g → 1]],
                {xB, 0.01, xlim[qdeux, 0.98, 0.55]}]}, {i, 1, 50, 1}];

In[186]:= Export["/home/lansberg/mathematica/mf_co_inf_m_500_scal.dat", Mlistwanted[[1]]];
          Export["/home/lansberg/mathematica/mf_co_750_m_500_scal.dat", Mlistwanted[[2]]];
          Export["/home/lansberg/mathematica/mf_co_700_m_500_scal.dat", Mlistwanted[[3]]];
          Export["/home/lansberg/mathematica/mf_co_700_m_550_scal.dat", Mlistwanted[[4]]];

In[205]:= Export["/home/lansberg/mathematica/mf_q2_inf_m_550_scal.dat", Mlistwantedb];
```

Plot de F2 à Q^2= 10 GeV^2

```
        {xB, 0.01, xlim[10, 0.138, Listdescoetmwanted[[j]][[1]]]}

In[191]:= ouch1 = {0.00001 + 0.01 * (i - 1), 0, 0, 0, 0}
          ouch2 = {0, 1, 1, 1, 1}

In[193]:= F2listwanted = Table[Table[ouch1[[j]] + ouch2[[j]] * gq210[[j]] ^2 * 18 / 5 *
                Re[F2c[Listdescoetmwanted[[j]][[2]] / 2, 0.98, Listdescoetmwanted[[j]][[1]],
                   10, 0.00001 + 0.01 * (i - 1)] /. g → 1] * UnitStep[
                 Re[F2c[Listdescoetmwanted[[j]][[2]] / 2, 0.98, Listdescoetmwanted[[j]][[1]],
                    10, 0.00001 + 0.01 * (i - 1)] /. g → 1]], {j, 1, 4}], {i, 1, 100, 1}];

In[194]:= Export["/home/lansberg/mathematica/F2_xB_scal.dat", F2listwanted];
```

Plot en fonction de Q^2 de l'intégrale sur x du rapport des contributions des deux types de diagrammes.

```
        ListPlot[Table[{a + b * (i - 1),
            Listdesg2[[i, 2]] * NIntegrate[Re[IntRapport[0.8, 0.138, 0.3, a + b * (i - 1), xB]] *
               UnitStep[Re[IntRapport[0.8, 0.138, 0.3, a + b * (i - 1), xB]]],
              {xB, 0.01, xlim[a + b * (i - 1), 0.138, 0.3]}]}, {i, 1, 40, 1}],
         Frame → True, Background → RGBColor[0.8, 0.9, 0.8],
         PlotJoined → True,
         PlotLabel → "Λ=800 MeV - Rapport - m_π=138 MeV- m_q=300 MeV",
         Axes → False, FrameLabel → {"Q² (GeV²)", "Int1/Int2", "", ""},
         RotateLabel → False]
```

Création d'une liste de fonction (à ploter) en fonction de la valeur de la masse du quark.

```
        F1lista = {F1a /. mq → 0.15, F1a /. mq → 0.2, F1a /. mq → 0.25, F1a /. mq → 0.3,
            F1a /. mq → 0.35, F1a /. mq → 0.4, F1a /. mq → 0.45, F1a /. mq → 0.5, F1a /. mq → 0.55,
            F1a /. mq → 0.60, F1a /. mq → 0.65, F1a /. mq → 0.70, F1a /. mq → 0.80};

        F2lista = {F2a /. mq → 0.15, F2a /. mq → 0.2, F2a /. mq → 0.25, F2a /. mq → 0.3,
           F2a /. mq → 0.35, F2a /. mq → 0.4, F2a /. mq → 0.45, F2a /. mq → 0.5, F2a /. mq → 0.55,
           F2a /. mq → 0.60, F2a /. mq → 0.65, F2a /. mq → 0.70, F2a /. mq → 0.80}
```

```
F2listsCG = {F2sCG /. mq → 0.15, F2sCG /. mq → 0.2,
  F2sCG /. mq → 0.25, F2sCG /. mq → 0.3, F2sCG /. mq → 0.35,
  F2sCG /. mq → 0.4, F2sCG /. mq → 0.45, F2sCG /. mq → 0.5, F2sCG /. mq → 0.55,
  F2sCG /. mq → 0.60, F2sCG /. mq → 0.65, F2sCG /. mq → 0.70, F2sCG /. mq → 0.8}

F2listc = {F2c /. mq → 0.15, F2c /. mq → 0.2, F2c /. mq → 0.25, F2c /. mq → 0.3,
  F2c /. mq → 0.35, F2c /. mq → 0.4, F2c /. mq → 0.45, F2c /. mq → 0.5, F2c /. mq → 0.55,
  F2c /. mq → 0.60, F2c /. mq → 0.65, F2c /. mq → 0.70, F2c /. mq → 0.80}

F2listd = {F2d /. mq → 0.15, F2d /. mq → 0.2, F2d /. mq → 0.25, F2d /. mq → 0.3,
  F2d /. mq → 0.35, F2d /. mq → 0.4, F2d /. mq → 0.45, F2d /. mq → 0.5, F2d /. mq → 0.55,
  F2d /. mq → 0.60, F2d /. mq → 0.65, F2d /. mq → 0.70, F2d /. mq → 0.80}

F2listcutoffa = {F2cutoffa /. mq → 0.3 /. cutoff → 0.2,
   F2cutoffa /. mq → 0.3 /. cutoff → 0.3, F2cutoffa /. mq → 0.3 /. cutoff → 0.4,
   F2cutoffa /. mq → 0.3 /. cutoff → 0.5, F2cutoffa //. mq → 0.3 /. cutoff → 0.6,
   F2cutoffa /. mq → 0.3 /. cutoff → 0.7, F2cutoffa /. mq → 0.3 /. cutoff → 0.8,
   F2cutoffa /. mq → 0.3 /. cutoff → 0.9, F2cutoffa /. mq → 0.3 /. cutoff → 1.0,
   F2cutoffa /. mq → 0.3 /. cutoff → 1.25, F2cutoffa /. mq → 0.3 /. cutoff → 1.5,
   F2cutoffa /. mq → 0.3 /. cutoff → 1.75, F2cutoffa /. mq → 0.3 /. cutoff → 2.0};


F1listcutoffa = {F1cutoffa /. mq → 0.3 /. cutoff → 0.2,
   F1cutoffa /. mq → 0.3 /. cutoff → 0.3, F1cutoffa /. mq → 0.3 /. cutoff → 0.4,
   F1cutoffa /. mq → 0.3 /. cutoff → 0.5, F1cutoffa /. mq → 0.3 /. cutoff → 0.6,
   F1cutoffa /. mq → 0.3 /. cutoff → 0.7, F1cutoffa /. mq → 0.3 /. cutoff → 0.8,
   F1cutoffa /. mq → 0.3 /. cutoff → 0.9, F1cutoffa /. mq → 0.3 /. cutoff → 1.0,
   F1cutoffa /. mq → 0.3 /. cutoff → 1.25, F1cutoffa /. mq → 0.3 /. cutoff → 1.5,
   F1cutoffa /. mq → 0.3 /. cutoff → 1.75, F1cutoffa /. mq → 0.3 /. cutoff → 2.0};

F2listcutoffc = {F2cutoffc /. mq → 0.3 /. cutoff → 0.2,
  F2cutoffc /. mq → 0.3 /. cutoff → 0.3, F2cutoffc /. mq → 0.3 /. cutoff → 0.4,
  F2cutoffc /. mq → 0.3 /. cutoff → 0.5, F2cutoffc /. mq → 0.3 /. cutoff → 0.6,
  F2cutoffc /. mq → 0.3 /. cutoff → 0.7, F2cutoffc /. mq → 0.3 /. cutoff → 0.8,
  F2cutoffc /. mq → 0.3 /. cutoff → 0.9, F2cutoffc /. mq → 0.3 /. cutoff → 1.0,
  F2cutoffc /. mq → 0.3 /. cutoff → 1.25, F2cutoffc /. mq → 0.3 /. cutoff → 1.5,
  F2cutoffc /. mq → 0.3 /. cutoff → 1.75, F2cutoffc /. mq → 0.3 /. cutoff → 2.0}

Plot[Evaluate[Re[F1lista]], {xB, 0.001, 1}, AxesLabel → {"xB", "F1"},
 PlotLabel → "From sig_T - g=3.2 - Q²=4 GeV² - m_π=138 MeV",
 PlotStyle → {{Thickness[0.005], GrayLevel[0.5]}},
 Background -> RGBColor[0.8, 0.9, 0.8], PlotRange → {0, 2}]

- Graphics -

Re[F2listcutoffNew]

Plot[Evaluate[Re[F2lista]], {xB, 0.001, 1}, AxesLabel → {"xB", "F2"},
 PlotLabel → "From sig_T - g=3.2 - Q²=4 GeV² - m_π=138 MeV",
 PlotStyle → {{Thickness[0.005], GrayLevel[0.5]}},
 Background -> RGBColor[0.8, 0.9, 0.8]]


ListPlot[Table[{i,
   Re[NIntegrate[Evaluate[Re[F1cutoffa /. nu → (i / 2 / xB) /. mq → 0.3 /. cutoff → 0.8] *
       UnitStep[Re[F1cutoffa /. mq → 0.3 /. cutoff → 0.8 /. nu → (i / 2 / xB)]]],
     {xB, 0.01, 0.8}]]}, {i, 0.5, 100.0, 10.0}], AxesLabel → {"Q² (GeV²)", "∫F1dx"},
 PlotLabel → "Λ=800 MeV g=3.2 m_quark=300 MeV m_π=138 MeV",
 Background -> RGBColor[0.8, 0.9, 0.8],
 PlotJoined → True]

Plot[Evaluate[Re[F2listsCG]], {xB, 0.001, 1}, AxesLabel → {"xB", "F2"},
 PlotLabel → "From sig_T+sig_L - sCG - Q²=4 GeV² - m_π=138 MeV",
 PlotStyle → {{Thickness[0.005], GrayLevel[0.5]}},
 Background -> RGBColor[0.8, 0.9, 0.8]]
```

List of Figures

Bibliography

[1] J.P. Lansberg, *Etats colorés et Fonction d'onde en QCD, application à la production de mésons lourds*, Undergrad. Dissertation, PTF-ULg, 2000.

[2] C-H. Chang, *Nucl. Phys.* **B 172** (1980) 425;
R. Baier and R. Rückl, *Phys. Lett.* B **102** (1981) 364;
R. Baier and R. Rückl, *Z. Phys.* **C 19** (1983) 251.

[3] F.Abe *et al.*, CDF Collab., *Phys. Rev. Lett.* **79** (1997) 572

[4] F.Abe *et al.*, CDF Collab., *Phys. Rev. Lett.* **79** (1997) 578

[5] F. Abe *et al.*, CDF Collab., *Phys. Rev. Lett.* **75** (1995) 4358.

[6] J.C. Collins, D.E. Soper and G. Sterman, *Perturbative Quantum Chromodynamics*, ed. by A.H. Mueller, World Scientific, Singapore, 1989;
G. BODWIN, *Phys. Rev.* D **31** (1985) 2616 and **34** (1986) 3932;
J. Qiu and G. Sterman, *Nucl. Phys.* **B 353** (1991) 105 and **B 353** (1991) 137.

[7] J.F Amundson, O.J.P. Éboli, E.M. Gregores, F. Halzen, *Phys. Lett.* B **372** (1996) 127;
J.F Amundson *et al.*, *Phys. Lett.* B **390** (1997) 323.

[8] P. Hoyer and S. Peigné, *Phys. Rev.* D **57** (1998) 1864 , *Phys. Rev.* D **59** (1999) 034011 .
N. Marchal, S. Peigné and P. Hoyer, *Phys. Rev.* D **62** (2000) 114001.

[9] A. Edin, G. Ingelman and J. Rathsman, *Phys. Rev.* D **56** (1997) 7317

[10] G.T. Bodwin, E. Braaten, G. Lepage, *Phys. Rev.* D **51** (1995) 1125;
G.T. Bodwin *et al.*, *Phys. Rev.* D **55** (1997) 5853.

[11] J.P. Lansberg, *Heavy quarkonium production in hadronic collisions*, Talk at 'JJC2001' (La Hume, France, December 2001) (hep-ph/0201111).

[12] H.Plothow-Besch, *PDFLIB, Users's Manual – Version 8.04, W5051 PDFLIB*, 2000.04.17,CERN-PPE and references therein.

[13] E. E. Salpeter and H. A. Bethe, *Phys. Rev.* **84** (1951) 1232.

[14] W. Buchmuller and S. H. Tye, *Phys. Rev. D* **24** (1981) 132.

[15] R. Barbieri, R. Gatto, R. Kogerler and Z. Kunszt, *Phys. Lett.* B **57** (1975) 455.

[16] F. Gross, *Relativistic Quantum Mechanics and Field Theory*, Wiley, New-York, 1993.

[17] M. Jaminon, P. Stassart and G. Ripka, *Phys. Lett.* B **227** (1989) 191.

[18] M. Jaminon, R. Mendez Galain, G. Ripka and P. Stassart, *Nucl. Phys.* **A 537** (1992) 418.

[19] V.D. Barger and R.J.N. Philips, *Collider Physics*, Addison-Wesley, Menlo Park, 1987.

[20] I.J.R Aitchison and A.J.G. Hey, *Gauge Theories in Particles Physics* (first edition), Institute of Physics Publishing, Bristol, 1982.

[21] C. G. Callan and D. J. Gross, *Phys. Rev. Lett.* **22** (1969) 156.

[22] I.J.R Aitchison and A.J.G. Hey, *Gauge Theories in Particles Physics* (second edition), Institute of Physics Publishing, Bristol, 1996.

[23] F. Halzen and A.D. Martin, *Quarks and Leptons: An Introductory Course in Modern Particle Physics*, Wiley, New-York, 1984.

[24] M. Gell-Mann and M. Levy, *Nuovo Cim.* **16** (1960) 705.

Index